

CR-86189

06414-6008-T000

# LUNAR MODULE/ABORT GUIDANCE SYSTEM (LM/AGS) DESIGN SURVEY

NASA/ERC  
Design Criteria Program,  
Guidance and Control

FACILITY FORM 602

**. N69-33430**

(ACCESSION NUMBER)

(THRU)

96

(PAGES)

(CODE)

CR-86189

(NASA CR OR TMX OR AD NUMBER)

21

(CATEGORY)

1968 September

Prepared for:

National Aeronautics and Space Administration  
Electronics Research Center  
Cambridge, Massachusetts  
Contract NAS 12-110

**TRW**  
SYSTEMS GROUP

ONE SPACE PARK • REDONDO BEACH, CALIFORNIA

DON STEVER



06414-6008-T000

# **LUNAR MODULE /ABORT GUIDANCE SYSTEM (LM/AGS) DESIGN SURVEY**

**NASA/ERC**  
*Design Criteria Program,  
Guidance and Control*

1968 September

Prepared for:

National Aeronautics and Space Administration  
Electronics Research Center  
Cambridge, Massachusetts  
Contract NAS 12-110

**TRW**  
SYSTEMS GROUP

ONE SPACE PARK • REDONDO BEACH, CALIFORNIA

DON STEVER

LUNAR MODULE/ABORT GUIDANCE  
SYSTEM (LM/AGS)  
DESIGN SURVEY

NASA/ERC DESIGN CRITERIA PROGRAM  
GUIDANCE AND CONTROL

Prepared for

National Aeronautics and Space Administration  
Electronics Research Center  
Cambridge, Massachusetts

Contract NAS 12-110

1968 September

Approved: N. W. Trembath  
N. W. Trembath  
LM/AGS Program Manager

Approved: T. W. Layton  
T. W. Layton  
Study Manager  
Contract NAS 12-110

## FOREWORD

This report is one of a series of design surveys being produced by industrial contractors as part of the NASA Design Criteria Program. The objective of the Program is to provide a unification of design approaches for the development of space vehicles and their major components. The surveys are intended to document design experience gained from specific NASA projects and will be used as an aid in identifying suitable topics for design criteria monographs.

This report summarizes TRW's design experience to date in developing the Lunar Module Abort Guidance System for the Apollo Program, and relates this experience to the NASA/ERC Design Criteria Program for Guidance and Control.

The preparation of this report was supervised and coordinated by Dr. T. W. Layton and J. A. Vanderlaan. Major sections were prepared by: J. A. Vanderlaan, H. D. Blow, G. M. Petrov, F. A. Evans, W. M. Ashley, P. B. Aubol, M. L. Obright, and D. Sargent. Additional contributors of technical content were J. S. Hill, H. A. Irwin, L. N. Jenks, D. Wedelund, T. A. Fuhrman, W. W. Benjamin, R. E. Morse, and H. A. Pudewa.



PRECEDING PAGE BLANK NOT FILMED.

## CONTENTS

1.	SUMMARY	1
2.	SYSTEM DESCRIPTION	2
2.1	CONFIGURATION	2
2.1.1	Abort Sensor Assembly	2
2.1.2	Abort Electronics Assembly	2
2.1.3	Data Entry and Display Assembly	2
2.2	OPERATIONAL CHARACTERISTICS	5
2.2.1	Lunar Module Mission	5
2.2.2	Major LM/AGS Functions	5
2.3	PERFORMANCE CHARACTERISTICS	7
2.4	ENVIRONMENTAL CONSIDERATIONS	8
2.4.1	Thermal Environment	8
2.4.2	Vibration Environment	8
3.	HISTORICAL SUMMARY OF AGS DESIGN DEVELOPMENT	10
3.1	EARLY DESIGN DECISIONS	10
3.1.1	Computer Concept	10
3.1.2	Sensor Assembly Concept	10
3.2	MAJOR DESIGN CHANGES	11
3.2.1	Modifications Caused by Changes in Functional Requirements	11
3.2.2	Modifications Caused by Changes in Mission Requirements	12
3.3	HISTORICAL SUMMARY OF DESIGN DEVELOPMENT OF THE ABORT SENSOR ASSEMBLY	13
3.3.1	Early History	13
3.3.2	Design Concepts at Program Start	13
3.3.3	Outline of Design Evaluation	14
3.3.4	Chronological Outline of Design Changes, Problems, and Solutions	14

## CONTENTS (Continued)

3.4	HISTORICAL SUMMARY OF DESIGN DEVELOPMENT OF THE COMPUTER SUBSYSTEMS (AEA AND DEDA)	24
3.4.1	Early Design Decisions	24
3.4.2	Design Development History of AEA Subsections	26
3.5	HISTORICAL SUMMARY OF SOFTWARE DESIGN DEVELOPMENT	29
3.5.1	Early History	29
3.5.2	Program Modifications Subsequent to DMCP	30
4.	MAJOR DESIGN PROBLEMS	33
4.1	DISCUSSION OF MAJOR DESIGN PROBLEMS OF THE ASA	33
4.1.1	Sensors	33
4.1.2	Sensor/Electronics Loops	36
4.1.3	Electronics and Interface	40
4.1.4	Thermal and Mechanical	41
4.1.5	Testing	42
4.2	DISCUSSION OF MAJOR DESIGN PROBLEMS OF COMPUTER SUBSYSTEMS (AEA AND DEDA)	47
4.2.1	Major Design Changes	47
4.2.2	Mechanical Design Problems	49
4.2.3	Residual Problem Areas	50
4.3	DISCUSSION OF MAJOR DESIGN PROBLEMS OF SOFTWARE	51
4.3.1	Softwired Program	51
4.3.2	Hardwired Program	54
4.4	DISCUSSION OF MAJOR PROBLEMS IN SYSTEMS LEVEL TESTING	54
4.4.1	Integration Test Problems	54
4.4.2	System Performance Test Problems	55
APPENDIX:	DETAILED DESCRIPTION OF MAJOR SUB- ASSEMBLIES, SOFTWARE, AND SYSTEM LEVEL TESTING	57

## ILLUSTRATIONS

2-1	Abort Guidance System Assemblies	3
2-2	AGS Functional Block Diagram	4
2-3	Co-Elliptic Rendezvous Flight Profile	5
2-4	ASA Linear Vibration Requirement	9
2-5	ASA Rotational Vibration Requirement	9
2-6	AGS Design Limit Sinusoidal Vibration	9
2-7	AGS Design Limit Random Vibration	9
4-1	Capacitor C4 Adjust in Accelerometer	35



## ABBREVIATIONS

ACE	Automatic checkout equipment
AEA	Abort electronics assembly
AGS	Abort guidance system
ASA	Abort sensor assembly
BTME	Bench test maintenance equipment
CDH	Constant delta h
CDU	Coupling data unit
CLR	Clear
C/O	Checkout
CSD	Gross spectral density
CSI	Coelliptic sequence initiate
CSM	Command and service module
D/A	Digital/analog
DEDA	Data entry and display assembly
DMCP	Design mission computer program
DRB	Design Review Board
DTL	Diode transistor logic
EMI	Electromagnetic interference
ENTR	Enter
EPC	Earth prelaunch calibration
ERC	Electronic Research Center
FDAI	Flight Director Attitude Indicator
FEB	Functional electronic block (thin-film hybrid circuit)
FP	Flight program
FS	Flight simulation
g	Acceleration due to gravity

GAEC	Grumman Aircraft Engineering Corporation
GMT	Greenwich Mean Time
GSE	Ground Support Equipment
HVSIR	H-vector spin input rectification
Hz	Hertz
ICS	Interpretive computer simulation
ID	Identification
IMU	Inertial measurement unit
I/O	Input/output
KHz	Kilohertz
LM	Lunar Module
LOS	Line of sight
LSB	Least significant bits
MIT/IL	Massachusetts Institute of Technology Instrumentation Laboratory
MSB	Most significant bits
MSC	Manned Spacecraft Center
MSFN	Manned space flight network
MTBF	Mean time between failure
PGNCS	Primary Guidance, Navigation, and Control System
PPS	Pulses per second
PSD	Power spectral density
PTSA	Pulse torque servoamplifier
RCS	Reactor control system
RFP	Request for proposal
SCP	Software change proposal
SMRD	Spin motor rotation detector
TLM	Telemetry
TPI	Transfer phase initiate
UACSC	United Aircraft Corporation System Center
WSMR	White Sands Missile Range

## 1 SUMMARY

This report presents a survey of the design and development of the Abort Guidance System for the Apollo Lunar Module.

The Lunar Module Abort Guidance System, which is described in Section 2, is a strapdown, all-attitude, inertial guidance system being developed and produced by TRW Systems Group for NASA's Manned Spacecraft Center under subcontract to Grumman Aircraft Engineering Corporation. This system provides the capability for safely returning the astronauts to the Command Module in the unlikely event of a Primary Guidance, Navigation, and Control System (PGNCS) failure either during descent, while the Lunar Module is on the lunar surface, or during ascent from the lunar surface to the Command Module. The abort guidance

system also provides a means of monitoring the performance of the PGNCS for fault detection.

Section 3 documents the evolution of the Abort Guidance System (AGS) design and summarizes the historical design development of subassemblies and software. Section 4 presents the major design problems that have developed to date. Since the system is in the late stages of development, but has not yet been flight-tested, it is possible that additional problem areas will appear, and design changes will be required. In any event, it may be desirable to write an addendum to this report at the end of the development cycle after the system has been subjected to operational usage. A detailed description of the major AGS subassemblies, software, and system level testing is contained in the Appendix.



## 2. SYSTEM DESCRIPTION

This section contains a physical and functional description of the Lunar Module Abort Guidance System (LM/AGS). A typical LM mission from lunar liftoff to rendezvous is briefly described to establish the terminology used in explaining the functional capabilities of the AGS. Performance characteristics are discussed in detail.

### 2.1 CONFIGURATION

The LM/AGS consists of the following three major assemblies, as shown in Figure 2-1:

1. Abort Sensor Assembly
2. Abort Electronics Assembly
3. Data Entry and Display Assembly

Table 2-1 lists the general characteristics of the system's constituent assemblies. Figure 2-2 is a functional block diagram of the AGS.

#### 2.1.1 Abort Sensor Assembly

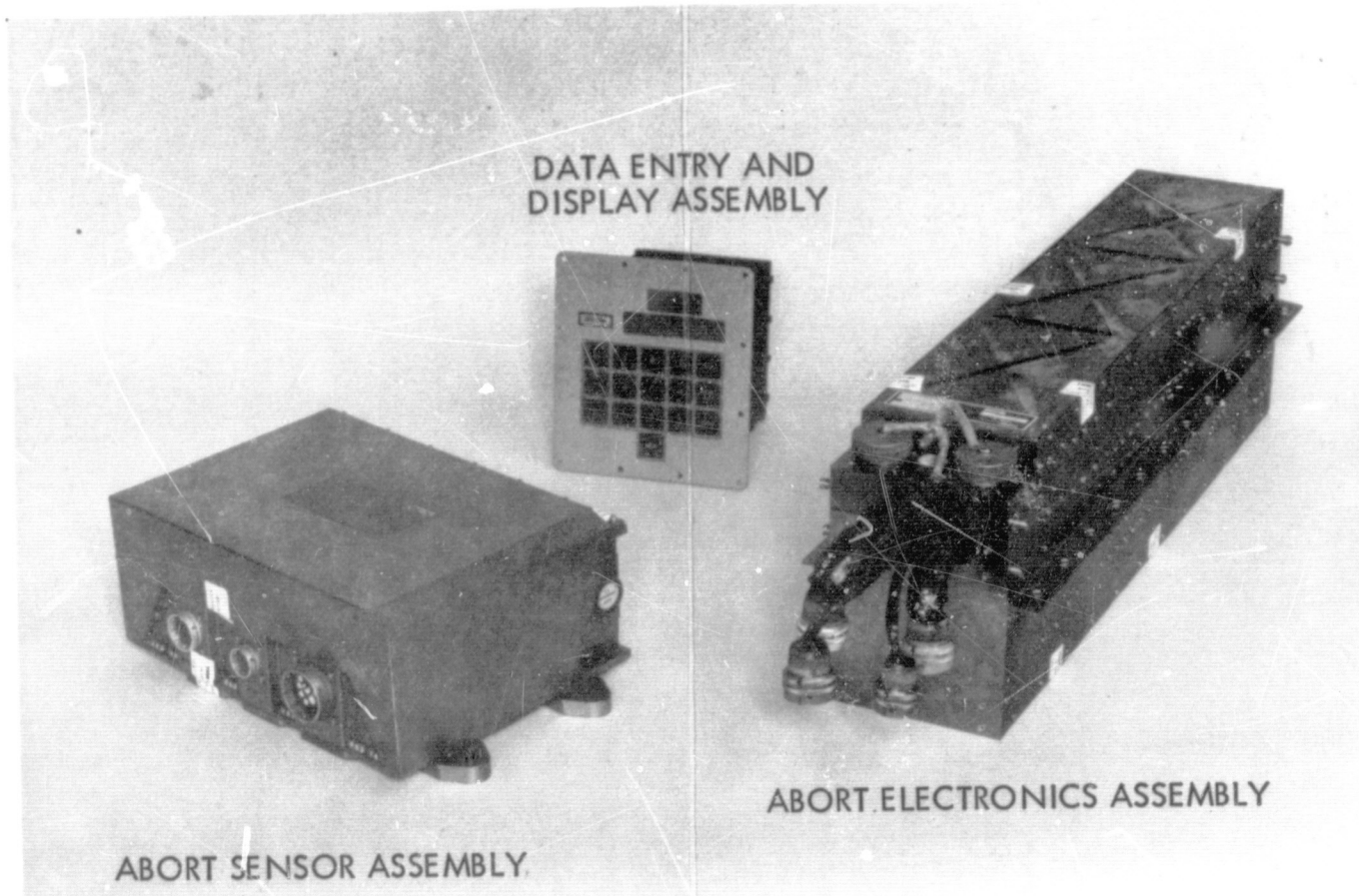
The Abort Sensor Assembly (ASA) consists of three strapdown, pendulous accelerometers; three strapdown gyros; and associated electronic circuitry. The ASA is located on the LM navigation base above the flight crew. The ASA provides incremental angular rotation information about the vehicle X, Y, and Z axes, and incremental velocity changes along the vehicle X, Y, and Z axes. These incremental data, in the form of pulses, are used in the Abort Electronics Assembly to maintain knowledge of attitude, position, and velocity of the LM vehicle.

#### 2.1.2 Abort Electronics Assembly

The Abort Electronics Assembly (AEA), located in the LM aft equipment compartment, is a general-purpose digital computer that solves the guidance and navigation problem. The computer includes a special-purpose input-output unit, its own power supply, and an internal clock. The AEA is a fixed-point, 18-bit machine with 17 magnitude bits and 1 sign bit, using 2's complement arithmetic. The AEA memory is of conventional ferrite-core construction with a 4096-word capacity. Half of this capacity, called the softwired memory, can be programmed electrically and operates read-restore. The other half, called the hardwired memory, is programmed at manufacture and operates read only.

#### 2.1.3 Data Entry and Display Assembly

The Data Entry and Display Assembly (DEDA) is a general-purpose, flight-crew, input-output device for the LM/AGS. The DEDA, located on the right-hand side of the cockpit, consists of a keyboard, electroluminescent address, and digital data displays. By means of this device, the flight crew selects the desired system mode, inserts the desired targeting parameters into the AEA, and monitors appropriate quantities throughout the mission. Selection of a system mode or insertion of data always requires the entry of three digits (the word address), followed by a plus (+) or minus (-), followed by the value to be inserted (which always consists of five digits). Read-out of any parameter requires the entry of three digits (the address of the desired word) followed by the pressing of the READOUT pushbutton.



13432-66

Figure 2-1. Abort Guidance System Assemblies

Table 2-1. General Characteristics of AGS Assemblies

ASA	AEA	DEDA
<ul style="list-style-type: none"> <li>• Three Body Mounted Norden RI-1139B Gyros</li> <li>• Three Kearfott 2401 Accelerometers</li> <li>• Dimensions - 9.00 x 11.50 x 5.12 in.</li> <li>• Weight - 20.7 lb</li> <li>• Power - 74 watts</li> <li>• Location - Navigation Base</li> </ul>	<ul style="list-style-type: none"> <li>• General Purpose, Parallel, Random Access, Ferrite Core Digital Computer</li> <li>• Memory Capacity - 4096 18-Bit Words 1/2 Fixed (Hardwired) 1/2 Temporary (Softwired)</li> <li>• Speed - 10 <math>\mu</math>sec add - 70 <math>\mu</math>sec multiply</li> <li>• Instructions - 27</li> <li>• Dimensions - 23.75 x 5.25 x 8.00 in.</li> <li>• Weight - 32.5 lb</li> <li>• Power - 12.5 watts (standby) - 91.0 watts (operate)</li> <li>• Location - Aft Equipment Bay</li> </ul>	<ul style="list-style-type: none"> <li>• Address and Data Displays</li> <li>• Clear, Readout, Hold, Enter Push Buttons</li> <li>• 12 Data and Sign Push Buttons</li> <li>• Limited Operator Error Detection and Indication</li> <li>• Dimensions - 5.50 x 6.00 x 5.19 in.</li> <li>• Weight - 8.4 lb</li> <li>• Power - 10 watts</li> <li>• Location - Right side of control panel, waist level</li> </ul>

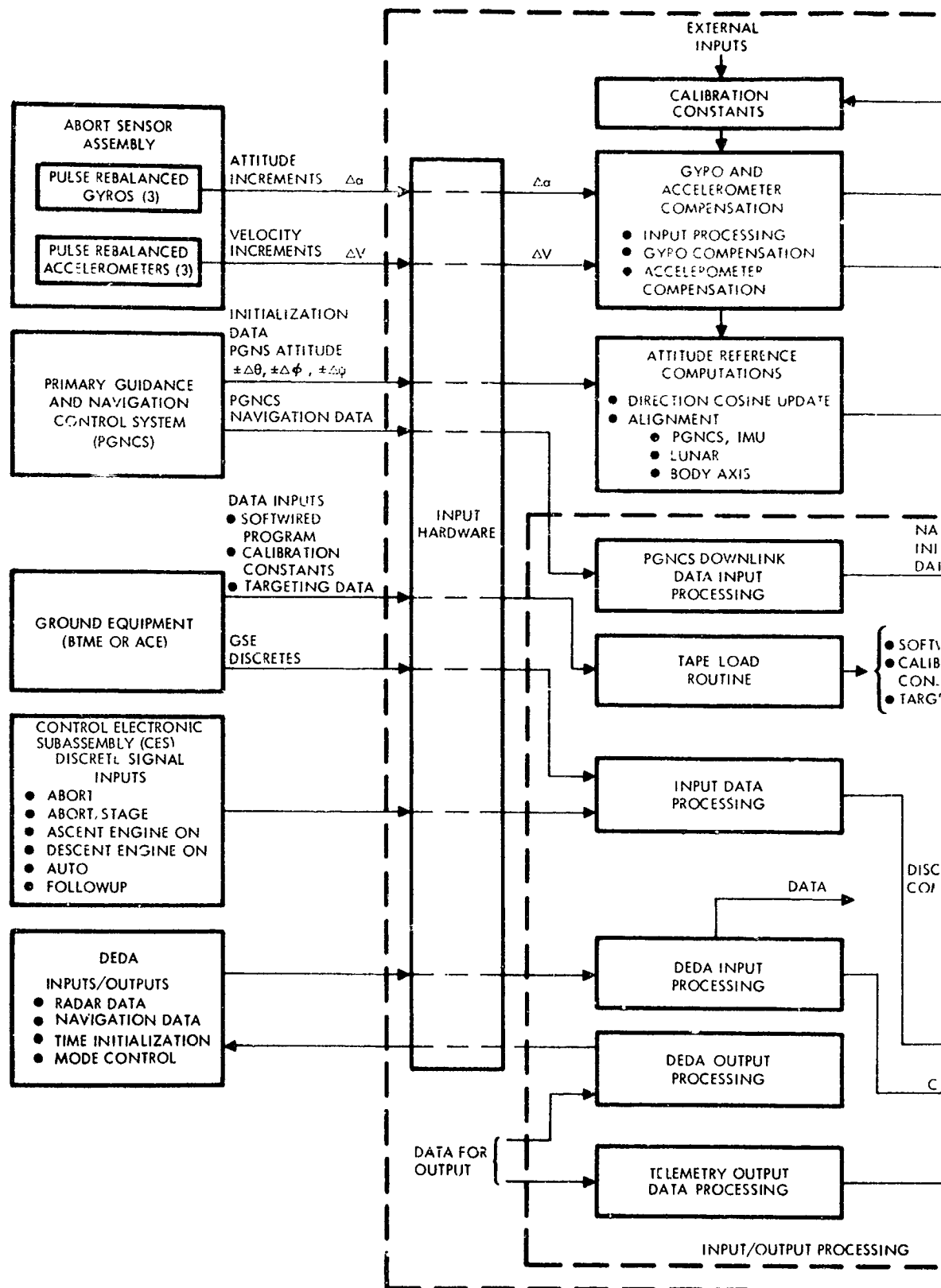
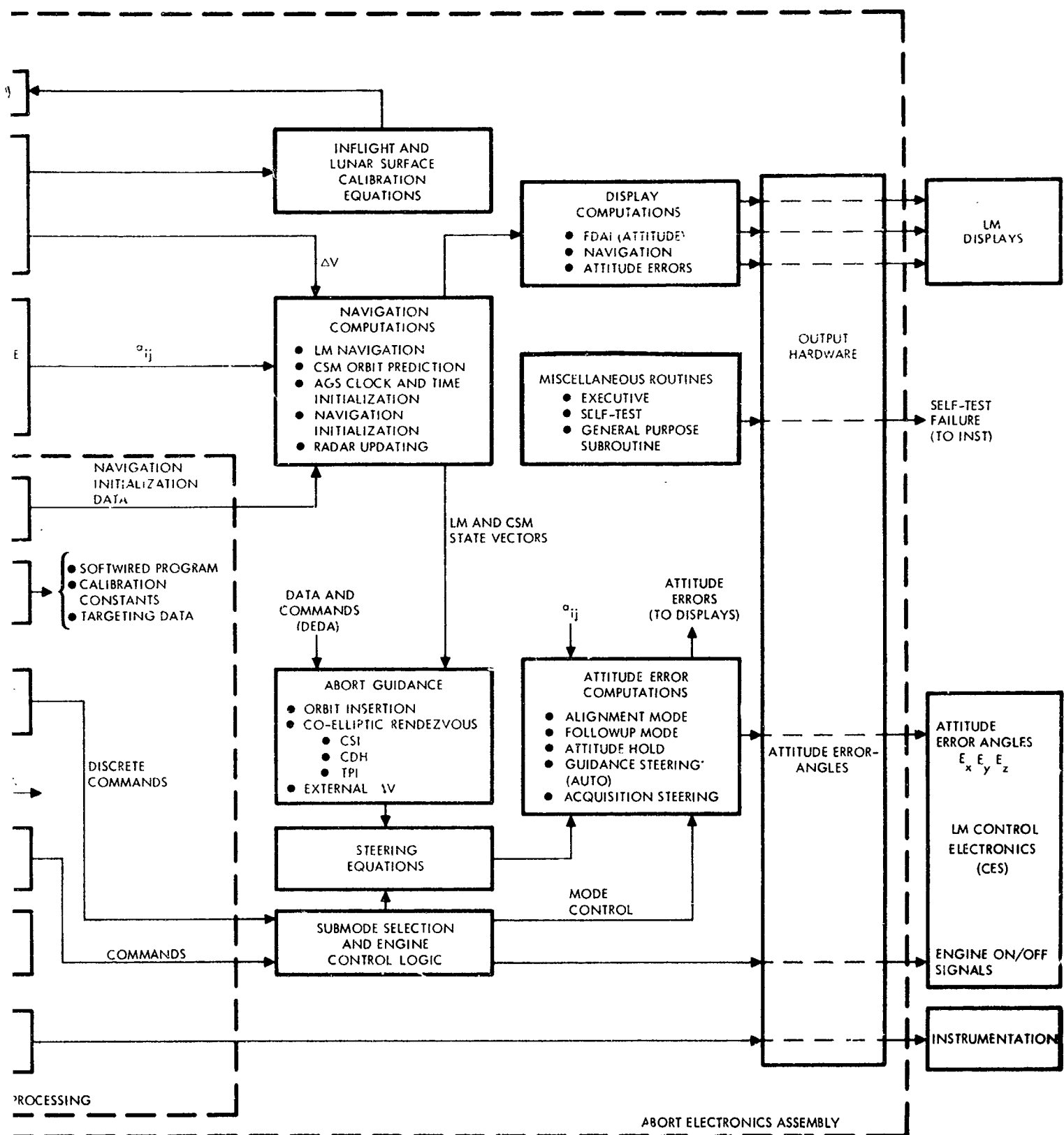


Figure 2-2. AGS Functional Block Diagram





## 2.2 OPERATIONAL CHARACTERISTICS

### 2.2.1 Lunar Module Mission

The mission for which the AGS is designed is the co-elliptic rendezvous of the LM with the Command Service Module (CSM), which provides abort initiation at any time after separation of the LM from the CSM. To illustrate the various maneuvers required and introduce some needed terminology, the flight profile following an abort on the lunar surface is discussed. (See Figure 2-3.)

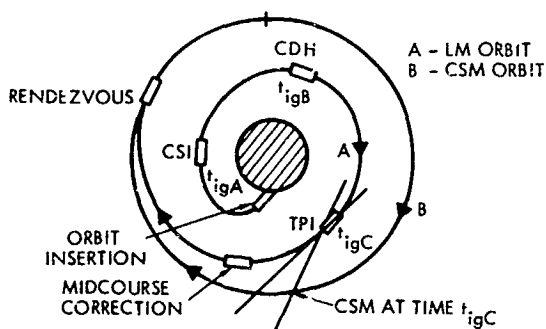


Figure 2-3. Co-Elliptic Rendezvous Flight Profile

The CSM travels in a circular orbit at an altitude of about 60 n. mi. The AGS is initialized prior to liftoff, and then controls the targeted orbit-insertion maneuver to drive the LM to a desired altitude, altitude rate, and horizontal velocity with a zero cross-plane velocity. The LM then coasts until absolute time,  $t_{igA}$ , which positions the LM at about  $90^\circ$  around the orbit from orbit insertion. At that point, the co-elliptic rendezvous flight profile begins with the co-elliptic sequence-initiate (CSI) maneuver. The magnitude of this CSI burn is determined by an iterative technique in which trial values of the horizontal burn magnitude are selected and a resultant error criterion evaluated. The error criterion is established such that, following the constant delta  $h$  (CDH) maneuver (see below) at a specified time ( $t_{igC}$ ), a desired relationship exists between the positions of the LM and CSM. Successive values of the CSI burn magnitudes are chosen to drive the error criterion

to zero. The co-elliptic (CDH) burn is performed at the predicted time of the LM orbit apofocus (or perifocus). The magnitude of this burn makes the LM orbit co-elliptic with the CSM orbit: i. e., the lines of apsides of the two orbits are aligned and, essentially, a constant differential altitude between the orbits exists. The terminal-phase initiate (TPI) burn is performed at the time the desired line-of-sight ( $\theta_{LOS}$ ) between the LM and CSM is achieved. The transfer time to rendezvous is specified, and the rendezvous point is the predicted position of the CSM at the specified time. An iteration is then performed to determine parameters of the transfer orbit, which passes from the present LM position to the rendezvous position in the specified time. Once the orbit is determined, the velocity impulse needed to achieve the desired trajectory is calculated. The midcourse maneuver is obtained in the same manner.

Aborts may occur any time after a separation of the LM from the CSM. The sequence of events followed after the abort depends upon the abort situation. That is, if the abort occurs when the LM is near the lunar surface, the above sequence of events would be desired. If the abort occurs when the LM is high above the lunar surface, it may be desirable to begin immediately with the co-elliptic sequence. Finally, there is always the possibility of transferring directly to rendezvous, which can be accomplished by utilizing the direct transfer modes (TPI) available. Built-in mission planning capabilities are available when these modes are employed.

### 2.2.2 Major LM/AGS Functions

The major functions of the LM/AGS during the lunar landing mission are as follows.

#### 2.2.2.1 Maintain Attitude Reference

The AEA accepts the strapdown gyro inputs from the ASA and updates the direction cosines between the LM body axes and the inertial reference system every 20 milliseconds.

#### 2.2.2.2 Perform CSM and LM Navigation

Navigation for both the CSM and LM is performed continuously, assuming that the motion is in a spherical gravitational field. The classical  $f$  and  $g$  closed form expression is used to navigate the CSM, while navigation of the LM is performed by integrating the equations of motion. State-vector initialization is provided by the PGNCSS or entered manually via the DEDA. The gravitational constant used for both vehicles is adjusted to account for aspherical harmonics for the particular mission under consideration.

#### 2.2.2.3 Solve Guidance Problems

The LM/AGS has five distinct guidance routines that can be used in any sequence. These routines and their functions are discussed in the following paragraphs.

Orbit Insertion. The orbit insertion guidance routine has been designed to drive the LM vehicle to a prescribed altitude above the lunar surface with specified values of altitude rate and horizontal velocity. In addition, steering in this mode is such that the LM is driven into the CSM orbit plane with an out-of-CSM-orbit-plane velocity component of zero at completion of the maneuver. The equations have been designed to maintain the derivatives of acceleration (radial and out-of-plane) constant. By limiting the allowable range of the acceleration rate, the desired turning rate of the LM is also limited. The effect is that as the velocity-to-be-gained decreases, the system concentrates more on attaining the targeted velocity conditions than on attaining the position conditions.

Co-Elliptic Sequence Initiate (CSI). The CSI guidance routine has been designed to compute the magnitude of a horizontal burn so that, following the co-elliptic maneuver (CDH), the desired line-of-sight between LM and CSM will be achieved at nominal TPI time.

Co-Elliptic or Constant Delta  $h$  (CDH). The CDH guidance routine computes the maneuver to place the LM in a

trajectory such that the differential altitude between the CSM and LM orbits is essentially constant.

Terminal Phase Initiate (TPI). The TPI maneuver begins the direct transfer to rendezvous. The direct transfer guidance routine solves the following problem: What trajectory passes between two specified points in a given time  $T$ ? LM/AGS solves this problem by an iteration technique in which the iteration variable is the semi-latus rectum,  $p$ , of the transfer orbit. With the trajectory that passes between the desired two points known, the appropriate maneuvers (two impulse maneuvers) are then computed.

External  $\Delta V$ . In order to increase mission flexibility, this guidance routine is available to perform earth-calculated maneuvers. The external  $\Delta V$  routine accepts components of a velocity-to-be-gained vector in local vertical coordinates input via the DEDA. At the time of maneuver initiation, the velocity-to-be-gained is established in inertial space and the maneuver completed. This guidance routine can also be used to orient the LM vehicle to any desired attitude in the local vertical coordinate system. In particular, the vehicle can be pitched at the orbital rate to keep the Z-body axis pointed toward the moon.

All guidance modes have been designed so that the maneuvers can be performed with main engine thrusting (along the +X-body axis) or the velocity-to-be-gained can be removed by successive thrusting along each of the three-body axes. This latter capability is particularly useful for small  $\Delta V$  maneuvers or to remove residual velocities after a major maneuver.

#### 2.2.2.4 Provide Steering Commands

The LM/AGS has three steering modes: attitude hold, guidance steering, and acquisition steering. These are described in the following paragraphs.

Attitude Hold. The AGS generates attitude error commands to cause the LM to maintain the same inertial attitude that existed when the attitude hold mode was entered.



Guidance Steering. The AGS generates attitude error commands to cause the LM to orient to the desired maneuver direction. This direction is a result of the selected guidance routine.

Acquisition Steering. The AGS generates attitude error commands to cause the LM Z-body axis to orient toward the AGS indicated position of the CSM.

#### 2.2.2.5 Provide Engine Commands

The AGS outputs an engine ON or engine OFF command, continually. If the primary system is being used, the command is merely a followup of the actual engine condition. If the AGS is in control, engine ON can be transmitted only after the appropriate switches have been set and the flight crew initiates the maneuver by creating ullage. At the appropriate time, as determined by velocity-to-be-gained, the engine OFF command is sent.

#### 2.2.2.6 Perform Onboard Radar Updating

The AGS contains a digital filter that uses radar angle information and accepts radar range and range-rate information for updating LM navigation. The recursive filter is simplified to the extent that the same weighting is used to update all position components and another weight is used to update all velocity components.

#### 2.2.2.7 Provide Automatic Alignment

Alignment of a strapdown system consists of establishment of the correct direction cosines that relate vehicle body axes to the desired inertial coordinate system. The three basic alignment modes of the AGS are described in the following paragraphs.

PGNCS to AGS Align Mode. In this mode, the initial AGS direction cosines are computed from the PGNCS Eulerian angles  $\theta_p$ ,  $\phi_p$ ,  $\psi_p$ . Thus, the AGS inertial reference frame is the same as the PGNCS stable member coordinate frame.

Lunar Align Mode. On the lunar surface, the lunar align mode is employed

to orient the AGS X-inertial axis vertically and Z-inertial axis in a pre-determined direction. The AGS accelerometers are used for sensing the local lunar vertical. Azimuth reference data is input via the DEDA prior to the lunar align. The desired direction cosines are computed from this information.

Body-Axis Align Mode. The body-axis align mode may be used either on the lunar surface or in orbit. This mode establishes the inertial coordinate system as that of the LM-body axes.

#### 2.2.2.8 Provide Gyro and Accelerometer Calibration

The AGS is capable of calibrating the accelerometer bias in flight and the gyro bias either in flight or on the lunar surface. Gyro calibration is performed using a constant gain filter and the accelerometers are calibrated using a time average filter.

#### 2.2.2.9 Drive Attitude and Navigation Displays

In addition to the functions already described, the AGS computes and outputs various display quantities.

#### 2.2.2.10 Provide Telemetry Data

Each second a block of 50 words is placed on the telemetry channel. To achieve high efficiency, many of the words change meaning when the guidance mode is changed.

### 2.3 PERFORMANCE CHARACTERISTICS

AGS performance is judged by its ability to perform the critical functions during the mission described in Paragraph 2.2. System performance criteria are summarized in Table 2-2.

The mission performance estimate for abort-from-hover with the AGS is given in Table 2-3. This estimate is based on the current AGS error model for the lunar mission and includes initialization errors from the PGNCS and final navigation update from the Manned Space Flight Network (MSFN)

Table 2-2. Specified Mission Performance Mission

Mission Performance Parameter	Specified Criteria
Pericynthian altitude Mean - $3\sigma$	>30,000 ft
Available fuel after orbital injection Mean + $3\sigma$	349 ft/sec max (design goal)

Table 2-3. Mission Performance Estimate for Abort from Hover

Mission Performance Parameter	Performance Estimate
Pericynthian altitude Mean	59,220 ft
Mean minus $3\sigma$	32,010 ft
Residual fuel required after injection Mean	176 ft/sec
Mean plus $3\sigma$	274 ft/sec

prior to the TPI maneuver. This is only one of many possible abort conditions. However, these performance characteristics are typical. The AGS error model on which the above mission performance estimates were made is described in Paragraph 1.2.2 of the Appendix.

In general, the coefficients used in the error model reflect the time stability of the coefficients over a period of 120 days, including the effects of numerous shut-downs and temperature cycling of the ASA between the extremes of +70°F and +160°F, as well as transportation handling effects. To

reduce the AGS errors further, computer software provides a capability for calibration and compensation of the gyro drift rates and accelerometer bias. Therefore, the principal errors result from the time instability of these coefficients for periods ranging from 3 to 120 days.

#### 2.4 ENVIRONMENTAL CONSIDERATIONS

The AGS system is required to operate as specified when subjected to the thermal and vibration environments described in the following paragraphs.

##### 2.4.1 Thermal Environment

The LM/ASA is designed to be operated continuously when the mounting flanges or pads are attached to cold plates that will maintain the root of the mounting flange between approximately 60° to 80°F during maximum average power dissipation. The corresponding temperature range is 35° to 120°F for the AEA. The DEDA is mounted directly to the instrument panel with no coolant requirement. Ambient environments can vary between 30° and 130°F either at sea-level pressure or in a vacuum of  $10^{-6}$  mm Hg or less. The effects of ambient variations and radiative heat inputs are minimized by a low-emissivity coating on the outside surface of the unit. To achieve a high reliability, the internal thermal paths are sized to obtain a maximum temperature of 160°F at the case of the resistors, capacitors, and semiconductors in the unit when the root of the flange is 130°F.

##### 2.4.2 Vibration Environment

The environmental requirements that most affect AGS performance are the vibrational conditions in which the inertial sensor package must operate. Figures 2-4 and 2-5 are graphic depictions of these vibrational environments. In addition, the AGS must meet its performance requirements after exposure to the sinusoidal and random vibrations specified in Figures 2-6 and 2-7.

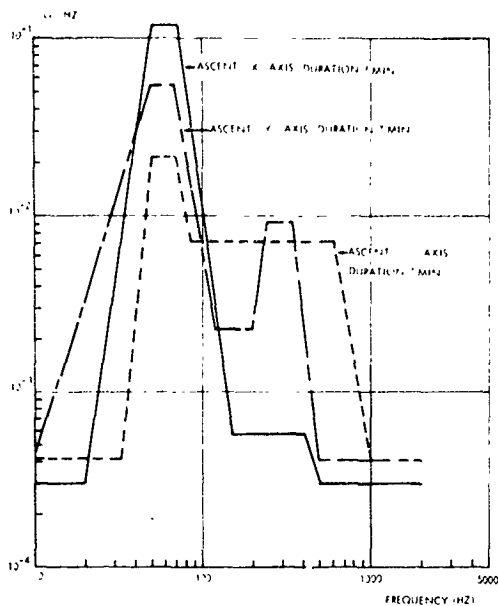


Figure 2-4. ASA Linear Vibration Requirement

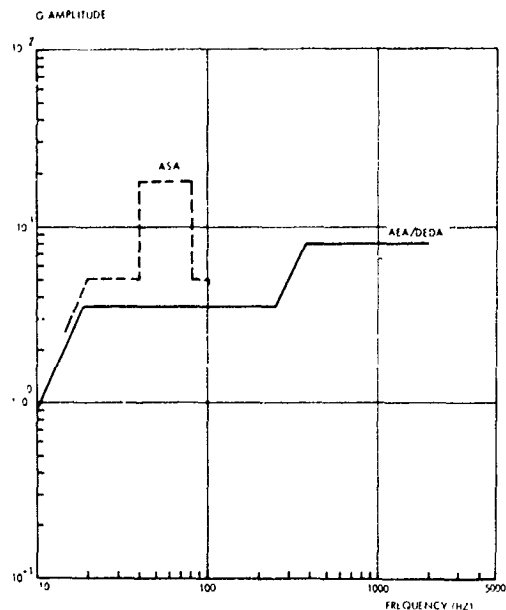


Figure 2-6. AGS Design Limit Sinusoidal Vibration

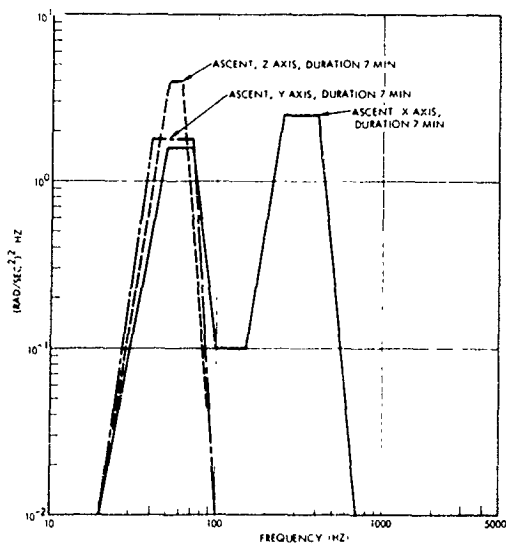


Figure 2-5. ASA Rotational Vibration Requirement

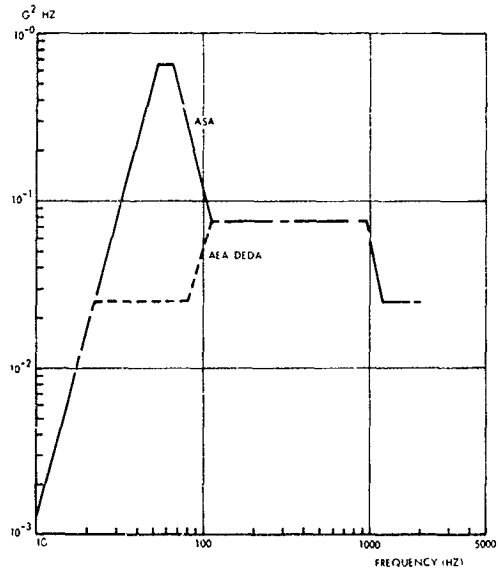


Figure 2-7. AGS Design Limit Random Vibration

### 3. HISTORICAL SUMMARY OF AGS DESIGN DEVELOPMENT

A brief development history of the overall system is contained in Subsection 3.1. In Subsection 3.2, a summary is given of the major design changes affecting the system as a whole, particularly changes in system functional and performance requirements, mission utilization, and vehicle interfaces. The design history of the various AGS subsystems and the system software are discussed in Subsections 3.3, 3.4, and 3.5.

#### 3.1 EARLY DESIGN DECISIONS

##### 3.1.1 Computer Concept

The initial system requirements presented by Grumman in the Request for Proposal (RFP) called for an attitude reference based on strapdown inertial instruments. Computing requirements were primarily those associated with computing and updating the direction cosine matrix relating a set of body-fixed coordinates to a set of inertial coordinates. During the initial proposal phases of the program, TRW considered meeting the computing requirements with a digital differential analyzer, containing about 300 to 400 integrators composed of integrated logic circuits and a hardwired core memory. Later in the proposal phase, it was determined that a general-purpose computer was the only approach that could meet all of the system specifications.

Based on the RFP requirements, 500 words of memory and 18-bit word length were determined as being adequate for the accuracy of the computations required. At that time, there were no requirements for variable mission

changes since the AGS was essentially an attitude reference system.

A major part of the proposal effort was directed toward keeping weight and power low. It was decided to use integrated circuits and hybrid, thin-film circuits wherever feasible and to utilize an extensive amount of hardwired core memory.

After the proposal was submitted, TRW continued design implementation of the specific technical approach taken. When the contract was awarded several months later, the design was well underway, at least in a conceptual and breadboard sense. But during the next few months, the computer grew due to major increases in system functional requirements and the memory now became 2000 words with a 500-word scratch pad. This required certain memory changes because the design was previously optimized for low power at a 500-word capacity.

##### 3.1.2 Sensor Assembly Concept

At initiation of the AGS program, TRW was directed to use the Abort Sensor Assembly concept under development by United Aircraft rather than the TRW design, and to subcontract with United Aircraft to supply this unit.

The initial design concept utilized three Norden RI-1139B gyros and three Bell Mod VII accelerometers, together with pulse-rebalance loops and an integral power supply, providing a self-contained sensor assembly. This unit is described in detail in Section 1 of the Appendix. In July 1968, the Bell VII accelerometers were replaced with Kearfott 2401 accelerometers.

### 3.2 MAJOR DESIGN CHANGES

#### 3.2.1 Modifications Caused by Changes in Functional Requirements

Table 3-1 summarizes major events in the history of AGS development.

The first major event occurred in February 1965 when the basic guidance scheme was changed from T-1 guid-

ance to rendezvous via either parking orbit or direct ascent. The T-1 guidance was a simplified abort guidance scheme providing only the orbit insertion guidance that had been developed by Grumman prior to initiation of the AGS development program.

Studies made by TRW in late 1964 showed that the T-1 guidance scheme was not sufficiently optimum with

Table 3-1. Major Events in AGS Development History

Date	Event
August 1964	Initial studies
October 1964	AGS full go-ahead
February 1965	Guidance requirements changed from T-1 guidance to rendezvous via parking orbit or direct ascent, AEA memory capacity increased to 4096 words. Data Entry and Display Assembly (DEDA) added to system.
July 1965	First hardwired memory (HO-1) program frozen*
January 1966	Rendezvous concept changed by NASA from direct ascent to co-elliptic
June 1966	Revised hardwired memory (HO-3) program frozen
August 1966	First AGS delivered
January 1967	TRW AGS software change control initiated
March 1967	First complete software package delivered: Design mission computer program (DMCP)
December 1967	First flight program delivered for operational usage (FP-2)
July 1968	Bell VII accelerometer replaced by Kearfott 2401
<p>*HO-1 was necessary to obtain a memory for the first production units to protect schedule and hence contained very little guidance information because its configuration had to be frozen at a very early date. HO-2 was considered to be the final version of the hardwired memory configuration. However, subsequent ICS testing indicated that the algorithm contribution to attitude drift rate under certain conditions was excessive. This was a scaling problem and was corrected by going to an HO-3 memory configuration.</p>	

regard to fuel consumption for abort guidance and could lead to mission failure due to fuel depletion. These studies also disclosed that the AGS suffered from severe operational limitations because there was no method of inserting data into the computer during the mission. TRW established that an "explicit guidance scheme" would be desirable and essentially required.

At this point in the program, the system concept had evolved from the initial concept of an attitude reference system plus simple programming functions into an actual guidance system. To implement the desired guidance system functions, it became necessary to provide an additional unit (DEDA) for use by the astronaut in communicating with the computer, and to increase the size of the memory from 2000 words (500 words of scratch pad) to a total of 4096 words with 2048 words of scratch pad and 2048 words of hardwired read-only memory. All of the computer design parameters that had been optimized over the preceding months were discarded and a completely new design was initiated. However, the basic circuit design concept and choice of parts remained the same.

Coincident with the changes in the memory capacity and the addition of the DEDA, several other changes in the AGS functional requirements were made by Grumman, resulting in substantial redesign of the AEA hardware. The primary changes were the addition of input/output channels to provide the capability of transferring navigation data from the PGNCs computer to the AEA via the PGNCs telemetry downlink channel, and to provide the capability of driving LM displays. AEA output channels were provided to drive the LM Flight Director Attitude Indicator (FDAI) and tape meters to display attitude, altitude, and altitude rate.

These memory and input/output changes required redesign of the AEA power supply. At the same time a requirement was added to provide the capability of accumulating input data during the computer warm-up mode. This necessitated separating the power supply into two parts.

### 3. 2. 2 Modifications Caused by Changes in Mission Requirements

The mission requirements on the initial explicit guidance scheme chosen to replace the T-1 guidance in February 1965 were that:

1. Pericynthian altitude be above 5 n. mi. after injection into orbit.
2.  $\Delta V$  expenditure be within a given constraint.
3. The AGS deliver the LM within 5 n. mi. of the Command/Service Module (CSM) with a navigation velocity error less than 30 ft/sec.

In early 1965 the constraint of minimum fuel or minimum time to rendezvous was added to the previous requirements. Within these constraints TRW was free to define the abort rendezvous mission in a manner that minimized the effects of errors inherent in the AGS. At this point of time TRW chose a direct-ascent rendezvous concept because of the apparent simplicity of the mission and the minimal amount of time expended in transit from the abort to the point of rendezvous (less than one orbital revolution).

Three maneuvers were employed. The first placed the LM on an intercept trajectory with the CSM. The coast orbit pericynthian was constrained above 5 n. mi. The point of intercept was selected by the guidance computer (AEA) to minimize the propellant expenditure. For the coast orbit, rendezvous radar data was inserted manually into the AEA via the DEDA to update the relative position and velocity of the LM with respect to the CSM.

At ranges of typically 30 to 40 n. mi., the second maneuver (a midcourse correction) was performed to account for guidance errors of the previous maneuver. The LM was again placed on an intercept trajectory with the CSM. The intercept point was either the originally chosen point or a new rendezvous point with a location that minimized subsequent propellant expenditure.

The final maneuver was the braking maneuver. Although not required by specification, the AGS had the capability of synchronizing the LM orbit with the CSM orbit during this maneuver at the point of closest approach.

Software required to perform the above mission was successfully designed and simulated. Aborts could be performed from any point of powered descent (LM landing phase) and powered ascent (lift-off from the lunar surface) trajectories. In the event of an "any-time" lift-off from the lunar surface (lift-off not within the direct ascent launch window), the AGS would automatically place the LM in a low, safe-parking orbit.

A second major event occurred in January 1966 when NASA/MSO promulgated a new rendezvous concept termed co-elliptic rendezvous. The rendezvous mission resulted from experience gained from the Gemini program, and represented a consensus of the flight crew and flight operations. The co-elliptic flight plan essentially placed the LM in a parking orbit after orbit insertion. A phasing maneuver was then performed so that the LM would achieve a prescribed relative position with the CSM at a prescribed location in space. From here, the LM would perform direct transfer maneuvers through a prescribed central angle to the point of rendezvous. The term "co-elliptic" was coined from a phase of the mission where the LM and CSM elliptical orbits are essentially concentric with semi-major axes aligned.

The change in mission concept had a major impact on the guidance software. Software designed to implement the co-elliptic rendezvous concept was successfully designed and simulated during 1966. In January 1967 the first complete AGS software package incorporating the new mission concept was delivered to NASA.

### 3.3 HISTORICAL SUMMARY OF DESIGN DEVELOPMENT OF THE ABORT SENSOR ASSEMBLY

#### 3.3.1 Early History

In 1959, United Aircraft began a company-sponsored development effort on strapdown guidance system techniques from which a design for a pulse-torque amplifier evolved. The amplifier was tested with a Norden RI-203 integrating gyro in 1960. A Mod X system, fabricated in 1961, combined pulse-torque amplifiers with timing circuits, temperature control amplifiers, a power supply system, Norden gyros, and Bell accelerometers. This unit was tested during 1961 and 1962, and favorable results led to the fabrication of a prototype sensor package (Mod I) in 1963 that utilized improved pulse-torque servoamplifiers (PTSA) and RI-1139X Norden gyros. Subsequently, a third generation inertial package (Mod II) was fabricated and extensively tested in 1963 and 1964 prior to the start of the UACSC LM/ASA Program.

#### 3.3.2 Design Concepts at Program Start

The conceptual design of the ASA existing during the proposal and negotiation effort that occurred between the summer of 1964 and November 1964 was similar to the final ASA design. The original conceptual design consisted of:

1. Three Norden RI-1139 gyros and their associated pulse-torque servoamplifiers.
2. One Bell VII thrust-axis accelerometer and PTSA.
3. Two Honeywell GG-116 cross-axis accelerometers and PTSA's.
4. A common power supply for the entire ASA.



5. A frequency countdown sub-assembly to convert the basic clock input to all those output signals with frequencies necessary for the operation of the power supply and the instrument/PTSA loops.
6. A fine temperature controller with associated heaters to maintain the block at 120° F using the concept of single-point temperature control.
7. A fast warm-up controller with associated heaters to provide additional power at turn-on in order to bring the block from ambient conditions to operating temperature as rapidly as possible.
8. A beryllium block on which the instruments and electronics are mounted, plus the associated suspension assembly, cover, etc.

Just prior to the program start in October 1964, a decision was made to make the three accelerometer channels identical. The two Honeywell GG-116 cross-axis accelerometers were dropped and three Bell VII accelerometers per ASA were used instead.

The proposed configuration of instruments and electronic subassemblies on the block was considerably different from that which evolved for the production ASA. This, however, was more a difference in design detail than in concept.

### 3.3.3 Outline of Design Evaluation

Aside from meetings, documentation, and the continuous monitoring of the vendor's design progress, three formal Design Reviews were conducted during the program (with corresponding Design Reports): the Conceptual, Preproduction, and Production Design Reviews.

The Conceptual Design Review was held in January 1965, two months after the program start, to review the design concepts in more detail than had been possible during the proposal and negotiation periods.

The Preproduction Design Review was held in August 1965 to review the design detail of the preproduction model ASA's. The preproduction design encompassed the first four ASA's. At this Design Review it was known that certain changes would be incorporated in the forthcoming production design.

The Production Design Review was held in April 1966 to review the final ASA design in depth. Approximately fifty Action Items resulted that had to be satisfied prior to design approval. These action items included additional analyses and hardware changes required from the vendor and specification clarification and/or relief required from the customer.

### 3.3.4 Chronological Outline of Design Changes, Problems, and Solutions

Table 3-2 gives a chronological history of the major ASA problems and changes in requirements, and the design changes or other solutions incorporated as a result. This history is somewhat subjective in the determination of those items considered to be major. However, the list does bring out those items which may prove beneficial to the development of future guidance systems and summarizes the problems and solutions.

After the production design was frozen, data provided from vehicle testing showed that the environment as originally specified was incorrect. The change in the environmental specifications did not require hardware changes, but did affect the assessment of inertial performance when the ASA was subjected to the new environments. Analyses and tests were performed to

Table 3-2. Chronological Summary of Major ASA Design Problems and Changes

Item No.	Date (approx.)	Problem/Change in Requirements	Solution
1	Jan '65	Customer directed change from Bell VII accelerometer to Bell III accelerometer.	Several mechanical design iterations evolved throughout the first several months of the program. Primary goal was optimum location of inertial instruments and major electronic subassemblies (e.g., power supply and PTSA's) to meet constraints of weight, envelope dimensions, mounting-hole dimensions, and thermal performance. A significant design iteration was the double change from Bell VII to Bell III and back to the Bell VII, in an attempt to meet reliability and weight requirements. The first change from the Bell VII to the Bell III was made to increase the ASA reliability by using the well-proven Bell III accelerometers. After extensive tradeoff studies, it was necessary to return to the smaller Bell VII instrument to meet the size and weight constraints.  In addition, specification relief on weight (from 17.0 to 20.7 pounds) and envelope dimensions was required to arrive at an acceptable final design. The basic configuration of the first ASA (001X, delivered 12-65) has been maintained throughout the program.
2	Mar 1965	Customer directed change from Bell III accelerometer to Bell VII accelerometer.	
3	Jan 1965	Misunderstanding on mounting feet and cover dimensional requirements in customer specification.	
4	Feb 1965	Customer required method of monitoring gyro wheel speed.	Spin-motor rotation detector (SMRD) incorporated in gyro design by adding platinum cobalt slugs in gyro wheel. Pickoff coil generates a pulse for each wheel revolution; SMRD amplifier for each gyro incorporated in interface electronics to amplify signal for external use.
5	Feb 1965	Application of the proposed RI-1139A gyro for ASA requirements and manufacturing difficulties.	There were several design changes in the RI-1139A gyro. In addition to SMRD (Item 3), minor changes included: longer torquer for increased torquer scale factor, change from beryllia to beryllium torquer frame because of potting difficulties, improved technique for output axis alignment, thermistor relocation, and improved magnetic shield at the bellows end.

Table 3-2. Chronological Summary of Major ASA Design Problems and Changes (Continued)

Item No.	Date (approx.)	Problem/Change in Requirements	Solution
6	Aug 1965	To prevent power supply failure by inadvertent shorting of voltage lines used throughout the ASA. Of particular importance when an ASA is operating with the cover removed during integration or maintenance periods. ASA specification also requires this protection.	Power supply overcurrent protection circuitry was incorporated so the power supply would turn off if excessive current was drawn from the generated secondary d-c and a-c voltage supplies.
7	Oct 1965	General electronic noise problem within the ASA became apparent with integration of first ASA. Inertial performance changed between having test connector outputs capped versus having them connected to test set. Noise problems were present throughout ASA development.	No single design change was found to eliminate noise problems despite extensive and continuing investigations. Changes found to help were: elimination of ground loops with the test set connected, rerouting of sensitive internal leads (e.g., rerouting raw power lines from interface electronics to the power supply through the block away from the PTSA's), tightly twisting instrument torquer leads instead of using shielded cable, using Netic-Conetic shields between PTSA's and the power supply, and internally connecting secondary power ground to chassis ground (required specification relief).
8	Oct 1965	Problems resulted from the lack of interface electronics definition between the ASA and interfacing electronics relative to the basic input and output characteristics and tolerances (including effect of cable between ASA and AEA), test points to be monitored (including characteristics, tolerances, and load impedances), and the type of connectors to be used.	To meet the program schedule requirements, it was necessary to proceed with the hardware design, even though the interface definition was incomplete. Meetings were held and analyses prepared to arrive at a mutually agreeable interface definition. Problems were resolved where possible by specification changes so as to minimize the impact on the hardware design.

Table 3-2. Chronological Summary of Major ASA Design Problems and Changes (Continued)

Item No.	Date (approx.)	Problem/Change in Requirements	Solution
9	Dec 1965	The first ASA (001X) had inter-connecting internal harnessing that employed flexible multi-layer printed circuit cable, primarily because of weight and volume limitations of conventional wiring. This method required more volume than originally anticipated, had an unsatisfactory appearance since it would not stay molded around corners, and was impractical from the standpoint of accommodating design changes which occur frequently during the development phases of a program.	A design change was immediately implemented. The second ASA used conventional point-to-point stranded wiring (or co-ax) with tied bundles.
10	Feb 1966	The ASA power supply is located between the main housing and the heat sink on both preproduction and production designs. The preproduction power supply was potted in BeOSil, a thermal-conducting compound, that allowed heat to permeate through the compound from the main housing and the power supply itself to the heat sink surface. However, the thermal conductivity of BeOSil was not as high as anticipated and a weight penalty was incurred when the relatively dense BeOSil was used as a potting compound.	The production power supply was designed such that all significant heat producing components and modules were heat sunk directly to the cold plate side of the power supply housing. A more conventional (less dense) potting compound could therefore be used, resulting in a significant weight reduction. Heat from the main housing was routed by two studs through the power supply to the cold plate (heat sink) surface. These studs incorporated adjustable slugs by which the thermal path between the main housing and cold plate could be varied. Thus, the capability of trimming total power consumption after ASA assembly was gained.

Table 3-2. Chronological Summary of Major ASA Design Problems and Changes (Continued)

11	Feb 1966	<p>The preproduction suspension system (feet) met the specified vibration requirements. However, long exposure to the environment resulted in fatigue failures. An additional difficulty was experienced in manufacturing. Each pair of preproduction feet was an integral unit at either end of the housing. Each individual foot contained a Mycalex ring to serve as a thermal barrier. Difficulty in machining the Mycalex was encountered.</p>	<p>An individual suspension system was incorporated for the production design. Each foot was attached to the block with a small enough thermal path to preclude the need for Mycalex. The body of each foot (titanium) was hollowed out and an aluminum slug covered with an elastomer was inserted to provide damping and prevent exceeding the resonance requirements of the specification.</p>
12	Feb 1966	<p>The preproduction cover that served as the support member for the three connectors was undesirable structurally and was difficult and time consuming to remove when maintenance and development problems occurred.</p>	<p>A separate structural member was designed to support the connectors. The cover was redesigned to accommodate this change as well as power supply and suspension system changes.</p>
13	Feb 1966	<p>Accelerometer scale factor temperature sensitivity was higher than could be tolerated to meet inertial performance requirements.</p>	<p>Temperature compensation was incorporated in the Bell VII accelerometer design employing a scheme previously used on other versions of this accelerometer.</p>
14	Feb 1966	<p>The preproduction electronics subassemblies (particularly PTSA's) were susceptible to broken internal solder joints. Also, other design aspects could be improved for production subassemblies.</p>	<p>Welded internal connections were used throughout the production subassemblies. A general repackaging of the individual subassemblies reduced weight, provided better heat sinking for critical components, and accommodated some components different from those used in the preproduction design.</p>

Table 3-2. Chronological Summary of Major ASA Design Problems and Changes (Continued)

Item No.	Date (approx.)	Problem/Change in Requirements	Solution
15	Mar 1966	A potential thermal runaway condition existed when the sensing thermistor controlling the fast warm-up opened or the trim resistor shorted. This condition could endanger other equipment on the LM adjacent to the ASA.	A normally closed thermostat set to open at 150° F was incorporated in series with the +12-v CAUTION and WARNING output signal. The ASA is manually turned off if the display indicates a malfunction on this line.
16	Apr 1966	The accelerometer bias was found to have an excessively long warm-up time, (as much as several hundred micro-g's) and several hour's time between initial and steady-state condition. The long warm-up was caused by: (1) an electrostatic charge build-up between the capacitor plates and torquer coil on the pendulum when the torquer coil potential was 16 volts above ground, and (2) a change in resulting electrostatic forces on the pendulum as the charge leaked off with time.	The problem was solved by adjusting the accelerometer electrical null for minimum shift in bias between the torquer at ground potential and at +16 volts. An alternative solution was the installation of bleeder resistors to accelerate leakage of the charge. However, schedule and cost limitations precluded use of these resistors at the time.
17	Aug 1966	The elastomer used in the production foot design (Item 11) deteriorated when subjected to extended periods of vibration such that exceedingly high resonances resulted.	Several other materials were tested for damping efficiency when inserted in the foot instead of the aluminum slug and elastomer. Although analysis indicated otherwise, a solid titanium foot did provide adequate damping and was much less difficult to manufacture.

Table 3-2. Chronological Summary of Major ASA Design Problems and Changes (Continued)

Item No.	Date (approx.)	Problem/Change in Requirements	Solution
18	Oct 1966	It was difficult to manufacture the cover that was built from the inside-out, so that the inner skin was made first, then honeycomb core material was bonded to it, and finally the outer skin was bonded to the honeycomb in sections.	Although a manufacturer was found who could produce single-piece outer aluminum skins to allow "outside-in" construction, the honeycomb core material was replaced with polyurethane foam to circumvent manufacturing problems.
19	Jan 1967	Under certain vibration and thermal-vacuum conditions, pins from the electronic sub-assemblies shorted to the inner aluminum skin of the cover by puncturing an insulating G-10 fiber-glass board. This was caused by a buildup of tolerances during assembly.	The inner aluminum skin was removed and replaced with G-10 fiber glass. The thermal effects of this change were negligible, and analysis showed that the effect on EMF radiation and susceptibility was acceptable.
20	Feb 1967	During the ASA qualification test the foam-core material of the cover was not strong enough to support itself under extended vibration and separated at the bond line.	A change was made from foam cores back to honeycomb cores and the manufacturing difficulties of Item 18 were overcome.
21	Mar 1967	Gyro output (bias, mass unbalance, or both) changed by as much as 0.7 deg/hr when the ASA was subjected to thermal/vacuum tests. The shift usually occurred when the vacuum was applied rather than when ambient temperatures changed.	Under the assumption that this problem was thermal, the gyro bores were enlarged to increase the gap between the gyro snoot and the ASA housing, and thereby minimize changes in heat flow from the gyro to the housing between ambient and vacuum conditions. When this action did not cure the problem, a thin layer of Wakefield thermal compound was applied to the gyro mounting seats. After a few iterations on proper thickness and method of application, the problem appeared to be solved. Maximum shifts of



Table 3-2. Chronological Summary of Major ASA Design Problems and Changes (Continued)

Item No.	Date (approx.)	Problem/Change in Requirements	Solution
21 (cont)			0.3 deg/hr are still observed occasionally, but these are acceptable from a mission standpoint.
22	Mar 1967	For a year or more prior to this time, investigation and testing were being performed to isolate an apparent sensitivity of gyro mass unbalance to storage position. Shifts of as much as 2 deg/hr/g were observed, particularly on earlier production gyros.	These mass unbalance shifts were postulated to be a result of fluid settling in which the more dense particles migrated with the gravitational field under extended periods of storage. The shifts were asymptotic and would become relatively stable. At the ASA level the solution was to always maintain the ASA in its launch-pad orientation (+X axis up) during nonoperating periods. The ASA shipping container, which is frequently used for storage, was modified to contain the ASA with +X axis up instead of +Z axis up, as had been the case previously. At the gyro level, the gyros were pre-assigned to a specific ASA axis and were stored in the corresponding position prior to mass unbalance trim. Subsequent to gyro acceptance they were maintained in this preferred orientation until installation in an ASA.
23	May 1967	The first of four gyros had extremely erratic output (as much as 25 deg/hr). When torn down, three of these were found to have particulate contamination (a fiber, a hair, and a carbonaceous particle) in the fluid. All these gyros had been installed in ASA's, had passed acceptance testing, and had been operating in the field for considerable time.	The three gyros torn down were all early production, nonflight units that were built in the midst of extensive changes and improvements to the gyro vendor's clean room and quality control processes and procedures.
24	July 1967	Accelerometer channel bias was the most erratic of all inertial performance parameters as observed for several	This problem is still under investigation. The mechanism causing the bias shifts is not presently known although it appears to be in the spring or epoxy joints that support the accelerometer pendulum. Initial

Table 3-2. Chronological Summary of Major ASA Design Problems and Changes (Continued)

Item No.	Date (approx.)	Problem/Change in Requirements	Solution
24 (cont)		months on all production ASA's. After an extended period of testing, a simple method for separating accelerometer bias from PTSA bias was found double polarity reversal at torquer and PTSA demodulator. The bias shifts were definitely attributed to the accelerometer, and single channel tests (accelerometer plus PTSA) subsequently showed these shifts to correlate with pendulum storage when the accelerometer was turned off. Peak-to-peak shifts of 600 micro-g's resulted when storage was alternated between 1A up and 1A down over 4 to 5 day intervals and when the storage temperature was 150° F. When storage was 120° F (normal ASA operating temperature), the peak-to-peak shifts were limited to less than 200 micro-g's with much longer time constants.	corrective action was taken to reduce the temperature of the shipping container (used extensively for storage in the field) from 145° F to 120° F in accordance with the results obtained from the single-channel tests.
25	Aug 1967	The first of several accelerometers had the pendulum stuck against the capacitor plates such that the full loop capability (3 g's) would not free it. At least three additional accelerometers failed such that the loop would not close, in most	When several accelerometers were torn down, different contaminants were found on the brass plates. The specific contaminant causing the situation has not been ascertained. An intensive review of materials used and of the manufacturing processes and procedures has been undertaken, however, and extensive changes have been incorporated. Most of the original accelerometers have been returned to the vendor for

Table 3-2. Chronological Summary of Major ASA Design Problems and Changes (Continued)

Item No.	Date (approx.)	Problem/Change in Requirements	Solution
25 (cont)		cases in ASA's that had been operating in the field for over a year. In subsequent tests, a large percentage of all accelerometers showed various degrees of sticking when tested by an open-loop method. A significant point is that the problem would probably never have been detected at the ASA level if the few accelerometers had not exceeded a sticking level of 3 g's.	rework.  The new materials, processes, and procedures did not eliminate the problem and in April 1968 a parallel configuration utilizing the Kearfott 2401 accelerometer was investigated. The results were so good that in July 1968 the decision was made to replace the Bell accelerometers with the Kearfott type.
26	Oct 1967	Gyro-scale-factor asymmetry of greater than 500 ppm for input rates at $\pm 3$ deg/sec was observed on most production ASA's. When it was realized that large dynamic errors (above mission requirements) would result during rotational vibration, an extensive test program was undertaken.	The digital outputs from the ASA should yield a precise measure of the current-time product of the current being fed back through the torquers, under the assumptions that the current level is constant and the digital pulses are equally spaced. However, the current level (1-kHz square wave with zero input) was found to have synchronous 8-kHz (used for d-c supplies, instrument excitation, and demodulators) noise. Further, the data pulses were not equally spaced because of the sensitivity of the single-shot multivibrator pulsewidth to noise on the +4-vdc line. This noise was generated at the data output transformers and, therefore, was also synchronous with the 1-kHz limit cycle. The solution was the incorporation of a new module to change the 8-kHz frequency to 8.258 kHz, which allows the noise effects to be averaged out over any sampling time of more than a few milliseconds. This module also eliminates the need for the single-shot multivibrator.

demonstrate that the ASA could perform successfully within these environments as designed.

At the outset of the program, a testing program was initiated, consistent with the program schedule and budget constraints. It was recognized at the time that the development risk was high. In retrospect, it appears that the program risk (and subsequent design changes) could have been substantially reduced by more extensive testing earlier in the program.

### 3.4 HISTORICAL SUMMARY OF DESIGN DEVELOPMENT OF THE COMPUTER SUBSYSTEMS (AEA AND DEDA)

#### 3.4.1 Early Design Decisions

During the proposal phase of this program, TRW initially decided that the technical approach toward solution of the problem would center about a digital differential analyzer. The analyzer was to contain about 300 to 400 integrators composed of integrated logic circuits and a hardwired core memory. Later in the proposal phase, TRW determined that a general-purpose computer was the only approach that could meet all of the system specifications.

TRW then decided to design a general-purpose computer based on technology evolved during in-house research and development programs. The computer is considered general purpose in the sense that it is capable of adding, subtracting, multiplying, etc., under program control. But this computer is actually special purpose because it was designed especially to solve the LM problem.

The sizing of the computer (speed, instruction repertoire, words of memory, word length, etc.) was based on software studies utilizing the Hypocomp Program. Hypocomp is a high-speed, interpretive, computer simulation that employs a subset of IBM 7094 orders usually found in airborne digital computers.

Initial estimates of memory capacity were about 500 words. An 18-bit word length was determined to be adequate for the accuracy of the computations required. At that time, there were no requirements for variable mission changes because the system under discussion was not truly a guidance system but rather an attitude reference system.

A major part of the proposal effort was devoted to keeping weight and power low. With respect to weight, it was decided to use integrated circuits and hybrid thin-film circuits wherever feasible. With respect to power, it appeared that the core memory should have an extensive number of hardwired, read-only words. Because the memory power is largely dependent upon the amount of scratch pad accessed, most of the power is dissipated in the Z-axis drivers during the rewrite cycle.

Because of the dynamic changes in semiconductor technology, it was decided to use the newest and most reliable components available. Some of the newer parts had not been fully qualified, and hence, were not carried on the TRW standard preferred parts list. This decision was to cause some difficulty during the design phase of the program because, simultaneously, components were being characterized, parameters were being agreed upon with vendors, and circuit design was being generated. In some cases, component specification negotiations with vendors made circuit redesign necessary.

DTL integrated circuit logic was selected at this time. This selection was based on the circuits having high-noise rejection, compatibility with functional and speed requirements, multiple sources, a history of satisfactory performance, and an established reliability.

After its proposal was submitted, TRW continued design implementation of the specific technical approach taken. When the contract was awarded several months later, TRW was well along in the design, at least in a con-

ceptual and breadboard sense. But during the next few months, the computer grew because of increased functional requirements, and the memory became 2000 words with a 500-word scratch pad. This required certain memory changes because the design was previously optimized for low power at a 500-word capacity.

During the ensuing three or four months, it was established that the guidance scheme (the system had now evolved into an actual guidance system as well as just an attitude reference system) was not sufficiently optimum from a fuel consumption point of view for abort guidance and rendezvous. An "explicit guidance scheme" was desirable and essentially required. To implement the explicit guidance scheme and to provide the necessary mission flexibility, it became necessary to add an input-output device (DEDA) to permit the astronaut to control the operating modes of the program and to read and enter data during the mission. In addition, it was necessary to increase the memory capacity to 4096 words with 2048 words of scratch pad and 2048 words of hardwired, read-only memory. All the design parameters that had been optimized over the preceding 4 months were discarded, and a completely new design was required. However, the basic design concept, the cores, the type of drive, and the type of sensing remained the same.

Because the requirements and capabilities of the computer expanded significantly during the early months of the program, two packaging design decisions were made. First, it was decided to abandon the cordwood module concept because the component part temperature requirement would compromise the weight and would also result in a subdivision of the unit into many small cubes. The complexity of the unit and the profusion of small parts were inappropriate to application of the cordwood technique (except in the power supply section with its large discrete components). Instead, it was decided to use the planar approach, much as though the computer consisted of a number of functional

slices. This method proved so practical that it has been generally adopted for most new designs. The planar approach reduces the levels of packaging to three: (1) parts and devices, (2) module circuit boards, and (3) interconnection matrix. Three packaging levels are the lowest practical minimum for equipment of this complexity. Studies showed that the addition of packaging levels between the first and second levels, in general, represents merely added connections, cost, and weight, without any noticeable improvement of other design factors.

The second basic decision stemmed from an apprehension of the third level package, the unit interconnection matrix. Experience and intuition indicated that this package, although undefined at the time, would be complex. Moreover, this package would be defined and designed last, thus allowing no time for major design change to correct any erroneous early judgments. Therefore, it was decided to lodge as much complexity as possible in the second level packages, and, where possible, even in the first level packages.

This decision led to the design of many complex multilayer circuit boards and some complex hybrid thin-film circuits. For instance, the judgment of the memory designers was that the memory should have its own interconnect matrix with logic interface signals on a connector. This would enable simplified testing by making the memory a true subassembly. But this proposal was rejected, mainly because of weight considerations. The memory designers then elected to run only logic signals in the matrix and to hardwire non-logic signals between boards within the memory subassembly.

The complexity of the circuit boards has been questioned in design reviews, but it is important to note that the packaging design did not create complexity. A fundamental level of complexity is established by the performance and reliability requirements, which in turn are achieved by the circuit design. In this case, complexity

was allowed at the first and second levels to prevent too great a complexity buildup in the third level. The use of the multilayer boards was compatible with electrical considerations. Ground and power planes made possible low-impedance power distribution (reducing ground noise) and reduced crosstalk between signals (mutual inductances in order of tenths of microhenries and mutual capacitances less than one picofarad were realizable). The multilayer boards also allowed controlled routing of signals, which was especially beneficial to the memory.

Although there has been considerable criticism of thin-film hybrid circuits (FEB's), they permit fabrication and test of functional circuits prior to installation on the circuit board. Moreover, their easy replacement enhances their maintainability. In addition to their small size and weight, they require short lead lengths and may be placed near to closely related parts. However, there are strong opinions that it would have been advantageous to expend the necessary effort to design these circuits with discrete components while maintaining the weight and volume requirements.

The early decision not to add any integrated circuits to the flight hardware used only for integration and test increased the reliability of the computer during flight; however, this decision complicated the checkout.

Another design feature, the hard-wired interconnection matrix, while increasing system reliability during flight, has increased the checkout time by several orders of magnitude.

### 3.4.2 Design Development History of AEA Subsections

#### 3.4.2.1 Power Supply

The power supply started out as an uncomplex, straightforward design and ended up as a very complex, sophisticated design, meeting very stringent requirements.

In order to meet the development schedule, it was necessary to proceed with the design before the requirements were fully determined. The final requirements specification was not released until January 1966, more than one year after award of the contract.

The power supply capability grew as the capability of the computer grew. Several events had large impacts on power supply design. For example, as the dynamic load changes became better defined, it became apparent that, for the power supply to meet its ripple specification, a large amount of capacitive filtering was required at the power supply outputs. This filtering occupied a considerable amount of volume. The laminated bus filtering on the logic, input-output, and memory cards aided in maintain a low-impedance power source throughout the computer.

As the memory increased in size, the memory drive voltages were increased. As the integrated circuit count increased, the power requirements of the logic voltages increased. These incremental changes had a severe impact on the power supply design, but they were unavoidable. It was not possible to overdesign in the first place and still meet the power dissipation requirements.

The addition of the voltage sequencing requirements (to prevent loss of scratch-pad memory) caused power supply redesign. Three separate converters, instead of the previous one, had to be used. Only the common input filter was salvaged from the previous design. Another requirement placed on the power supply was to provide energy for a period of time sufficient to complete a memory cycle in the absence of input power. This requirement resulted in the addition of more storage capability within the power supply. The decision to make the memory Z-driver supply voltage a function of temperature while increasing the overall reliability of the computer, presented a very difficult

challenge to the power supply designers.

The overall effect of the changes in the power supply requirements was an increase in size of the power supply. The modular (trays) packaging technique was used to increase packaging density. Had it been possible to anticipate the final requirements, the power supply might have been packaged on cards as was the rest of the computer. This would have simplified manufacturing and production testing. Another result of the design changes to the power supply was that some components had to be mounted external to the module of which they were a part. This greatly complicated the manufacturing test.

#### 3.4.2.2 Memory

The core memory was the outgrowth of Company-sponsored research and development. Prior to the AEA program, TRW had designed and built a scaled-down version of a 256-word memory. This memory increased to 500 words, then 2000 words, and then 4000 words during the development of the LM/AGS.

It was decided that TRW would design the electronics, specify, and then purchase a core stack from two of the six or so vendors capable of supplying the stack. Early in the program, 2048-word scratch-pad core stacks were purchased from Ferrox-Cube, RCA, and Fabri-Tek. Initial attempts by all three vendors to fabricate the core stack were not completely successful. One vendor selected an EMI core that was highly magnetostrictive and thus very difficult to string. After stringing and restringing the stack and not being able to make it work, the vendor dropped out of the competition. A core stack fabricated by a second vendor, after a long slip in the delivery schedule because of stringing problems, was placed in an engineering model breadboard memory. The electrical characteristics of the stack were quite satisfactory, but visual inspection of the stack revealed stringing problems. When TRW approached the vendor about hardwiring part of the stack, they

declined to bid. A third vendor delivered a stack for an engineering model; however, it did not meet the electrical requirements at the higher temperature. Because of this deficiency, and because of a doubt about meeting the other environmental requirements, this vendor was also eliminated.

During the time of the initial core fabrication efforts by the three vendors, EMI developed a new lithium core, less magnetostrictive than the core used in the engineering model. EMI discovered they could easily hardwire the stack and subsequently became one of the memory vendors.

About this time, Indiana General proposed to hardwire the core stack using a folded-plane technique which resulted in (1) an increase in reliability due to fewer solder joints and (2) a weight saving due to elimination of individual bit frames. Indiana General became our second vendor and later, because of superior electrical, mechanical, and scheduling performance, became our prime and only vendor.

The wiring of the core stack is somewhat unconventional: 2048 words are scratch pad and 2048 words are hardwired as read only. Through each core in the scratch pad are five wires: an X, Y, sense, and two-turn Z (inhibit current now required). The two-turn inhibit was selected to save power (half the inhibit current now required). In the read-only section, there are two or three wires through each core: X, sense, and sometimes Y. The threading of the Y wire through or around the core depends on whether that bit is required to be a one or a zero. Threading an AWG-40 wire through and then around the next core (cores have 18-mil holes, have 30-mil outside diameters, are on 30-mil centers, are at a 45° angle to the direction of the wire, and are staggered at 90° angles to each other) caused concern among several of the potential vendors. The threading technique of wiring zeros rather than chipping out the cores was selected because, by staggering currents, the signal-to-noise ratio of a conventional coincident-current core memory could be maintained.



Having two vendors supplying stacks with different mechanical sizes presented a difficult problem in the AEA packaging design. As a solution to this problem, it was decided to provide the vendors with end boards containing selection diodes to ease the interface problem. Interfacing with the drive wires directly would have meant connecting to 256 wires, while interfacing with the selection diodes reduced this interface to 32 wires. This caused some problems in determining vendor liability because the stack acceptance test was performed with end boards.

Selection diodes were chosen to be integrated circuits (16 packages) in order to increase reliability. Thirty-two components were then required rather than 512 with all matrix interconnections within the integrated circuit package. The electronic system required four diodes per line, rather than the conventional two diodes, to reduce the displacement currents, and thus the noise on the sense line caused by the direct drive scheme. The extra diodes were added when the memory was increased to 4096 words.

The stack-form factor allowed placement of boards around the stack. This proved quite beneficial from both an electrical and mechanical view. The inhibit (Z) drivers with high-power dissipation could be placed on two boards mounted directly to the computer side rails, providing a direct, low thermal-resistance path to the computer case. The sense amplifiers could be placed on two boards mounted above and below the stack, enabling these critical noise sensitive circuits to be isolated from the high-current drivers and to have short twisted pair leads to the source of their signals, the sense lines.

The selection of the sense amplifier was another major undertaking. It was decided that the sense amplifier should be an integrated circuit for reliability purposes, either one commercially available or one that TRW would design.

In final form, it became a combination of the two. TRW redesigned the sense amplifier used in the primary

guidance computer so that its ONE-ZERO threshold remained constant with temperature. Norden was selected as the supplier, with either Signetics or GME the second source. For various reasons, including the death of a key technical person at GME, the second source was eliminated. TRW then began building these circuits in-house for second-source supply. Some yield problems occurred due to the stringent performance specification dictated by our worst-case design. But a couple of iterations varying integrated circuit parameters solved the problems. The complete sensing circuit contained threshold-setting resistors and featured transformer coupling to the sense line, which increased the signal-to-noise ratio.

Requirements for the inhibit driver (18 per system) specified that the circuit supply a current through the inhibit wire that varied as a function of temperature. It was decided that the most reliable approach would be a voltage source varying with temperature, with a fixed resistor in series with the inhibit wire through an electronic switch between the voltage source and ground. The alternative would have been 18 current regulators, more parts, and high-power dissipation. The temperature-varying voltage source imposed a design burden on the power-supply designers. The fixed resistor was a specifically designed thin-film type, designed and built by TRW. The remainder of the circuit was suitable for FEB construction, which enabled the 18 inhibit drivers to be placed on the two boards mounted to the sidewalls of the computer.

The direct drive system was selected for X, Y drive. This eliminated the need for transformers in the drive scheme, saving volume and weight. The drivers and selection switches were adaptable to the FEB construction technique, resulting in size and weight reduction. The current in the lines was controlled by a feedback regulator designed to contain a built-in temperature coefficient so that read and write currents tracked core characteristics. In this way, the sensed output signal could be kept nearly constant over the

operating temperature, thus further simplifying the signal-detection problem in the sensing system.

Although timing generators using integrated logic circuits produce higher power dissipation than timing generators using glass delay lines (because of greater timing tolerances of current pulse widths), the use of integrated circuits was much the simpler design approach. In addition, glass delay lines would have involved mechanical problems.

The packaging of the memory resulted in the ten boards being functionally packaged. This has been of tremendous help to production testing.

#### 3.4.2.3 Central Processor

The original logical design of the central processor was used without any major modifications. The distribution of the logic resulted in two of the logic cards having 96 pin connectors instead of 64.

The use of ten layers (top and bottom pad layers, four logic layers, a clock layer, a ground layer, and two voltage layers) resulted in a workable system from both the electrical and mechanical viewpoint.

The DTL family of logic was selected for mechanization of the central processor. The different components were characterized, a set of logic rules were written, and the logic design was mechanized.

Two problems appeared in the clock distribution systems. The first problem concerned the design deficiencies in all of the available standard integrated clock-driver circuits. The more prominent deficiencies were the existence of too high a TRUE level and the occurrence of current spikes during switching. These characteristics could cause erroneous changing of states of the flip-flops. TRW designed a special clock driver to eliminate these problems.

The second problem, discovered on a breadboard computer, concerned under-shoots on the clock line that were of

sufficient magnitude to cause erroneous changing of flip-flop states. A clamping network had to be added to each slave clock input. This required the addition of a special transistor to the program with special characteristics such as inverse  $\beta$ . A redesign of the logic cards was required to incorporate these circuits.

#### 3.4.2.4 Input/Output Logic

The I/O logic development was similar to that of the central processor. However, there were some changes that affected the design and schedule, such as the input telemetry register, addition of altitude and altitude-rate registers, and the addition of dc D/A converter for lateral velocity. The number of discretes changed continuously, which also affected the design.

#### 3.4.2.5 Input/Output Buffers

The same factors affecting I/O logic design affected the design of the I/O buffers. Design could not be finalized until the interface specification was finalized.

During design considerations of the D/A converter, separate converters were specified for each input, rather than one converter, a sample-and-hold circuit, and AM modulation. The separate converter approach was chosen because it was not complex and would mean fewer components in the overall system.

The FEB approach was used for the register flip-flops to save power (the low power DTL was not available at the time). Other circuits were straightforward and approached optimum design.

### 3.5 HISTORICAL SUMMARY OF SOFTWARE DESIGN DEVELOPMENT

#### 3.5.1 Early History

The major events in the history of the AGS Software development follow the major changes of the functional requirements for the AGS system.

In February 1965 the basic guidance scheme was changed from T-1 guidance

to a rendezvous guidance concept. The T-1 guidance scheme was nonoptimum with respect to fuel consumption and operational procedures and was replaced with an explicit guidance scheme. In January 1966 NASA/MSC redefined the rendezvous concept from Direct Ascent to a co-elliptic rendezvous concept. This mission change had a major impact on the guidance software.

In January 1967, the first complete AGS software package was delivered to NASA. This program incorporated the concentric rendezvous flight plan and is known as the Design Mission Computer Program (DMCP). This program has served as a baseline for subsequent modifications.

A second major delivery, Flight Program 2 (FP2) was made in December 1967 to support a potential unmanned LM test flight in earth orbit. A third program (FP3) has been delivered in May 1968 to support the first Manned LM/CSM flight in earth orbit (Apollo Mission D). The fourth program FP 4 is identical with FP 3.

A fifth program (FP 5) is being prepared. This program will be a lunar program which incorporates many of the improvements of the previous programs.

The hardwired portion of the program has been developed via three configurations. The first one, HO1, was generated to support the production of the memory of the first production units. This program contained very little guidance information because its configuration was frozen at a very early date. The second version, HO2, was considered the final program. However, subsequent ICS testing indicated problems with the attitude equations and a rescaling was required. The final program, HO3, has not been changed since its generation in June 1966.

### 3.5.2 Program Modifications Subsequent to DMCP

Since January 1967 the AGS software has been under strict TRW and NASA/ MSC configuration control. All potential changes are processed as Software Change Proposals (SCP's) for TRW and NASA/ MSC approval.

Table 3-3 shows the status of the 45 SCP's processed to date, 6 of these are guidance constant changes, 13 are minor changes or general program improvements, 4 were disapproved, on 3 no action was taken, and 4 are not yet approved.

Table 3-3. Software Change Proposals

Software Change Proposal	Date	Program Affected	Title of Change	Source of Changes	Status
1	2-9-67	DMCP and subsequent	Rev. No. 1 to DMCP Equations	TRW	Approved
2	2-20-67	DMCP and subsequent	Change in Sign of FDAI Computations	MSC	Approved
3	2-22-67	DMCP and subsequent	Calibrated Accelerometer Bias Compensation Range Increase	MSC	Approved
4	2-28-67	DMCP and subsequent	Pitch and Yaw Steering Limits	TRW	Approved
5	2-28-67	DMCP	Predicted CDH Maneuver; removal of desired absolute time of CDH maneuver; predicted CSI and/or CDH time limited $\geq 0$	MSC/TRW	Approved
6	6-28-67	FP #2 and subsequent	Delete redundant reset of ullage counter to zero	TRW	Approved
7	6-28-67	FP #2 and subsequent	Removal of establishing particular values for $V_{dX}$ , $V_{dY}$ , $V_{dZ}$	TRW	Approved
8	6-28-67	FP #2 and subsequent	Delete $\Delta r_0$ and $T_{c0}$	TRW	Approved
9	6-28-67	FP #2 and subsequent	Input tangent of desired line-of-sight angle rather than desired line-of-sight angle	TRW	Approved
10	6-28-67	FP #2 and subsequent	Remove time sharing of $q_1$	TRW	Approved
11	6-28-67	FP #2 and subsequent	Delete Automatic Exit from Lunar Align	MSC/TRW	Approved
12	8-10-67	FP #2 and subsequent	Simplification of $S_{14}$ Logic	TRW	Approved
13	6-28-67	FP #2 and subsequent	Yaw steering for S Band communication	MSC	Approved
14	6-28-67	FP #2 and subsequent	DEDA "CLR" Change	TRW	Approved
15	6-28-67	FP #2 and subsequent	Calculation of apofocus altitude and time to perifocus	MSC	Approved
16	6-28-67	FP #2 and subsequent	Delete Abort and Abort Stage from steering loops	MSC	Approved
17	6-28-67	FP #2 and subsequent	Automatic selection of elliptic or circular equations for CSI	MSC	Disapproved
18	6-28-67	FP #2 and subsequent	Implement capability to perform CDH at first or third apsidal crossing	MSC	Approved
19	6-28-67	FP #2 and subsequent	Readout out-of-plane position and velocity at all times	MSC	Approved
20	6-28-67	FP #2 and subsequent	Capability of out-of-plane maneuvers at CSI and CDH	MSC	Approved
21	6-28-67	FP #2 and subsequent	Generate node $90^\circ$ from TPI	MSC	Approved
22	6-28-67	FP #2 and subsequent	Display h, and $\Delta r$ in nmi	MSC	Approved
23	6-28-67	FP #2 and subsequent	Accelerometer bias constant to decimal. Requires 6 program steps	MSC	Disapproved

Table 3-3. Software Change Proposals (Continued)

Software Change Proposal	Date	Program Affected	Title of Change	Source of Changes	Status
24	6-28-67	FP #2 and subsequent	Change ullage counter constant check	TRW	No Action
25	6-28-67	FP #2 and subsequent	Change lower limit on $a_T$ (4K34)	TRW	Approved
26	7-24-67	FP #2 and subsequent	Flight Crew selection of Yaw Steering Vector	MSC	Disapproved
27	8-1-67	FP #2 and subsequent	Changes to telemetry list	TRW	Approved
28	8-10-67	FP #2 and subsequent	Elimination of some inconsistencies between PGNCs and AGS in the external $\Delta V$ modes	MSC	Disapproved
29	9-14-67	FP #2 and subsequent	Variable Gyro Drift Compensation	MSC	No Action
30	11-30-67	FP #3 and subsequent	Deletion of S55 and change in selector address constraint	MSC/TRW	Approved
31	12-1-67	FP #2 only	Modifications for unmanned LM 2	MSC	Approved
32	12-5-67	FP #3 and subsequent	AGS/PGNCs Misalignment Correction	MSC	Approved
33	12-4-67	FP #3 and subsequent	Orient Z body axis to desired thrust direction	MSC	Approved
34	12-4-67	FP #3 and subsequent	Control limit on $V_d$ as a function of vehicle configuration	TRW	Approved
35	12-5-67	FP #3 and subsequent	Modification to Orbit Insertion Targeting Conditions	TRW	Approved
36	12-4-67	FP #3 and subsequent	Improved steering in TPI mode	TRW	Approved
37	12-4-67	FP #3 and subsequent	Elimination of attitude hold reference direction when in follow-up	TRW	Approved
38	11-21-67	FP #3 and subsequent	Navigation Sensed Velocity Threshold Constant Change	TRW	Approved
39	12-11-67	FP #3 and subsequent	PGNS Downlink Identification Change	MSC	Approved
40	4-23-68	FP #3 and subsequent	Program Timing Improvement	TRW	Approved
41	4-29-68	FP #4 and subsequent	LM Abort Insertion Targets	MSC	No action expected
42	6-28-68	FP #5 and subsequent	Altitude Update via DEDA	TRW	Not yet approved
43	6-28-68	TBD	Expanded Capability Radar Filter	TRW	Not yet approved
44	6-28-68	FP #5 and subsequent	DEDA Entry Protection	MSC	Not yet approved
45	6-28-68	FP #5 and subsequent	Program Step Savings		Not yet approved

## 4. MAJOR DESIGN PROBLEMS

### 4.1 DISCUSSION OF MAJOR DESIGN PROBLEMS OF THE ASA

#### 4.1.1 Sensors

##### 4.1.1.1 Accelerometers

The Bell VII B accelerometer used on the LM/ASA had one major problem, sticky pendulums; and two minor problems, a large turn-on time constant and bias instability. A fourth problem related to accelerometer mechanical saturation in the specified vibration environments (dependent also on the rebalance loop design) was satisfactorily resolved without any design changes. This problem points up the importance of high accelerometer damping in the design of inertial loops operating in severe vibration environments.

Sticky Pendulum. The sticky pendulum problem was readily detected by observing that the particular ASA output remained saturated for all levels of acceleration in a  $\pm 1$ -g field. Since the problem first appeared in August 1967 on ASA S/N 002, other accelerometers have been examined for sticky pendulums by performing a stiction test. This test determines the gravitational force required to pull the pendulum off the capacitor rings while the accelerometer is operating in open-loop storage. Tests indicated that an increase in storage temperature aggravated the problem.

The suspected cause of this problem was a viscous contamination between the capacitor plates and the pendulum. This contamination may have formed from various types of epoxies used

inside the accelerometer. Many of these epoxies with high outgassing characteristics were changed to gyro-grade epoxies with much improved characteristics.

Accelerometer fabrication techniques were changed drastically to incorporate state-of-the-art assembly techniques recommended by the Materials and Processes Department of Bell, United Aircraft, and TRW Systems. These procedures included the removal of adhesive tapes and Kester 1015 flux, and the elimination of chlorothene, tap water, silicone grease from vacuum pump processing equipment and vacuum brakes, and out-gas of all compounds in each unit before final seal. The accelerometer was then backfilled with 75 percent dry helium and 25 percent dry nitrogen. An attempt was made to solve the sticky pendulum problem through use of state-of-the-art superclean assembly procedures, which drastically reduced the number of different contaminants and the quality of contamination. The accelerometers passed all stiction tests up to the final temperature cycle, that ranged between  $+200^{\circ}$  and  $-100^{\circ}$ F. After temperature cycling, however, some units still failed, probably due to remaining contamination. In the meantime a parallel solution, utilizing a Kearfott 2401 type accelerometer was investigated. The results were excellent and finally it was decided to replace the Bell accelerometer with the Kearfott type.

Bias Instability. The Bell VII accelerometer bias changes exponentially as a function of accelerometer storage time. Storage temperature greatly



affects this rate of change. For a storage temperature of 150°F the bias spread can be as high as 900 g's peak-to-peak when the accelerometer storage position is changed from IA up to IA down or vice versa. The accelerometer bias was separated from the PTSA bias by measuring the total loop bias, reversing the PTSA input and output, and again measuring the total loop bias. The sum of the two biases divided by 2 is the accelerometer bias.

The cause of this problem is not definitely known. Tests have been performed by Bell. In their opinion the creep rate of the epoxy joint between the flexures and the pendulum is causing this instability.

To accommodate bias instability, the ASA can be recalibrated in flight to determine the latest accelerometer bias. A correction is made in the computer to compensate for any change.

It was determined from various tests that accelerometer bias instability could be improved by reducing storage temperature and storing the unit in the position in which it is ultimately used. Reducing the storage temperature to 120°F will reduce the bias instability to approximately 300 g's peak-to-peak. Because of the gyro stratification problem it was decided to store the ASA in only one orientation. This should further reduce the spread in bias to approximately 150 g's peak-to-peak.

Turn-On Time Constant. The Bell VII accelerometers experienced a turn-on problem early in the program where the bias failed to reach a steady-state value between  $\pm 30\mu\text{g}$ 's within 25 minutes after the accelerometer-PTSA loops were closed. This problem prevented the AGS from meeting the mission requirements.

The accelerometer torquer is operated at a 15-vdc potential relative to ground due to the particular PTSA design. This potential causes an electrostatic charge to build up between the pendulum and the capacitor plates that is inversely proportional to the relative distance between the pendulum and the capacitor plates. If the pendulum is

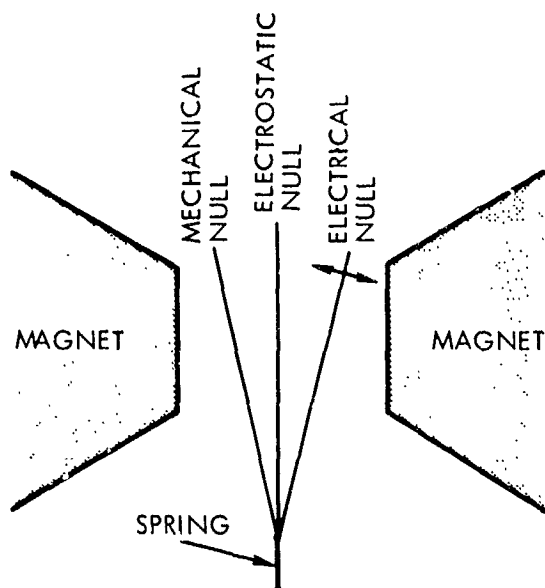
not centered between the plates physically, one plate will exhibit a greater force on the pendulum than the other. Because of the very low leakage rates of the bridge circuit capacitors that exhibit a very large time constant, the electrostatic forces require a long time to settle out. This time period causes the effective bias to change proportionally.

In closed-loop operation the pendulum operates around electrical null. Adjustment of capacitor C4 is made such that the electrical null coincides with electrostatic null. Thus, in closed-loop operation, the net electrostatic force on the pendulum is approximately the same regardless of the dc torquer potential and the charge on the capacitor plates. This adjustment of C4 does not affect the charge on the capacitor plates, but does minimize the change in bias during warm-up or turn-on, during which time the charge on the capacitor plates is changing. This is illustrated in Figure 4-1,

Accelerometer Damping. The original accelerometers chosen for the ASA were gas filled, and hence lightly damped. Under such circumstances, the accelerometer loops saturate at relatively low acceleration levels. Analysis has shown that simple changes in the loop design to increase the dynamic range of the accelerometer and its rebalance loop are not possible. Initial analyses of the accelerometer loop performance in the specified LM mission environment showed a potential mechanical saturation (bottoming) of the accelerometers. Although this problem was resolved satisfactorily without requiring design changes to the accelerometer or its rebalance loop (see Paragraph 4.1.2.4), it emphasizes the importance of using highly damped inertial instruments in inertial loop designs of the ASA type. Such instruments minimize pendulum or float motion and are inherently better suited for operation in a severe vibration environment.

Had the importance of this problem been fully appreciated early in the program, it is likely that an alternate accelerometer would have been chosen to replace the Bell VII.





#### Notes:

- Electrical Null — That pendulum position that gives zero electrical output. Adjustment of capacitor C4 affects only this null.
- Electrostatic Null — That pendulum position at which the net electrostatic force on the pendulum is the same ( $\sim$ zero) regardless of whether the torquer coil is at zero or +15-vdc potential.
- Mechanical Null — That pendulum position at which there is no flexure in the spring.

Figure 4-1. Capacitor C4 Adjust in Accelerometer

#### 4.1.1.2 Gyros

**Mass Unbalance Instability.** Initially in the program the magnitude and stability of mass unbalance terms exceeded the requirements of the ASA specification. The variations manifested themselves in two ways: (1) an initial shift in mass unbalance was observed from the tests performed at Norden (torque to balance and servo) to the tests performed at UACSC (pulse torquing) and (2) a long-term unidirectional variation occurred at both Norden and UACSC.

The effect of the problem was that the attitude drift rates in flight would have exceeded specification. The problem was more severe in the X channel

because of the orientation of the gyro in the ASA. Another effect was that the characteristic instability of the mass unbalance terms made it difficult to use mass unbalance instability as a failure indicator.

In an effort to isolate the problem, testing at UACSC and Norden was directed toward eliminating the responsibility of known effects and discovering any new effects that could be responsible for the variations. A gyro circle test was designed to determine the relationship between the gyro storage position and the gyro mass unbalance. The test consisted of storing two gyros in a fixed orientation until the change in the measured IA and SA mass unbalance terms was less than 0.2 deg/hr-g during a 72-hour period. The orientation was then changed and the above procedure repeated. The orientation sequence was IA up, IA down, SA up, SA down, IA up, etc.

The testing program indicated that the initial shift from analog torquing to pulse torquing was due to the difference in power levels applied to the torquer in these two tests (1.3 watts during the pulse torquing mode compared to 0.7 watt in the analog mode). The cause of the long-term variation, however, was due to storage orientation sensitivity as a result of fluid stratification. This appears to be a common problem in gyros utilizing two-cut flotation fluid, as is used in the R2-1139B gyro.

The shift in mass unbalance resulting from the two test modes was resolved by performing the final mass unbalance adjustment with 1.3 watts dissipated in the torquer. The long-term unidirectional variation problem was resolved by storing the gyros in the same orientation in which they will ultimately be used.

In summary, experience in the ASA development program indicates that if the design of the gyro requires a two-cut flotation fluid, precautions should be taken to assure proper storage orientation. It appears that the stratification problem is bounded and does not result in a catastrophic failure; however, a more stable design could be attained utilizing a single-cut fluid.

Gyro Bias Shifts due to Thermal/Vacuum  
During some of the initial thermal/vacuum testing of the ASA it was found that the temperature difference between the housing and the gyros increased by 0.5 to 2.0°F when the chamber pressure was decreased to 10<sup>-5</sup> Torr. or less. This value was significantly higher than the predicted analytical value of 0.2°F maximum. As a result of this variation, additional testing on the entire unit was performed using the thermal vacuum chamber. During these tests, Wakefield Interface Compound (zinc-oxide-loaded silicon grease) was placed between the interface of the gyro and the housing to prevent the thermal resistance across the interface from being affected by pressure variations from ambient pressure to a hard vacuum.

The potential problem of interface thermal conductance changing from ambient atmosphere to hard vacuum was emphasized almost from the inception of the program, and the possibility of using an interface material was discussed. Very crude preliminary tests indicated that bare interfaces would be adequate; however, this information was not in complete agreement with all of the literature available. An additional problem was that use of Wakefield Compound might induce an undesirable misalignment. It was verbally recommended and planned to build a mock-up of the housing and test one gyro in the housing in both air and vacuum conditions. This mock-up could also have been used to determine misalignment effects. The need and feasibility of an interface compound could have been determined early in the program without the high cost of evaluating the method on a system thermal vacuum level. The decision not to build a separate mock-up for these tests was based upon budget considerations.

#### 4.1.2 Sensor/Electronics Loops

##### 4.1.2.1 The Low-Frequency Resonance Problem and H-Vector Spin-Input Rectification

The first evidence of a low-frequency resonance problem came from tests conducted at United Aircraft. It was

found that if an ASA were subjected to a skew axis vibration test with sinusoidal inputs in the 3 to 5 Hz frequency range, the gyro loops could show very large drift errors. The error source may be described as follows: In an unperturbed condition the rotor of the gyro spin motor (i.e., the gyro wheel) rotates in synchronism with the stator field. Torques are applied to the rotor by either the stator field (through a magnetic spring) or by windage and bearing friction. The coupling of the rotor to the stator field is well modeled as a second-order system.

If a very low frequency sinusoidal angular rate is applied to a gyro about its spin axis the wheel will remain in synchronism with the stator field. If the frequency of this spin axis sinusoidal rate is increased above 5 Hz, however, the magnetic spring will no longer be strong enough to drive the wheel in synchronism with the stator field and the wheel will not follow the sinusoidal stator motion. Somewhere between these extremes of total synchronism and total asynchronism of the wheel and stator field the wheel is excited at a resonant frequency. Small angular rates about the spin axis at this frequency can cause large deviations in instantaneous wheel speed.

The angular momentum of the gyro, however, is proportional to wheel speed. If a sinusoidal rate is applied about the spin axis the wheel speed will be perturbed in a sinusoidal fashion. This means that the angular momentum of the gyro will also be sinusoidally perturbed. Assume sinusoidal inputs of the same frequency and phasing are applied simultaneously about the spin and input axes of the gyro. The spin axis rate will cause the angular momentum to momentarily increase when a positive rate is applied about the input axis, and to momentarily decrease for negative input rates. This will cause greater float precession for positive than for negative inputs and a positive gyro drift rate. This error source is the H-vector spin-input rectification (HVSIR).

The basic cause of HVSIR is the inability of the magnetic spring to

force the wheel into synchronism with the stator field at frequencies above 3 Hz.

HVSIR is another gyrodynamic rectification error and will have to be accounted for both in the LM/AGS and in future systems. However, for an error to exist, it is necessary that the inputs about the spin axis and input axis be of the same frequency. For the error to become large, it is necessary that the frequency of the applied input axis and spin axis rate be very near the frequency where wheel resonance occurs. On the LM project it was assured that these conditions did, in fact, not exist. Grumman simulated the attitude control systems and found the moments of inertia about the various LM vehicle axes were different enough to ensure that the limit-cycle frequencies about each LM axis were at no time the same.

To a great extent HVSIR is unavoidable and will remain so as long as lightly damped magnetic drive spin motors are used in gyros. This error source should not be a problem during the mission, however, because of the need to have correlated inputs about both the spin and input axes of any one gyro. HVSIR could be an appreciable error during skew axis vibration testing, however, when correlation between inputs about different gyro axes is indeed common.

Limit cycling of the LM vehicle as a result of the reaction jet control system operation is the only significant source of excitation of HVSIR. During the initial design of any attitude control system care should be taken to examine possible limit-cycling frequencies. HVSIR may be eliminated if the frequencies of limit-cycling about different vehicle axes are not coincident.

#### 4.1.2.2 The Sensor Loops

##### Evaluation of Cross Spectral Density Dependent Rectification Errors.

Although stable platform inertial navigation systems are essentially immune to rotational rates, a strapdown system is not. If the strapdown system housing is rotated, either because of vehicle

motion or angular vibration, the instruments will also rotate. Under these conditions such errors as spin-input rectification, spin-output rectification, HVSIR, etc., may be appreciable error sources. The problem was to predict the values of these rectification errors first from the specified environment and second from actual vibration test data taken at White Sands Missile Range (WSMR), New Mexico. These tests are described below.

Methods for evaluating errors were developed first for sinusoidal inputs and later for random vibration inputs. The methods show that these errors depend on loop design and on the cross correlation between motions about or along different instrument axes (e.g., spin and input axes angular rates for the HVSIR error described above). Also, actual data from the WSMR tests show that during a simulation of the actual vibration environment these errors were quite small. The reason for this is the dependence upon cross spectral densities (CSD). If the CSD phase angle changes rapidly, as a function of frequency, error cancellation will occur. That is, one frequency component of the CSD may induce a positive error from any one error source; another frequency component may induce a cancelling negative error. These errors add up algebraically across the frequency spectrum. If there is substantial cancellation, as there was in the WSMR test data, there is little opportunity for error build-up.

The technique described above has general applicability for CSD dependent errors and may be used in their evaluation of future systems. It requires, however, a knowledge of the vibrational CSD's, that is not always readily available.

##### Computer Effects on Coning Error.

Coning errors fall in the class of CSD dependent errors discussed in the previous paragraph and therefore may be evaluated as previously explained. However, coning has one unique feature. The presence of an error is evident only after processing of the gyro angular rate data by the computer. Rectification is not evident at the sensor

loop outputs. For this reason the effects of the computer on the computation of coning rate must be considered. The relevant effect is that the computer has a non-unity transfer function for coning caused by the fact that the computer sampling frequency is finite. The problem was to modify the method of computing coning rates to reflect this frequency response.

The basic cause of the problem is that the computer in the AEA samples the sensor loop outputs at a rate of 50 Hz. This limits the frequency range in which coning can be detected, and hence compensated for in the computer, to about 10 Hz and below. As an example, if the sampling rate had been 500 Hz, the range in which coning could be reasonably well detected would be from 0 to about 100 Hz.

The effect of the problem was to introduce an unknown performance uncertainty. It was necessary to fully understand the coning phenomena and to develop a method for determining the effects of coning on mission accuracy.

A computer simulation was performed wherein coning inputs were fed into a simulation of the LM/AEA direction cosine update equations. By varying the amplitudes, frequencies, and phase angles of the sinusoidal inputs, a computer transfer function for coning

$$\frac{\sin(\omega\tau)}{\omega\tau}$$

was developed where  $\omega$  is the input frequency about the two coning axes and  $\tau$  is the sampling period.

This transfer function was used to modify the calculations of CSD dependent errors described above. The resulting values of expected coning error during the mission were acceptable.

This problem area highlighted what could have been a large gyro drift error. Attention should be directed to the design of the support structure around the sensor package to ensure that a tendency toward coning is not built into

the structure. If coning is expected from the environment of any future system, it should be assured that the computer can calculate the coning rate successfully. It should also be noted that the coning transfer function given above is good for the direction cosine method of angular rate updating. If some other method were used (e.g., quaternions), the applicable coning transfer function for that method may or may not be the same and would also have to be found, probably by simulation.

#### 4.1.2.3 Gyro Loop Problem (Asymmetry)

All hardware is to some extent nonlinear. To that extent, asymmetry was known to be a problem since the inception of the LM program. However, in about November 1966, after design proof testing results had been analyzed, gyro asymmetry was recognized to be a major error source. Asymmetry drift may be defined as follows: A gyro loop with zero bias is subjected to a time-varying angular rate about its input axis, which has an average value of zero. However, it is found that the average value of the output of the gyro loop is nonzero, that is, the loop is nonlinear and the input motion has, in some way, been rectified. There were two parts to the problem. First, tests showed that asymmetry error could be quite large. Second, our ability to predict asymmetry under any given set of circumstances was very poor.

The cause of this problem was:

- a. The linearity of pulse torquing loops, such as in the ASA, is directly dependent upon precise timing of the ASA clock pulses. This clock timing was influenced by noise on the +4-volt line.
- b. A second cause was cross talk in the ASA between an 8-kHz demodulator signal and the regulators for torquing current.

The first effect of the problem was that our ability to predict AGS performance was seriously questioned. As the

asymmetry phenomenon became more fully understood, a second effect appeared, an ASA yield problem. Certain ASA's had unacceptable asymmetry, others had acceptable asymmetry. This meant that without circuit changes some ASA's would not have been flightworthy. If the situation had not been corrected, there would have been an obvious impact on cost and schedule.

There were two parts to the remedy. United Aircraft developed circuit changes that eliminated the susceptibility to the +4-volt-line noise. The 8-kHz crosstalk problem was effectively squelched by the development of an asynchronous 8-kHz demodulator. With this latter modification, crosstalk of the demodulator with the current regulators no longer caused drift errors. As a second part of the remedy, TRW developed a method for predicting asymmetry drift during either mission or tests. This method was used to show that the LM/AGS would meet mission requirements.

It should be recognized that future pulse torque loop designs may also be susceptible to clock timing problems. Proposed designs for future systems should be analyzed to determine the effect of imprecise clock pulse timing.

#### 4.1.2.4 Accelerometer Loop Problem

##### Measurement of Frequency Response

Part of the original analysis of the ASA included the prediction of accelerometer loop frequency response curves. These curves were verified by single-axis testing. The predicted frequency response resembled a second-order system; flat at a level of 0 db from 0 to about 100 Hz, a 3 to 6 db peak at about 400 Hz, and a rolloff from that point on. Loop performance was analyzed and error predictions were made, based in part, on this frequency response. When actual frequency tests were performed, it was found that accelerometer loops had a double peak frequency response. An unexpected peak in the 30 to 50 Hz region was observed as was a peak in the 400-Hz region. It also appeared as if the roll-

off that should have followed the 400-Hz peak had begun about 200 Hz, so that in many instances the 400-Hz peak appeared to occur partially down a frequency rolloff.

Unfortunately, the basic cause cannot be pinpointed. Probably a frequency dependent timing or crosstalk phenomenon was at fault. This problem has not been pinned down because the modifications to the clock and 8-MHz circuitry within the ASA caused the double-hump accelerometer frequency response phenomenon to disappear. ASA's with the asymmetry modification have frequency response characteristics as originally anticipated.

Before the appearance of the double-hump phenomenon, it had been intended that the accelerometer frequency response be used as a check of ASA performance. That is, a check that the actual loops in an ASA fell in that class of loops that had been theoretically analyzed. When the double-hump phenomenon appeared, this simplifying process could no longer be used. It therefore became necessary to perform translational vibration tests during acceptance testing. This ensures, in a positive but relatively costly manner, that the accelerometer loops function properly.

If only one accelerometer loop in an unmodified ASA is excited at a given time, the double-hump phenomenon does not appear. Therefore, in future systems it is suggested that performance of any single loop be compared with performance of the same loop in the system.

Mechanical Saturation of the Accelerometer Loops. Under certain vibration environment conditions, the accelerometer loops exhibited very large biases (e.g., 20,000  $\mu\text{g}$ 's). The reason for such biases was unclear because the accelerometer loop has a mechanical saturation (i.e., mechanical pendulum stops), two electrical saturations, and torque limiting in the torquing circuitry, all of which interact. Two questions emerged: Should the accelerometer loops be changed? And, if so, how?

The vibration environment for the ASA, specified at the inception of the LM program, was sinusoidal vibrations between 14 and 60 Hz. To refine this environment, Grumman produced a model of the whole LM structure. This model showed the vibrational propagation paths from the ascent, descent, and Reaction Control System (RCS) engines to the ASA. This allowed calculation of a detailed vibration environment at the ASA. The new environment differed markedly from the original environment. It soon became obvious that the new environment was incompatible with proper operation of the accelerometer loops.

As a result of this problem, the ability of the accelerometer loop design to operate in the LM mission environment was questioned. To better understand the problem, digital computer simulations were performed both at TRW and United Aircraft in conjunction with nonlinear loop analysis. Performance of digital computer simulations showed which saturations were important and at what levels of vibration the present loop design would operate successfully. In addition, Grumman conducted tests at WSMR in which the LM/RCS jets and the descent engine were fired. Vibration data was taken and reduced to PSD's and CSD's. Analysis of this data showed that the specified translational vibration level could be lowered. As a result, it was concluded that the present ASA accelerometer loops were satisfactory.

To prevent recurrence of this problem in future programs, it is recommended that:

- a. Structural models similar to the LM model produced by Grumman should be encouraged to aid the prediction of vibration environments for future systems.
- b. Highly damped inertial instruments should be used for future inertial loop design. Such instruments minimize pendulum or float motion and are inherently better suited for operation in a severe vibration environment.

#### 4.1.3 Electronics and Interface

Specification LSP-300-37D and SS2-1C required the signal ground and the chassis ground to be isolated by 10 megohms. During the integration and inline testing of ASA S/N 001 in late March and early April 1966, UACSC encountered susceptibility of inertial performance to noise between the two lines, and different loading effects upon the two lines when the test connector was attached and removed. Tests at TRW confirmed this change in bias on both gyro and accelerometer outputs between operation with the test connector connected and disconnected. This phenomenon was also noted on units 001X, CSC-1 and 002. ASA S/N CSC-1 typically showed an accelerometer bias shift of 450  $\mu$ g's and a gyro shift of 3 deg/hr for test connector on/off tests.

The basic causes of the problem were: (1) the existence of many ground loops, e.g., the accelerometer has a designed-in ground loop since the 8-kHz excitation to the bridge is through the chassis and the output is with respect to signal ground, (2) failure of test equipment to simulate specification loads, (3) failure to check the performance with specification loads, and (4) minor discrepancies between LSP 37D and SS2-1C concerning the kinds of cables, bundling, shielding, etc.

The problem was solved by shorting the chassis ground to the signal ground internal to the ASA and requiring performance to be met with a breakout box with exact specification loads. Ground loops were removed as a result of the investigation.

To prevent recurrence of this problem, each component of the system should be selected to be consistent with the grounding philosophy, and care should be taken during the design of a system to ensure that attention is given to proper grounding. Additionally, since the Bell accelerometer used in the system had an inherent ground loop, the effect of which could only be minimized by tying the two grounds together, it should have been discovered earlier that the two grounds were in fact tied

together less than 3 feet away from the ASA on the LM structure. The final solution was axiomatic after months of investigation were expended to find a solution other than connecting the chassis and signal grounds together.

#### 4.1.4 Thermal and Mechanical

##### 4.1.4.1 Thermal Problem with Thermal Path to Cold Plate

At the time of the conceptual design review of the ASA, the thermal design of the electronic subassemblies and the power supply were based upon the use of a beryllium-oxide-loaded silicone elastomer, which according to the manufacturer, had a thermal conductivity of 21 Btu/hr-ft-°F. Subsequent investigation of this material revealed that the actual conductivity was only in the order of 0.3 Btu/hr-ft-°F, or 1/70 of the reported value.

As a result of this difference, the thermal design of the electronic assemblies and the power supply required was redesigned to provide adequate thermal paths. In addition, the method of achieving the proper thermal attenuation between the ASA and cold plate was significantly changed.

As a general rule, whenever a material or device has properties significantly different from those expected, careful evaluation of the item should be made before a design becomes dependent upon it.

##### 4.1.4.2 Thermal Problem with Heat Sink Surface Specification

From the beginning of the program until a few months before qualification thermal vacuum testing, the specification for the thermal interface for the unit stated that the heat sink surface of the ASA would be maintained between 60°F and 80°F and that the heat density of the heat sink surface should not exceed 1.6 watt/in<sup>2</sup>. This was a rather awkward and poorly defined interface, because the gradient that might be imposed on the heat-sink surface was not defined and was dependent upon the parameters of the cold plate that would be attached to the heat-sink surface. The problem of demonstrating that the

power did not exceed 1.6 watts for any square inch was practically an impossibility experimentally; it could only be shown analytically. Even then, some basic assumptions regarding the parameters of the cold plate were required.

The changes required late in the program presented numerous practical problems in obtaining the necessary equipment to provide the required coolant to the cold plate. Because of schedule problems, the unit could not be calibrated when the flight cold plate and other equipment were used.

To obtain more realistic tests that would simulate actual flight conditions and resolve basic problems, the specification was changed to include the cold plate and its associated parameters along with a range of the inlet temperatures. In addition, qualification testing was to be performed with an actual flight cold plate.

It is felt that the comparison between calibration and flight would have been more realistic if the units had been calibrated with flight cold-plate conditions rather than at a heat-sink surface temperature of 60° to 80°F.

##### 4.1.4.3 Feet Redesign for Foot Fatigue and Vibration Environment

As part of the initial design concept, an isolation system was proposed for the ASA in order to present an attenuated vibration spectrum to the sensors which were known to be vibration sensitive. Considerable time and effort were expended to develop an adequate system of isolation considering the specified environment to be applied as an input at the mounting foot interface. As the interface design developed at GAEC, it became obvious through analysis and tests that the mounting structure of the navigation base influenced the ASA input to the extent that no isolation system could be effective.

Because of the incomplete interface definition early in the program, overly conservative specifications of the vibration environment were used for design purposes. The specified environments were considered as equipment

inputs ignoring the structural response of the navigation base with the ASA mounted on it.

To eliminate this type of problem, a complete understanding of the end use of the equipment, mounting location, and mounting procedures must be obtained by the subsystem design engineers early in the program. Installation drawings and interface mock-ups should be completed early in the conceptual design stage, and analyses made of the complete mounting structure to define the environment at the sensitive component as precisely as possible.

#### 4.1.5 Testing

The discussion that follows deals primarily with problems encountered while testing the ASA at TRW (i.e., problems encountered in the test technique and test equipment when accomplishing the evaluation of an ASA in the laboratory). This discussion is not intended to cover those ASA design problems uncovered by the test program. Of course, some of the design features of the ASA give rise to testing problems, the principal ones of which are discussed herein.

##### 4.1.5.1 General Problems

Two classes of problems were encountered in laboratory testing the ASA:

Testing Problems. The nature of the strapdown configuration (i.e., rigid mounting of the sensor components directly to the navigational base as opposed to an inertial platform system) results in the following test conditions that require special attention by the test engineer.

##### a. Isolation of Dynamic Stimulation

Dynamic testing exposes the ASA to all dynamic conditions present in the test environment, regardless of their interest or application to the test underway. This exposure propagates all the errors in various degrees from the error sources of the strapdown instruments. These

errors are often sufficiently large to mask the data of interest during the test. A typical example is the presence of high-frequency angular vibration errors during a low-frequency coning test. These unwanted dynamics are always present to some degree. The test designer is therefore faced with the problem of achieving precision alignment of the inertial instruments and tightly controlling the dynamic stimulation to minimize the effects of dynamics that are of no interest to the test.

##### b. Pulse Counting

The use of precision pulse torquing in the ASA design poses another problem for the test engineer in the area of accurate pulse counting and timing. This problem is primarily reflected in the design of ASA special test equipment used to monitor loop outputs.

ASA Design Problems. Various characteristics, in some cases problems, of the ASA design give rise to the following types of test problems.

##### a. Inertial Component Parameter Nonrepeatability

ASA design problems that are difficult to detect often pose test problems because of the nonrepeatability of the test results. An example is the gyro flotation fluid stratification problem, that appears as shifts in certain gyro mass unbalance terms. Before the problem was resolved, additional test effort was required to review test methods and to search for gyro malfunctions.

##### b. ASA Ground Sensitivity

This sensitivity of ASA outputs to ground loops and EMI conditions within the ASA results in parameter shifts and uncertainty when the ASA



is integrated with the test equipment. The test designer is faced with the problem of creating a test configuration that minimizes the sensitivity of the ASA performance to ground-loop configurations and changes thereto.

c. ASA Mounting Technique

The ASA reference planes are determined by the plane of the mounting feet and the center of the precision holes on two of the feet. Early in the program, no special effort was made to locate the center of the holes or to obtain a consistent reference other than that provided by the special guidepins on the mounting fixture. As a result of this mounting technique and the large tolerances in the diameter of the precisely located holes in the ASA feet, the reference planes were not consistently established.

In addition, non-uniform torquing of the holddown bolts and flatness problems of the ASA feet contributed to ASA misalignment problems.

4.1.5.2 Solution

During the ASA test program at TRW, most of the above classes of problems were alleviated by refined test planning and modifications to the test equipment. The major fundamental goals of the test program were achieved. The discussion of specific problems in Paragraph 4.1.5.3 includes the TRW solution of these problems and recommendations for courses of action to be followed on any new program. It is well to point out that some areas identified as problems in one case are the causes of additional problems in other cases. There is frequent interaction between various identified problems.

4.1.5.3 Specific Problems

Gyro Mass Unbalance Measurement. Considerable test effort was expended

in evaluating the cause of large changes in certain gyro mass unbalance terms that were mistaken as an indication of a malperforming sensor. Additional testing revealed continuing shifts in the same direction. These results were disturbing because the normal values were expected to show a random-walk type progression from one value to another, with no tendency toward a net change. After sufficient time lapse, the values of the unbalance terms stabilized at new values.

The basic causes of the additional test effort and the loss of confidence in the gyros were the shift in the values of the Y-gyro input axis mass unbalance and the Z-gyro spin axis mass unbalance.

The basic cause of the shifting unbalances was stratification of the flotation fluid in the gyro during the period of storage at high temperature. The two fluids used for the flotation separated over a period of time. The more dense fluid settled. When the ASA orientation was changed, the stratified fluids began to move slowly around the float to reestablish equilibrium with the more dense fluid at the bottom. Up to four or five days were required for the fluids to reach equilibrium. While the fluids were in motion seeking the equilibrium, they were acting on the float by cohesion, thereby causing changes in mass unbalance.

The cost of the testing effort increased, and confidence in the gyros and the testing methods decreased. Before the cause of the shifts was traced to the gyro flotation fluid stratification, the sensors were not considered to be flightworthy. The stability of the unbalance terms was questionable, and the shifts were considered indicative of a reliability or, at least, a performance problem.

The remedy to the test problem was to circumvent the ASA problem. After identifying the nature and time constant of the cause of the unbalance shifts and demonstrating that the resulting error was bounded, an adequate solution was found in maintaining the storage position of ASA's, from manufacture until

the flight, in the flight orientation, X-axis up. In this orientation, the X-gyro spin axis mass unbalance shifts to the limit and stabilizes. Other unbalance terms are not affected by the stratification.

#### Sensor Misalignment Measurement

Large apparent shifts in the sensor misalignment angles were observed during calibration testing. Upon investigation, these apparent shifts in sensor misalignments proved to be shifts in the calibration fixtures.

The apparent basic shift problem appears to result from unstable test fixtures during the calibrations. The fixture instability may be attributed to both design inadequacies and procedural errors. Because the coefficient of friction between the two polished surfaces is very low, the fixture sometimes slips during calibrating of the ASA.

Before the problem in the calibration fixture was identified, the apparently shifting misalignment angles reduced the confidence in the ASA. When the specification limits were exceeded, the unit was not considered flightworthy.

The remedy for the alignment shifts has been an increase in the bolt torque to hold the fixture more securely. Other methods such as increasing the number of bolts and etching the surface may be more successful. A two-axis dividing head would help solve this problem.

Calibration Repeatability. Some difficulty has occurred with ASA alignment repeatability during calibration tests. Bubble levels rather than optical devices were chosen to establish the verticality of the ASA. Since alignment requirements were not extremely critical, this method was considered more feasible, faster, and cheaper; but with bubble mounting surfaces available in only two of the six calibration positions, this method has worked marginally. An improved method would be to have bubble mounting surfaces available in every test position. Bubbles are practical and may be more expedient than optics where alignment requirements are not in the arc-second range.

Test Set Counting Accuracy. The AGS test set, which was designed to test both ASA's and AGS's, has exhibited inconsistent pulse counting of the ASA sensor loop digital output. This inconsistency, which occurred intermittently in the early portion of the program, caused a number of ASA performance tests to be rerun. In those test configurations where the AEA was utilized to accomplish parallel counting, the inconsistent test set counts could be easily identified. The AEA routinely yielded consistent and accurate counts. The problem became aggravated when the ASA was tested by itself, the AEA not being available for cross-check.

This problem was caused primarily by the poor signal-to-noise ratio in the test point monitor and the difficulty in adjusting the buffer amplifiers in the transfer unit of the test set.

This situation resulted in numerous test reruns and extended time expenditure for adjusting the ASA test-set counter circuitry to perform accurately. After the circuitry was modified, the test crews became very adept at adjusting this level to match each ASA under test.

A circuit change has been incorporated in the test point monitor that improves the buffer circuit signal-to-noise ratio and satisfactorily diminishes the problem.

Test Set Clock Jitter. Large apparent gyro-scale-factor nonlinearities caused by test set clock jitter were measured.

The ASA uses a time-modulated, constant-current torquing scheme, and is extremely sensitive to jitter of its clock signal (128 KHz) if the jitter is coherent with the 1-KHz torquer switching frequency. An equivalent drift of 1 deg/hr will occur for 5 nsec of coherent jitter on a particular clock pulse.

Such jitter occurred in the AGS test sets (up to 30 nsec) and caused unsuspected problems in bias nonrepeatability and vibratory test errors and, finally, very apparent discrepancies in gyro scale factor nonlinearity measurements.

Jitter in the test set is suspected to be principally attributable to the countdown circuitry. This countdown circuitry provides numerous signals at a wide range of frequencies for various functions within the test set. Transients from simultaneous switching of the various countdown circuits probably induce the clock pulse jitter. Such transients are not pulse to pulse, but cyclic.

The large apparent scale factor errors indicated that the units were not flightworthy. The synchronous jitter in the test set resulted in an apparent asymmetry characteristic of the ASA scale factor when under test. The results of such tests were erroneous in that excessive or out-of-specification performance was falsely attributed to the ASA.

A modification to the countdown circuitry within the test set is being incorporated that will bypass the other countdown circuitry and thus isolate ASA clock pulses. The resulting total jitter after incorporation of this circuitry is in the region of 2 nsec. The difficulty encountered when attempting to measure pulse jitter in the picosecond range is that available test equipment is noise limited below about 1 nsec. It appears, however, that by limiting the jitter to the 1 nsec range, the ASA asymmetry problem has been reduced to tolerable levels.

Ground Loop Sensitivity. Shifts were observed in values of the ASA calibration parameters from one test configuration to another. The ASA design appears to be sensitive to ground loop configurations within the test equipment. This situation is particularly aggravated by the test configuration normally consisting of the AGS test set, the Inland rate table, and various lengths of cables connecting the ASA to the test equipment.

This problem is undoubtedly caused by many ground loops within both the test set and the ASA. In general, violation of the single-point ground concept within the ASA is felt to be the principal contributor to this situation.

As indicated, such grounding sensitivity results in inconsistent performance parameter measurement across the various test configurations.

The effect of this ground condition was greatly reduced by careful design of the test cabling and judicious application of an external grounding means to tie the various items of test equipment (as well as the ASA) together, and thus minimize ground loop occurrence.

Generation of Pure Test Dynamic Stimulation. As previously pointed out, a strapdown sensor assembly is subject to all the dynamics present under any test conditions. That is, the sensor assembly is not mechanically isolated in any manner from both angular and linear vibration motion. This can result in corruption of the test data of interest in any one particular test.

These unwanted dynamics (e.g., cross-axis vibration and coning) cause noise in the dynamic stimulating equipment (particularly angular and linear shakers) and special equipment such as the EPC sway simulation machine and the coning machine. Such noise, resulting from inaccurate sensor alignment, stimulates the sensors in question by dynamics along axes other than the axis of interest or by unwanted dynamics along the axis of interest.

This situation corrupts the test data, making it difficult, even impossible, to analyze the data for the evaluation of the various parameters under investigation.

Test fixture extraneous motion (noise) is minimized by equipment design and modifications (isolation, damping, etc.) and by careful choice of test techniques. The residual test set dynamic noise is somewhat offset by accurate measurement of this noise prior to the test, followed by adjustment of the test data for the measured amount of dynamic noise. Such measurements can be achieved (particularly on vibration equipment) by use of a mirror arrangement on the dynamic simulator and two-axis automatic auto-

collimator recordings during a dynamic run. This method was used to establish, for example, the amount of coning noise that was present in the angular vibration shake equipment.

The alignment errors can be alleviated by the use of precision techniques in mounting and aligning the sensor assembly. The test crews who handle the equipment must exercise extreme care and practice strict cleanliness in their work. Fixtures should be stored in special padded boxes and must be cleaned and inspected prior to each use.

Rate Table Reversing Error. Occasionally, the rate table exhibited a difference in angular rate between the clockwise and counterclockwise directions for the same rate setting. This problem occurred during rate tests when the test set was operating in an automatic mode. It did not cause inaccurate test results because a computer program in the AEA indicated the problem and the tests were rerun manually.

This rate table reversing error is caused by rate table ground currents flowing through a common portion of signal ground in the rate table electronics.

The basic effect of such a problem is extended test time due to repeat testing. This is true in that angular rate is not a critical feature of the scale factor and misalignment calibrations as long as the angular traverse and the time of traverse is known.

The problem has been corrected by relocating the rate table ground circuitry in the rate table console.

Mounting Instability During Thermal Vacuum/EMI Testing. In ASA performance tests, during thermal vacuum exposure in a chamber, the ASA had to be mounted on a fixture within the chamber. Due to the size and construction limitations of the chamber, this fixture was supported directly by the chamber.

Since the chamber was not designed with inertial stability in mind, a situa-

tion resulted wherein an ASA was mounted on a rather dynamically unstable support.

This condition contaminated ASA performance data collected during ASA operation while under thermal vacuum conditions by the dynamic movements transmitted to the ASA through this unstable mounting configuration. The effects of thermal vacuum conditions on ASA performance were then difficult to separate from the effects of such phenomena in the data. This situation was somewhat circumvented by establishing the static drift of the ASA while it was mounted in the thermal vacuum chamber under ambient conditions, and then subtracting these drift measurements from those drift measurements obtained under thermal vacuum conditions. While in theory this would establish the ASA thermal vacuum performance, the confidence in such a scheme is marginal due to instability, and it is felt that the more precise manner of determining the effects of thermal vacuum on ASA performance should have been utilized.

If the tests were to be rerun and funding was available, TRW would have constructed a vacuum installation utilizing a stable pier mounted on a seismic pad as part of the test configuration. The stable pier mounting surface would have been available within the thermal vacuum chamber but the pier construction would have been mechanically isolated from the chamber construction so as to minimize the effect of thermal stresses on pier stability. While the construction would have accomplished such mechanical isolation, it would, in turn, have also achieved the necessary thermal vacuum insulation.

EMI Test Problem. During EMI susceptibility testing of the AGS, the ASA sensor outputs were monitored, both with and without EMI stimuli applied, to determine the effect of EMI on the sensors. The test was conducted in a screen room without a stable pier. Both the floor and bench in the screen room were much less stable than expected and, as a result of the dynamic noise level present in the sensor outputs, evaluation of the EMI effects

became very difficult without extensive statistical treatment of the data. Since the dynamic noise level varied in a random fashion and was at least partially dependent on the activities of the test crew, it sometimes happened that the level was lower during the EMI portion of the test, since the test crew tended to remain in one position throughout the test. A stable pier in the screen room would clearly have made evaluation of the data much easier and would have improved the level of confidence in the test results. The discussion regarding the thermal vacuum testing problem remedy applies to this EMI test.

Test Cabling Problems. Because many of the ASA performance tests required rotation of the ASA on the rate table, considerable bending stress was placed on the test cables between the ASA and the test set. This resulted in excessive cable failure, which in turn caused poor data and test re-run.

This problem occurred because of the layout of the test configuration of the ASA rate table. The test cables went from the ASA directly through a fixed hanger arrangement that suspended the cables over the ASA for rotating to the test set. Rotation of the ASA caused flexing of these cables at the hanger which resulted in considerable cable wear and continuous difficulty in maintaining cable continuity and acceptable signal-to-noise ratio. This difficulty in cable maintenance and troubleshooting was aggravated by molded/potted construction of the cables.

This situation resulted in occasional intermittent signals from the ASA to the test set that exhibited themselves in erroneous test counts. While these were usually identified by the test conductor, in some cases the performance change was more subtle and it was possible to generate erroneous performance data not obviously attributable to cabling intermittency. This situation resulted in frequent cable rework and troubleshooting, which in turn resulted in extensive test time and inefficiency.

If redesign of the ASA test facility were possible with sufficient funding, we would probably abandon the cable flexing approach and utilize slip-ring connectors between the ASA rate table and the test set. Considerable design analysis would have to precede the design to achieve a satisfactory method of using slip-rings; however, this appears to be a more feasible way to approach this problem. If the flexing cable scheme is to be used, it would be wise to abandon molded cables and use vinyl sleeve connectors for easier maintenance. The cables should be designed for flexing by making them flat and thin. They should be precoiled and have a device for changing the direction of the coil as the table rotates. This arrangement would increase cable flexibility, increase cable life, simplify maintenance, and reduce drag on the rate table.

#### 4.2 DISCUSSION OF MAJOR DESIGN PROBLEMS OF COMPUTER SUBSYSTEMS (AEA AND LEDA)

##### 4.2.1 Major Design Changes

The major design change discussed herein were made after the start of production. Earlier design changes are discussed in the historical summary of Section 3.

The first design change affecting production computers was the addition of the requirement for the dc D/A converter. Fortunately, the change was anticipated and involved only the redesign of one I/O board.

During qualification of the AEA, there was a memory failure: drive lines were opening within the core stack. Investigation revealed that a hat bracket used as part of the structure had cracked, stressing the wires and eventually breaking them. The problem was solved by redesigning the hat bracket. No further failures have occurred.

After fabrication of several computers, a problem was found in the memory. The memory appeared to be pattern sensitive, that is, the content

of the memory was erroneously changing when certain computer programs were being performed. The problem was traced to current undershoot in a drive line, causing partial switching of cores. Redesigned timing circuitry eliminated the undershoot, solving the problem. This problem was a vexing one because associated symptoms appeared only when the memory was physically in the computer. On the memory test fixture the problem did not exist. If a production prototype computer had been available to Engineering, this problem could have been eliminated prior to production.

A memory word loss problem was first noted on computers S/N 16 and 17. A noisy falling edge of the memory-read clock pulse was coupling into and false-triggering the memory-write clock one-shot. The probable cause was minor variations in transistor characteristics. However, a marginal design factor, resulting from a packaging layout that placed sensitive circuits adjacent to noisy circuits, should be cited as well. The loss of words from the memory was more pronounced at lower temperatures. The problem was remedied by slowing down the memory-read clock pulse falling edge and logically clamping the input to the one-shot. This prevented the false triggering. In retrospect, it appears obvious that the production-configured memory should have been thoroughly design-evaluated by Engineering. However, such action was effectively eliminated by the dollar and schedule constraints imposed by the customer.

An AEA-DEDA interface problem was detected during LM vehicle testing. It was noted that an extraneous triggering of the DEDA clock pulse was causing faulty transmission of data. The double triggering of the DEDA logic clock pulse was caused by inflection of the incoming waveshape (from the AEA) at the DEDA. In turn, this occurrence was caused by unterminated transmission line characteristics of the actual vehicle cabling. This problem of improper data transmission was solved by modifying the clock output from the AEA to the DEDA. The pulse width was reduced from 2

to 1 msec. Shortening of the clock pulse produced, in effect, a DEDA insensitivity to transmission line characteristics. Apparently, reflection was not considered in the original customer interface specifications or in the circuit design. Initial interface specifications should have considered the vehicle cable characteristics.

Another major change in the system was the addition of an internal clock. A circuit was designed, a circuit board was redesigned, components were specified, and production was underway when a problem arose. The internal clock was found to oscillate at other than the required frequency. This oscillation was due to unwanted modes of the crystal. The crystal was respecified and the circuit was redesigned to correct the design error.

There were several component design changes and manufacturing process changes made in the FEB's. Capacitors used in the D/A converters required redesign after numerous failures occurred. Mechanical design deficiencies within the transformers used in the memory necessitated a vendor change for transformers. Computers containing these defective components are being retrofitted. A vendor change for the switching transistor used in the computer was made after vendor failure in parts qualification occurred. These transistors were unreliable because of purple plague.

During the course of production, numerous product design and manufacturing design changes were made. The most predominant change required wire-wrapping seven or eight matrix boards a second time because of problems with the wire-wrap pigtails.

On the DEDA, a bracket with a rubber gasket was placed over the electroluminescent display and then compressed against the front panel. The panel was trapped in a groove on the front panel and further restricted from movement by the rubber gasket. In addition, a potting compound was used as a sealer for the contacts of the wires exiting from the rear of the

enclosure. However, during assembly of the front panel, manufacturing allowed the potting compound to flow around the face of the electroluminescent display and bond the glass to the front panel. During vibration, the front panel transmitted enough stress to shatter the glass. The problem was solved by removing the potting compound from the glass surface. In addition, the rubber gasket was eliminated as a part of the design. In the final mounting arrangement, the electroluminescent panel was bonded to a bracket with an epoxy and the bracket was mounted to the front panel with four corner studs.

During qualification testing, the electroluminescent display separated from the mounting bracket. Salt spray testing of the same unit also disclosed the inadequacy of the terminal seal potting configuration. Analysis indicated that the separation of the electroluminescent display from the bracket was due to thermal stresses and interferences existing between the DEDA front panel and the electroluminescent display case.

The following actions were taken to ensure the integrity of the electroluminescent display/panel assembly:

1. Tighter process controls were established to ensure adhesive bonding without contamination of the adherents.
2. The front panels were remachined in the vicinity of the electroluminescent display mounting area to remove all possible interference with the front panel.
3. A rubber compound was used to form a gasket between the electroluminescent panel and the front panel. In addition, the rubber was used as a sealer for the electroluminescent panel terminals and the pins on the rear connector. Two important design features were accomplished here:

- a. The electroluminescent panel was essentially captured between the bracket and the front panel.
- b. All terminals associated with the electroluminescent panel were protected from contamination.

The original specification on the electroluminescent display states that all distortion on the electroluminescent display surface shall be kept to a minimum. In the initial display design the vendor inserted a center bar through the center of the electroluminescent display for additional structural support which later had to be removed in order to minimize the distortion of the electroluminescent surface.

The DEDA switches are of the two-pole, double-throw type. The inherent delay between poles of the switch was such that either (1) erroneous information was displayed or (2) discretes were received from the computer before the DEDA was capable of operating on the discrete. The latter is typically a function of the READOUT or ENTR pushbutton on the DEDA front panel.

The wiring on each pushbutton switch pole was changed so that all functionally independent switch poles were made functionally interdependent.

#### 4.2.2 Mechanical Design Problems

The flatness specification on the side plates and the hole location for mounting the AEA in the vehicle were stringent requirements specified by Grumman that were very difficult to achieve in the unit. Meeting these requirements required an extensive amount of tooling in the unit. To maintain the hole spacing across the width of the box, TRW had to use holes to the outside extreme edge of the tolerance allowed and then attempt to pull in the distances between holes during mounting of the assemblies. Compliance with the flatness requirement caused increased thermal resistance between surfaces. Also, the surface tended to

bow or bend as bolts were placed in the holes. A flat surface completely across the plate could not be achieved.

Another constraining requirement was the tight tolerance on the size of the hole itself for mounting the equipment. Later analysis by GAEC showed that the flatness requirements and the tolerances on the mounting holes were unnecessarily tight.

The initial specifications for all three AGS units (AEA, DEDA, and ASA) imposed a vibration transmissibility limitation of 10 on the design. Interchange with Grumman dynamicists resulted in an agreement between the technically responsible personnel that a limitation of this design factor was not critical, but only one indication of an acceptable design. Consequently, a change to a design goal of 10 with a maximum limitation of 20 was implemented. Although this change was incorporated only in the AEA specification, and not in the DEDA specification, it was shown to the satisfaction of TRW and Grumman dynamicists that the high Q is not detrimental to the design, as evidenced by satisfactory passage of qualification testing. AEA and DEDA maximum transmissibility factors ranged from 9 to 24, based upon the design verification test results.

Another requirement from Grumman, enabling them to freeze their interconnection wiring throughout the spacecraft, as that the AEA have pigtail cables exiting from the AEA to mate with Grumman cables that were rack-mounted. An alternate configuration which would have simplified the AEA design would have been to provide box-mounting connectors on all units and mate the spacecraft cables to each unit.

Another point worth emphasizing is the lack of an engineering model. Had it been possible within the schedule and budgetary constraints of the program to build an engineering model instead of a dynamic model, many manufacturing problems would have been more readily solved, tolerances could have been relaxed, and circuit design problems could have been corrected prior to entering the manufacturing phase.

Throughout development of the entire system, because of unit size, volume, and weight requirements, state-of-the-art methods and techniques were required with respect to packaging densities, circuit boards design and fabrication, and interconnection techniques. The matrix, which was very costly, had considerable impact upon scheduling of the unit during the design cycle. The large number of outputs required on each board (due to packaging density on the board itself) forced TRW into a "TRW-make-connector" situation instead of allowing us to use off-the-shelf items or available hardware from other connector companies. TRW designed and built its own connectors to serve this function primarily because of the one-tenth center spacing necessary to get the required connections off the board. The center spacing was dictated by the pitch required between boards to maintain the total length of the unit.

#### 4.2.3 Residual Problem Areas

The major problems remaining are (1) the higher-than-expected rate of random component failures and (2) the determination of causes of these and other intermittent failures during and after acceptance testing. As a result of reliability and weight tradeoff studies a decision was made early in the program to design for minimum weight flight hardware and not for ease of checkout and test. This has increased system reliability, but has also made the computer difficult to troubleshoot and repair.

As a consequence of this design philosophy a minimum number of external test points were provided and all internal test points (covers off) were eliminated because of weight considerations. As a result, the capability for failure isolation testing at the box level is uncomfortably limited. The DEDA essentially has no test points, and the AEA has far too few test points to permit thorough troubleshooting at the module or top level. Board or component level troubleshooting is not, of course, adversely affected by lack of test points on the computer. TRW believes that an adequate number of



test points should have been provided, even at the expense of a small weight penalty. Certainly computer diagnostic capabilities would have been immeasurably improved thereby.

Another problem area concerns the computer test equipment, which has limited diagnostic capabilities. It should be emphasized that this test equipment was designed only as an exerciser and a GO/NO GO indicator. Inherently, very little diagnostic capability was built in. The design philosophy involved ties in closely with the lack of test points on the AEA and DEDA. The unavailability of top level (module) testing, while admittedly an encumbrance, is nevertheless a logical evolutionary product of the original test equipment design philosophy.

#### 4.3 DISCUSSION OF MAJOR DESIGN PROBLEMS OF SOFTWARE

The major software design changes discussed herein were made after the delivery of the baseline Design Mission Computer Program (DMCP). Earlier design changes are discussed in the historical summary of Section 3.

##### 4.3.1 Softwired Program

###### 4.3.1.1 Add Range Rate Input to the Radar Update Equations (SCP1)

The change to the co-elliptic rendezvous mission resulted in insufficient accuracy of the onboard navigation update from the rendezvous radar. This was caused by the longer range, the reduced capability of the MSFN for this case, which placed more reliance on the radar, and the reduced LM fuel budget. The radar update equations were kept simple in the early design stage to save on memory space and were inadequate to handle the mission change.

The solution to this problem was the addition of range rate input (R) to radar update equations which required about 11 additional computer words. Mission changes seem to be unavoidable and, therefore, it is advisable to provide ample equation accuracy as well as

adequate memory space in the airborne computer, provided that other factors such as volume, weight and power consumption remain within the general system constraints.

##### 4.3.1.2 Change in Sign of FDAI Computations (SCP 2)

The LTA-8 tests being performed at GAEC identified an incorrect interface between the AEA and Flight Director Attitude Indicator (FDAI). The FDAI rotated in the wrong direction, due to the wrong sign of the  $\sin \alpha$  output. The LM/AGS Performance and Interface specification provided by GAEC was in conflict with the FDAI instrument.

Two fixes to the problem were considered. One was to reverse the wiring connections in the AEA  $\sin \alpha$  output and the other was to modify the software to "patch" over the hardwired equation. The last solution was considered to be less expensive and was implemented at the cost of six cells of the software memory. The change required a program reassembly, a limited recheck of the program coding and a limited repeat of the program verification testing. It is recommended that more comprehensive coordination and evaluation be invested in the area of interface specification.

##### 4.3.1.3 Predicted CDH Maneuver, Removal of Desired Absolute Time of CDH Maneuver; Predicted CSI and/or CDH Time Limited $\geq 0$ (SCP 5)

It became desirable to allow the crew to examine the predicted CDH solution (via the DEDA) and also to orient the LM to the predicted, desired thrust attitude relative to the real-time local horizon coordinate system (radial, tangential, transverse) prior to the CDH burn. The AGS software did not include this capability.

The flexibility of the original software program was limited due to lack of computer space. Several other modifications made space available, which could be used to increase the software capability and to simplify the crew operating constraints.

The software was modified to provide the required capability. The change included addition of the predicted CDH capability, removal of the Predicted Absolute Time of the CDH maneuver, and limiting of the prediction time to CSI to be  $\geq 0$ .

#### 4.3.1.4 Delete Automatic Exit from Lunar Align (SCP 11)

The automatic exit from lunar align as originally implemented, could result in a loss of a portion of the attitude error pulse counts, resulting in a degradation of the alignment. The automatic exit was eliminated entirely. This solution saved nine program steps.

#### 4.3.1.5 Yaw Steering for S Band Communication (SCP 13)

A new requirement from MSC to maintain earth communication with the LM vehicle required the continuous orientation of the S-band antenna toward the earth, and consequently a specific vehicle attitude about yaw. The steering equations permit the vehicle to continuously rotate about the X body axis under certain circumstances (depending on pitch and yaw angles). The new requirement requires the elimination of this rotation.

The equation for the attitude error about the X body axis was modified. The new mechanization saved two program steps when compared with the original one.

Communication, telemetry and tracking requirements are bound to change during the development of a spacecraft program and consequently, vehicle attitude control equations should be designed with sufficient flexibility to cope with such situations.

#### 4.3.1.6 DEDA "CLR" Change (SCP 14)

A difficulty was encountered in the DEDA operation. Occasionally, double actuation of the CLR pushbutton on the DEDA panel was required for entry of data. That is, the CLR pushbutton had to be depressed twice in succession instead of only once. The basic cause of this malfunction was found to be a logic error in the DEDA. An AEA com-

puter software change was used to fix the problem and required one additional program step. This solution was preferred over a modification of the DEDA.

#### 4.3.1.7 Calculation of Apofocus Altitude and Time to Perifocus (SCP 15)

It became desirable to provide the flight crew with more trajectory information such as apofocus altitude and time to perifocus. The original AGS software did not have this capability. The non-essential navigation computations were limited at the start of the program due to lack of computer space. The equations were modified in order to provide apofocus altitude and time to perifocus. The cost of implementing this change was approximately 15 program steps.

#### 4.3.1.8 Delete Abort and Abort Stage Discretes from Steering Loops (SCP 16)

The initiation logic of the AGS guidance steering was specified by GAEC to include the presence of the abort or abort stage discrete. Consequently, RCS maneuvers could not be executed without arming the descent and ascent main engines. This was considered to be undesirable and MSC requested a modification of the program to increase system flexibility.

A change of guidance logic was incorporated in the computer program, so that the capability of steering without arming the engines will be available at the expense of only one additional program step.

#### 4.3.1.9 Implement Capability to Perform CDH at First or Third Apsidal Crossing (SCP 18)

In order to increase the system capability, it appeared desirable to implement the capability in the AGS to compute the CDH maneuver at either the first or third apsidal crossing. This capability was included in the software. The CSI routine is utilized in exactly the same way as presently done for the first and second apsidal crossing. This modification required 22 additional program steps.

4.3.1.10 Capability of Out-of-Plane  
Maneuvers at CSI and CDH  
(SCP 20)

It became desirable to increase mission flexibility and to be able to perform out-of-plane maneuvers to set up inplane rendezvous maneuvers. The AGS guidance software did not include this capability and a software change was made. The out-of-plane maneuver will be done in the external  $\Delta V$  mode. Only one component of velocity (out-of-plane) need be entered and the usual procedures for performing external  $\Delta V$  followed. The implementation of this technique required ten additional program steps.

4.3.1.11 Generate Node 90° From  
TPI (SCP 21)

In order to allow the final portion of rendezvous to occur in the CSM orbit plane, the TPI maneuver was required to be performed so as to create a node 90° downrange. The midcourse maneuver will then be performed at the node causing the CSM and LM to be in the same orbit. This mode was not available in the existing software, which only provided for a direct transfer mode. It was decided to make this modification which required seven additional program steps.

4.3.1.12 AGS/PGNCS Misalignment  
Correction (SCP 32)

Measurements taken on equipment during the system integration of the LM vehicle at Bethpage indicated a gross attitude misalignment between PGNCS and ASA inertial measurement units. Such misalignment is important in view of AGS to PGNCS alignment and inflight gyro calibration. It was assumed that the ASA was misaligned with respect to the LM body axes. Consequently, software changes were made which allowed the correction of such misalignments. However, it was found afterwards that the measurements had been in error. Therefore, it seems advisable that all input data concerning hardware deficiencies should be thoroughly evaluated and their accuracy absolutely established prior to incorporating software changes.

4.3.1.13 Control Limit on  $\ddot{r}_d$  as a  
Function of Vehicle  
Configuration (SCP 34)

The orbit injection equations were designed to place the LM vehicle in a pretargeted orbit in preparation for the co-elliptic rendezvous sequence. In order to eliminate excessive vehicle maneuvers, a steering constraint was imposed and implemented by limiting radial jerk  $\ddot{r}_d$  in the computations. However, it appeared that the narrow limits on  $\ddot{r}_d$  reduced the ability of the LM to achieve the targeted insertion conditions from a wide range of orbit conditions. It was decided to modify this by allowing larger trajectory perturbations to be removed when ample fuel remains. For this purpose, the  $\ddot{r}_d$  limiting was made a function of vehicle configuration and thrust magnitude. This modification was made at the cost of 12 program steps.

4.3.1.14 Improved Steering in TPI  
Mode (SCP 36)

AGS controlled midcourse maneuvers may be accomplished in the terminal phase initiate (TPI) mode. The AGS computed steering vector appeared to be noisy in these midcourse situations. This steering noise is caused by quantization in the TPI guidance computations. Those factors contributing to noise are small velocity-to-be-gained magnitude and small central angle between LM and CSM target. The effect of this steering oscillation is poor RCS fuel utilization, in addition to disturbing effects upon the flight crew. The steering oscillations are eliminated by using manual steering and AGS attitude hold for attitude control. The midcourse burn is accomplished manually by firing the RCS thrusters until the  $\Delta V$  components as displayed via the DEDA are zero within their noise. This modification saved 14 program steps.

4.3.1.15 Coupling Data Unit  
Deficiency

The AGS receives PGNCS gimbal angle information via the Coupling Data Unit (CDU) and uses this information for alignment and gyro calibration.

Results of test at MIT/IL indicated the existence of CDU transients which would result in large AGS alignment and calibration errors. A hardware change was developed and tested by MIT/IL to eliminate the transients. However, there are no plans to implement this hardware change because of the relatively high cost involved. AGS software changes, which would allow the detection of such CDU transients during the critical periods, would require 45 program steps. No memory space is presently available. Therefore, "work around" procedures were developed by means of which the astronaut could orient the vehicle manually to regions where the CDU transients could not occur.

#### 4.3.2 Hardwired Program

##### 4.3.2.1 Attitude Reference Algorithm

The attitude reference algorithm computes body direction cosines from body axis angular increments. During testing of this algorithm on an interpretive computer simulation, drift rates greater than the design goal of 0.2 deg/hr were noted under low-rate limit cycle environments. These unacceptable drift rates were attributable to quantization in the attitude reference algorithm. The scaling of these equations, and thereby the quantization, is constrained by the maximum abort turning rates of 25 deg/sec per axis and the 17-data-bit computer word size.

These quantization errors could result in significant attitude reference drift during coasting flight. This drift would cause undesirable navigation errors during subsequent thrusting maneuvers and would also degrade the radar update of the LM state.

The remedy was to decrease the quantization errors at low vehicle rates by creating a program with two-way scaling. At low vehicle rates, the attitude reference equations would be scaled to reduce the quantization errors, and at high rates the scaling would return to the original values that were necessary to prevent overflow. The attitude reference algorithm tests the magnitude of the angular increments

from the gyros to determine scaling. Since these equations were in the hardwired memory, a new hardwired program (HO-3) was necessary to accommodate two-way scaling.

#### 4.4 DISCUSSION OF MAJOR PROBLEMS IN SYSTEMS LEVEL TESTING

##### 4.4.1 Integration Test Problems

Test equipment interface, timing, cabling, and logic changes were made to establish proper operation. Some AGS software revisions and minor hardware changes were required for proper test equipment interface. These problems were typical of initial system/GSE integration efforts. Detailed discussion is not warranted, but typical examples follow.

###### 4.4.1.1 GSE Register Loading

An inability to load the GSE register was noted. The cause was that a program error in the GSE service routine caused the AEA to look for GSE 1 instead of TLM stop pulse. The effect was that the AEA could not be loaded from the test set. The GSE service routine was revised. No specific recommendation is applicable. This account illustrates the importance of an exhaustive integration test to discover such routine problems before the production model design is frozen.

###### 4.4.1.2 Counting ASA Output Pulses

An inability to properly count ASA output pulses in the GSE was noted. The deficiency was caused by oscillation of the GSE buffer amplifier. The buffer amplifier was redesigned. No specific recommendation is applicable. This was a typical developmental problem that points out the need for a thorough integration test to disclose such problems before a production model design freeze.

###### 4.4.1.3 Reading AEA Memory

An inability to read from the AEA memory with the test set was noted. A timing problem was involved. An

AEA 20-msec delay instruction was found to be incompatible with the test-set timing requirements. The delay instruction was deleted. It should be noted that numerous similar problems with timing, cabling, switch bounce, etc. were discovered and resolved satisfactorily.

#### 4.4.2 System Performance Test Problems

##### 4.4.2.1 Vibration Test Equipment

The basic problem was extraneous motion, particularly coning, in the vibratory test equipment. Reduction of this motion was mandatory.

Test tables, sway fixtures, vibration fixtures, shakers, etc. have significant noise sources, random and sinusoidal, linear and angular, and over broad frequency ranges. This extraneous motion interferes with inertial equipment performance measurement. A strapdown system is particularly vulnerable to angular vibration, particularly sensitive to correlated cross-axis angular vibration, and hypersensitive to coning.

Initial equipment design must suppress all unwanted motion. Equipment evaluation, with vibration transducers and high-speed optical means, was necessary to measure coning and cross-axis motions before equipment designs were modified to suppress the motion. Power spectral density and cross-spectral density analyses of vibration data were required to identify phase correlations and coning motion. Accurate error modeling was required to identify sensitivities to the extraneous motion.

##### 4.4.2.2 Sway Simulator

The sway simulator machine developed for Earth Prelaunch Calibration (EPC) testing produced excessive angular vibrations at the ASA mounts. This angular vibration masked the test results. The EPC program instrumented in the AEA filters the effect of sway motion and low-frequency coning. The superposition of high-level angular vibration and high-frequency coning caused uncertainties larger than the error being measured.

Equipment mounts, brakes, bearings, and damping were modified and adjusted to reduce vibration. Counter rotation was used to cancel some coning errors and spectral analysis of recorded data identified error term which could be used to correct the resulting test data.

Successful strapdown inertial system dynamic performance testing required accurate error modeling to identify sensitivities to extraneous motion. Extensive monitoring and control of test facilities should be employed as required to constrain errors.

##### 4.4.2.3 Electromagnetic Interference Tests

Performance of the AGS was difficult to establish when exposed to conduct and radiated EMI. When EMI tests were conducted in the established screen room, the AGS was not on a stable foundation. Although it was assumed that short-term stability would be sufficient to detect any effects of electrical interference, the lack of a stable pier seriously hampered the evaluation. In later testing of a similar system, this problem was avoided by setting up the EMI equipment in an inertial lab for susceptibility testing.

PRECEDING PAGE BLANK NOT FILMED.

# APPENDIX DETAILED DESCRIPTION OF MAJOR SUBASSEMBLIES SOFTWARE AND SYSTEM LEVEL TESTING

## 1. DESCRIPTION OF ABORT SENSOR ASSEMBLY

### 1.1 FUNCTIONAL DESCRIPTION

The Abort Sensor Assembly (ASA), a self-contained assembly of the Lunar Module Abort Guidance System, contains inertial sensors and associated electronics. A block diagram of the ASA is shown in Figure 1-1. The ASA senses angular displacements about the LM vehicle orthogonal axes and vehicle accelerations with respect to

vehicle orthogonal axes. The unit utilizes three Norden RI-1139B single degree-of-freedom, floated, rate-integrating gyros, and three Bell Mod VII pendulous accelerometers as inertial instruments. (The Bell accelerometers have been replaced since July 68 with Kearfott type 2401 accelerometers. The ASA description pertains, however, to the old configuration.) The ASA subassembly includes, in addition to inertial sensors, an integral power supply, six inertial sensor pulse rebalance amplifiers,

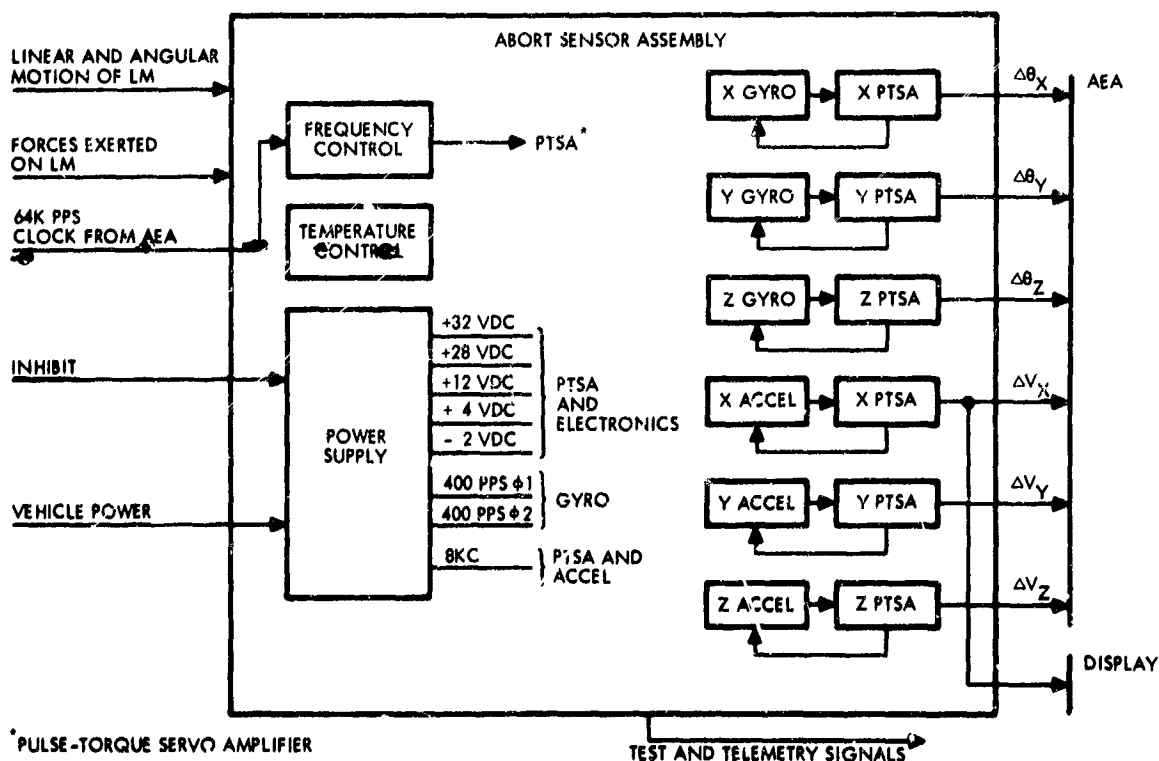


Figure 1-1. ASA Block Diagram

thermal control electronics, a frequency countdown and synchronization unit, and a housing subassembly. The gyros sense angular rotation of the LM about each of the vehicle axes and are pulse torqued to remain at null. The pulses represent incremental body rotations,  $\Delta\theta$ . Similarly, the pulse rebalanced accelerometers measure incremental velocity changes.

These pulses are proportional to incremental vehicle velocity components,  $\Delta V$ , along the respective accelerometer input axes. General requirements of the ASA are:

Maximum design turning rate	$\pm 25$ deg/sec
Maximum design acceleration	$\pm 100$ ft/sec <sup>2</sup>
Sensor scale factors (approximate)	
Angular	$2^{-16}$ rad/pulse ( $\approx 3$ arc sec/pulse)
Translational	$0.00325$ ft/sec-pulse

The gyros and accelerometers are both operated in a torque rebalance or forced-limit-cycle mode. The forced-limit-cycle torquing concept utilizes time modulated, alternating positive and negative current periods synchronized as follows. The switchover from negative to positive is under control of a 1-KHz signal synchronized with a higher frequency pulse train for precise quantization (64-KHz). The switchover from positive to negative is controlled by a servo loop from the sensor's error signal that is summed with a 1-KHz sawtooth voltage but synchronized by the 64-KHz pulse train. This concept is implemented in the LM/ASA Pulse Torque Servoamplifier (PTSA).

The ASA is designed for operate, standby, warmup, and off modes as commanded from the LM control panel assembly. The off mode occurs when no power or signals are provided; the warmup mode occurs when 28-volt LM power and a warmup signal are provided;

the standby mode occurs when only the 128-KHz clock signal and 28-volt LM power are provided; the operate mode occurs automatically under two conditions:

1. A minimum of 40 minutes has elapsed after initiating the warmup signal, including 15 minutes of warmup and 25 minutes of standby.
2. A minimum of 20 minutes of standby has elapsed when the ASA has previously stabilized at operating temperature, normally after a prolonged warmup mode.

#### 1.1.1 Input Signals

The ASA receives three electrical input signals in addition to linear and angular motion input to the sensors.

<u>Signal</u>	<u>Function</u>
28 vdc	Vehicle power
128k pps	Reference for all internal synchronization
Warmup Signal	To select warmup or standby/operate mode

#### 1.1.2 Output Signals

The ASA provides the following outputs:

##### 1. Angular Increment Signals

These signals are developed through gyro rebalance and represent incremental angular changes about the X, Y, and Z axes.

##### 2. Velocity Increment Signals

These signals are developed through accelerometer rebalance and represent incremental changes in velocity along the X, Y, and Z axes.

### 3. Outputs to Display

Separate lines are provided for positive and negative  $\Delta V_X$  signals along the thrust axis. All pulses on an individual line have the same magnitude. The time between successive pulses is some multiple of  $\Delta t$ .

### 4. Block Temperature Signal

This signal is obtained from block temperature sensor No. 1 and is in the form of a resistance output.

### 5. Caution and Warning Voltages

Because this is a man-rated system, the following ASA signals are supplied to the instrumentation subsystem for caution and warning displays.

- a. 28 vdc (precision)
- b. 12 vdc
- c. 29 vac, 400 Hz, phase A.

### b. Test Signals

The ASA provides test signals that are available at the GSE test connector.

## 1.2 PHYSICAL DESCRIPTION AND OPERATING CHARACTERISTICS

### 1.2.1 Physical Characteristics

The physical characteristics of the ASA are:

Weight	20.7 pounds
Size	11-1/2 x 8 x 5-1/8 inches
Power	74 watts

The system can operate within the performance requirements at body rates of up to  $\pm 25$  deg/sec and accelerations to  $\pm 100$  ft/sec. The ASA is designed to meet a MTBF of 4000 hours.

### 1.2.2 Performance Capability

Estimated ASA capability and expected errors during the lunar mission as a function of expected parameter variations are shown in Table 1-1.

### 1.2.3 Thermal and Vibration Environments

The ASA is designed to be operated continuously when the mounting flanges or pads are attached to cold plates that will maintain the foot of the mounting flange between approximately 60 to 80° F during maximum average power dissipation for the ASA.

The system is designed to perform as required in the vibrational environment given in Figures 2-4 and 2-5 of Section 2.

## 1.3 SUBASSEMBLIES/COMPONENTS

### 1.3.1 Inertial Sensors

#### 1. Gyro

The RI-1139B gyro has a permanent magnet torquer that is designed for precision pulse torquing in strapdown applications. The gyro characteristics include torquing capability up to 28 deg/sec with 1.62 watts  $\pm 5$  percent applied to the torque winding, spin-motor rotation detector (SMRD), and ability to operate in a vacuum without a change in thermal paths affecting performance. This sensor weighs 1.53 pounds.

#### 2. Accelerometer

The Bell VII B-8 accelerometer is an electromagnetically restrained permanent magnet torque coil, spring pivoted, hermetically sealed accelerometer weighing 0.38 pound.



Table 1-1. ASA Mission Capability Estimate

Error Source	Unit	Predicted Error
<b>Gyro Fixed Drift Stability</b>		
Time instability (8 days)	deg/hr	0.14
Electrical power variation	deg/hr	0.03
EMI	deg/hr	0.07
Thermal effects	deg/hr	0.04
Vacuum effects	deg/hr	0.11
Magnetic effects	deg/hr	0.01
Residual vibration	deg/hr	0.06
Bias discrepancy	deg/hr	0.07
Total Error (RSS)	deg/hr	0.22
<b>Gyro Vibration and Limit Cycle Induced Error (Powered Ascent)</b>		
Nonlinearity (asymmetry)	deg/hr	0.24
Spin -- Input rectification	deg/hr	0.02
Spin -- Output rectification	deg/hr	0.00
H-vector Spin -- Input rectification	deg/hr	0.02
Anisoelastic drift	deg/hr	0.01
Total Error (RSS)	deg/hr	0.24
<b>Gyro Spin Axis Mass Unbalance Instability</b>		
Time instability (8 days)	deg/hr/g	0.10
Thermal effects	deg/hr/g	0.07
Vacuum effects	deg/hr/g	0.18
Total Error (RSS)	deg/hr/g	0.22
<b>Gyro Scale Factor Instability and Nonlinearity</b>		
Time instability (120 days)	ppm	147
Residual shock	ppm	57
Check instability	ppm	10
Nonlinearity	ppm	65
Total Error (RSS)	ppm	171
<b>Gyro Input Axis Misalignment</b>		
Initial Alignment	arc sec	44
Instability	arc sec	10
Total Error (RSS)	arc sec	45
<b>Accelerometer Bias Instability</b>		
Time Instability (120 days)	$\mu g$	200
Electrical power variation	$\mu g$	2
EMI	$\mu g$	8
Thermal effects	$\mu g$	11
Vacuum effects	$\mu g$	18
Magnetic effects	$\mu g$	2
Residual vibration	$\mu g$	5
Residual shock	$\mu g$	36
Total Error (RSS)	$\mu g$	204

Table 1-1. ASA Mission Capability Estimate (Continued)

Error Source	Unit	Predicted Error
Accelerometer Nonlinearity and Vibration Induced Error		
Nonlinearity	μg	26
Vibration induced Error	μg	30
Total Error (RSS)	μg	40
Accelerometer Scale Factory Instability		
Time instability (120 days)	ppm	34
Residual shock	ppm	6
Check instability	ppm	5
Total Error (RSS)	ppm	35
Accelerometer Input Axis Misalignment		
Initial alignment	arc sec	42
Instability	arc sec	6
Total Error (RSS)	arc sec	42

### 1.3.2 Pulse Torque Servoamplifiers

The ASA contains six pulse torque servoamplifiers (PTSA), one for each of the three gyros, one for each of the two cross-axis accelerometers, and one for the thrust-axis accelerometer.

The gyro accelerometer PTSA's have the same general mechanization, the major differences being in the torquing power levels and frequency compensation networks for the PTSA-instrument loop. The thrust-axis accelerometer PTSA is identical to the cross-axis accelerometer PTSA except for the additional electronics that scale the PTSA data output pulses used in the AEA.

The PTSA supplies the inertial instrument torquer with current to restrain its float or pendulum about its null. The amount of current applied to the instrument is proportional to the inertial inputs. This current is measured by applying torquer current in known discrete amounts. The instrument is rebalanced about its null in this manner every millisecond. The output data is a pulse train whose rate represents a measure of the current supplied to the instrument.

The PTSA contains four components, connected as shown in Figure 1-2.

1. An ac amplifier and pulse-sensitive demodulator
2. A quantizer
3. A current-switching bridge and driver
4. A constant current source.

When the gyro is rotated about its input axis or an acceleration is sensed by the accelerometer, an 8-KHz signal from the instrument pick-off indicates the displacement of the float or pendulum from null. This signal is amplified, demodulated, and applied to the quantizer. By summing the demodulated signal with a 1-KHz ramp function and detecting a prescribed level an output waveform is generated with a duty cycle proportional to the amplitude of the input 8-KHz signal. The zero crossings of the resultant wave furnishes the on-off switching to produce a 1-KHz width-modulated waveform.

The variable duty-cycle waveform is then quantized and used to drive a

four-transistor bridge that reverse current in the torquer for various portions of the limit cycle. The net dc current applied is approximately proportional to the input 8-KHz signal from the instrument. The peak current output is maintained constant through the torquer by the current regulator. The net current supplied to the instrument is of a polarity required to return the instrument float to its null position. The final result is to supply current that balances the acceleration or angular velocity received by the instrument.

The output is a pulse train whose rate is a direct measure of the current feedback to the instrument. Each pulse represents an incremental velocity for the accelerometer-PTSA and incremental angle for the gyro-PTSA.

### 1.3.3 Temperature Control Loops

The ASA contains two temperature control loops: the fast warm-up controller and the fine temperature controller. The fast warm-up controller provides the necessary power for initial warm-up. It uses thermistors and requires less critical control than the fine temperature controller. During calibration the fast warm-up controller turn-off is trimmed to a point just below operate temperature to maximize the unit's heating capability.

The fine temperature controller provides the close temperature control required during the operate mode. The circuit incorporates two platinum sensors and has a pulsewidth modulated output. The fine temperature controller operating point is trimmed during calibration.

### 1.3.4 System-Timing Module

The system-timing or frequency-countdown module accepts a 128-KHz clock input signal and provides as an output all of the timing signals required by the ASA for analog to digital conversion, synchronization, range limiting, and thrust axis signal conditioner data processing.

The frequency countdown also provides 400-Hz and 8-KHz synchronizing signals to the power supply.

### 1.3.5 System Power Supply

The power supply accepts raw LM power as it appears at the output of the EMI filter and processes it through a switching preregulator. This processed voltage is fed to a dc-to-dc converter which takes the preregulator output and generates the ASA dc voltages. The dc-to-dc converter has a self-starting internal oscillator. When the 128-KHz clock is applied, the system timing module provides 8-KHz

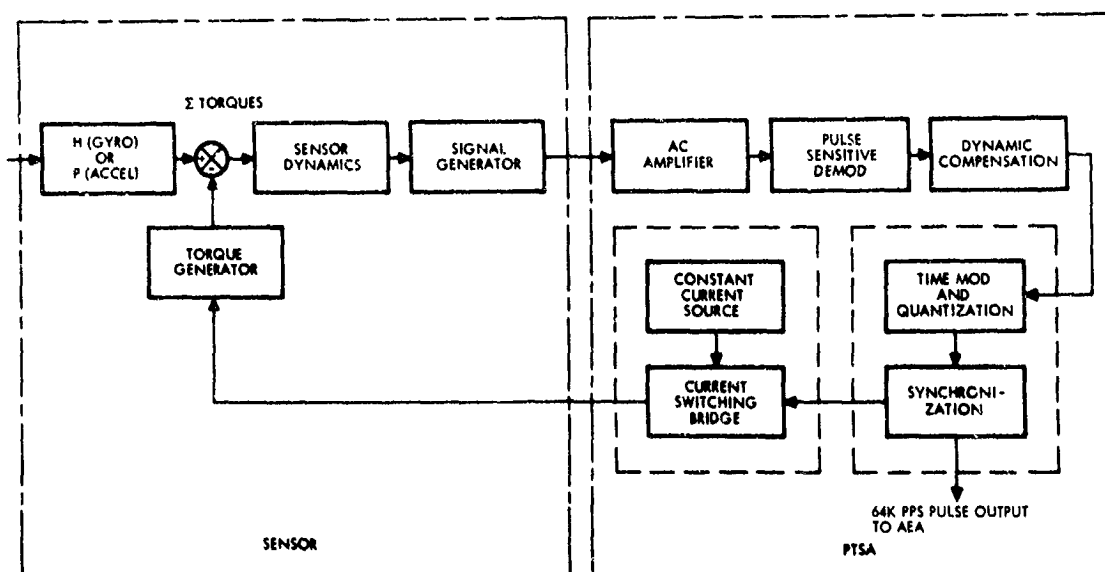


Figure 1-2. Sensor Loop Functional Diagram

synchronization to the converter and the converter synchronizes itself to the timing module. A sense winding on the converter provides feedback to the preregulator for regulating the voltage on the converter output.

A second set of outputs in the form of an 8-KHz square wave is fed from the converter to an 8-KHz filter that filters out the harmonics and provides 8-KHz for the inertial instrument pick-off excitation and PTSA demodulator references. A third converter output is fed to the 28-volt precision regulator that provides the critical bridge bias voltage from which gyro and accelerometer torquer current is derived.

A 400-Hz inverter is in parallel with the converter, across the output of the preregulator. The inverter generates three-phase, 400-Hz drive power for the gyro motors from the preregulated voltage and the 400-Hz synchronization signal from the system timing module.

The power supply has overcurrent and overvoltage protection to turn off the unit when either condition is present.

### 1.3.6 Interface Electronic Module

The interface electronics module provides the signal conditioning and EMI suppression required by the ASA for input/output signal processing. Principally, the module contains the input power filter, spin-motor rotation detector amplifiers, data pulse transformers, and short circuit protecting resistors in the dc outputs.

## 2. COMPUTER SUBSYSTEM (AEA AND DEDA)

### 2.1 COMPUTER DESCRIPTION

#### 2.1.1 Functional Description of the Abort Electronics Assembly

The Abort Electronics Assembly (AEA) is a compact, microminiaturized, high-speed, general purpose computer that contains input/output equipment and a power supply. Figure 2-1 illustrates the computer. The AEA

computer incorporates parallel arithmetic using a data word length of 17 bits plus sign, and utilizes a core memory with a 5-microsecond cycle time. The design incorporates a substantial amount of input/output equipment for the extensive LM interface. All circuits have been designed using "worst-case" design philosophy to meet the stringent reliability requirements of the LM program.

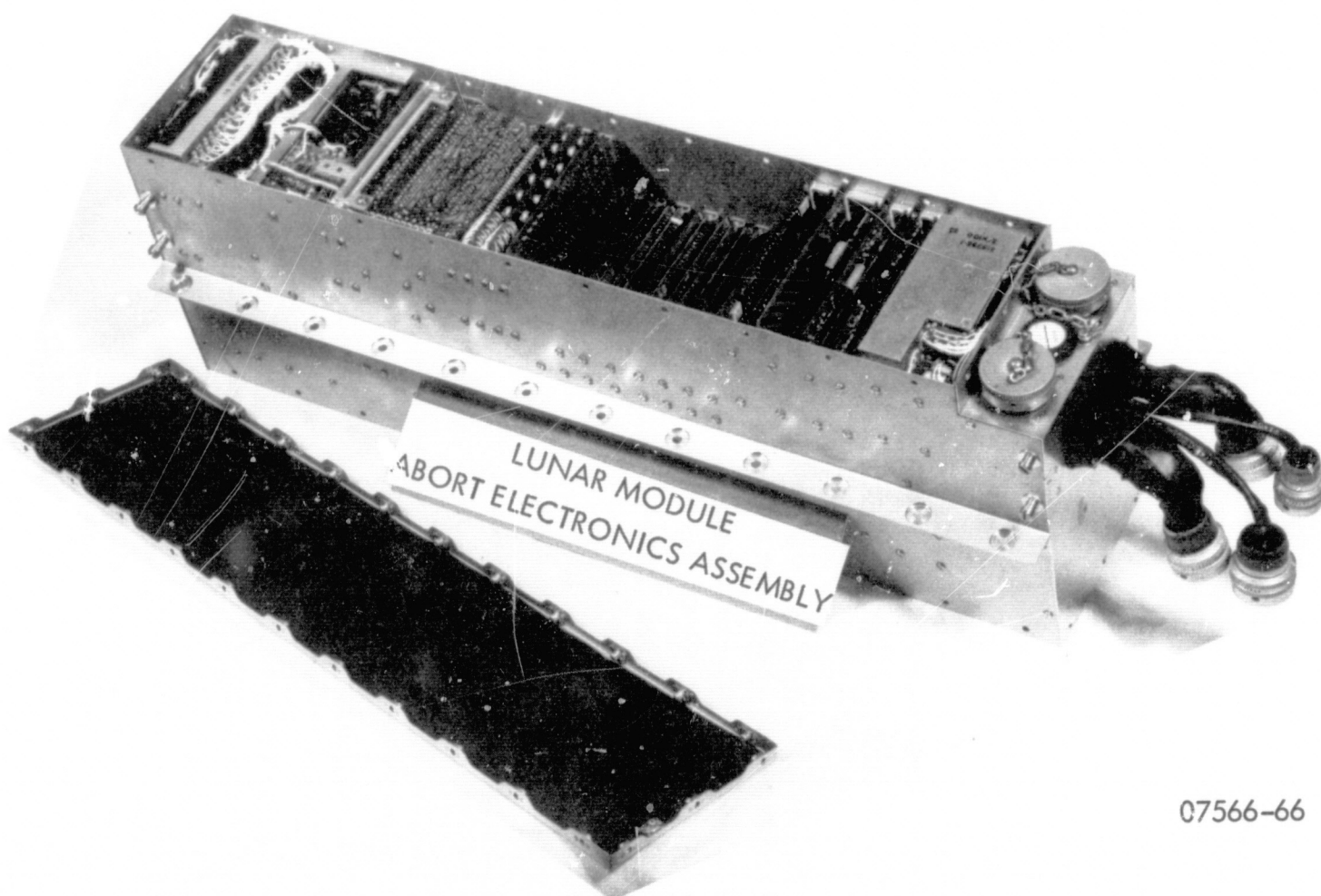
The general characteristics of the AEA are as follows:

- Memory capacity      4096 words
- Clock frequency      1.024 MHz
- Word length            18 bits
- Repertoire             27 instructions
- Computation time:
  - Add      10 microseconds
  - Multiply 70 microseconds

The AEA is contained in a 34-pound package 8 inches high, 5 inches wide, and 23.75 inches deep. The AEA is mounted by attaching the mounting flanges to a set of cold rails to provide fluid cooling. Operating temperature range of the computer is 30 to 120°F.

The AEA requires three power input signals: a 28  $\pm$ 6 vdc line capable of supplying 92 watts, a 400-Hz 115  $\pm$ 2.3 vac line capable of supplying 3.5 watts, and an 800-Hz 28-vac reference signal. All other voltages and reference signals required by the computer are derived from these inputs.

To attain a single-point grounding system in the LM vehicle, the AEA was required to have a minimum of 10 megohms isolation between the computer ground and the chassis and all input/output signals were ac coupled with the exception of certain input discretes. These discretes were switch closures controlled through isolated contacts on a switch or a relay.



07566-66

Figure 2-1. Abort Electronics Assembly

The memory system is a partially hardwired, partially scratch pad, 18-bit, 5-microsecond cycle time, ferrite core type. The memory is currently half hardwired and half softwired with 512 words of the softwired portion being scratchpad. The logic design incorporates an expansion capability for extension from 4,096 words of memory to 8,192. The softwired memory is electrically alterable through established loading equipment.

The AEA must maintain attitude reference, compute attitude errors, perform the explicit guidance computations required, perform inertial navigation with radar updating, calculate midcourse corrections, and generate attitude and navigation display signals. Figure 2-2 is a detailed block diagram of the AEA computer. To accomplish these extended tasks, a complete software package has been developed for the AEA that provides for:

- Symbolic assembly of programs
- Complete bit-bit computer system simulation, including input and output
- Program maintenance, simulation and checkout
- A core-stack wiring program permitting automatic wire listing of the permanent memory.

All logic functions within the computer are implemented from a series of eight types of integrated circuit diode-transistor logic (DTL) elements of the Signetics SE100, milliwatt logic line, the Fairchild 930 element, and an integrated circuit slave clock driver designed by TRW.

The central processor employs a parallel, fractional-two's complement arithmetic unit for 18-bit data words



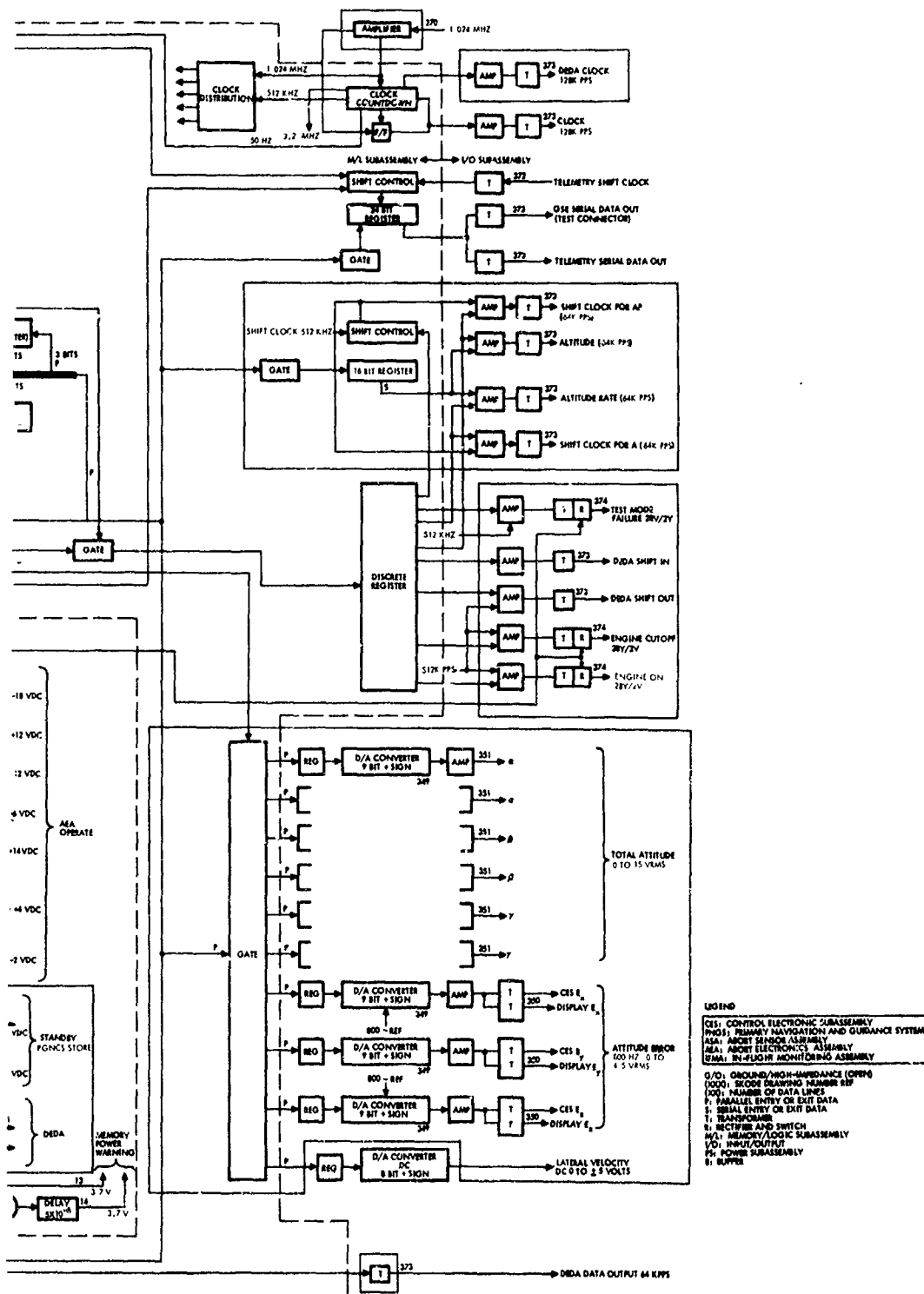


Figure 2-2. AEA Computer Block Diagram

consisting of a sign and 17 magnitude bits. Instruction words consist of 18 bits that contain the 5-bit order code, one index bit, and the address at which the order is to be executed. In cases where an address is not required, the address field is replaced by other data pertinent to the instruction, such as the number of places the data is to be shifted or the number to be placed into the index register.

The memory is of conventional ferrite core construction. It has a capacity of 4096 words.

The AEA instruction repertoire includes 27 instructions that have been selected to provide optimum performance in processing the sensor package inputs and accomplishing other required program functions, while maintaining power consumption at a minimum.

Those instructions most often used, that cause data words to be extracted from the memory, have two modes in which they may be used. The data word may be restored in memory. Or, if there is no further requirement for the data word, the location may be zeroed, thereby reducing the memory power depending upon the I/O bit pattern in the word.

#### 2.1.2 Functional and Electrical Design Characteristics of Major AEA Subassemblies

The memory is an 18-bit, 4096-word, 3-axis coincident current, ferrite core memory system employing a 5-microsecond cycle time and having an access time of 2 microseconds. The memory is divided into two sections of 2048 words each, with the lower address section being volatile and the upper address section containing permanently wired program information. The core material is lithium ferrite, which is oxidation resistant over the operating temperature range, thus eliminating the requirement for a hermetic seal.

The electrical characteristics permit switching times of 0.2 to 2 microseconds, allowing circuit element choices consistent with the memory

cycle time. A sufficiently large voltage-second product of output signal is available to minimize the sense amplifier and timing circuit design.

An analysis of the ONE/ZERO pattern of the data and instructions contained within the volatile section of memory indicated that the number of ZEROS exceeded the number of ONES. Therefore, it was decided to store the information in the core in inverted form, using inhibit current to write ONES instead of ZEROS.

The data inversion is accomplished between the memory buffer register and the cores. Since most of the power consumed in the memory is dissipated in the inhibit drivers, this inverted storage feature significantly reduces the power required by the memory. A further reduction in power is achieved by using a two-turn inhibit winding, thereby reducing the required inhibit current to one quarter select.

The information storage in the memory's non-volatile section is accomplished by bypassing those cores that contain a ONE with the X-axis drive line and eliminating the inhibit winding from this section. Under these conditions there can never be an output from a core that is wired for a ONE and there will always be an output from a core that is wired for a ZERO. If for any reason the information in one of the non-volatile locations becomes altered, it can be restored to its original contents by reading out the location. This is accomplished automatically each time the computer is turned on to assure that the contents of all non-volatile memory addresses are correct.

The read/write drive system employs a closed-loop current regulator to establish precise magnitude of all drive currents.

#### 2.1.2.2 Central Processor

The central processor consists of the following registers and/or functions:

1. Order register
2. Order decode



3. Timing and control
4. Accumulator
5. Adder
6. Quotient register
7. Data bus
8. Index register
9. Cycle counter
10. Program counter
11. Address register.

The central processor is designed to handle fractional numbers with negative numbers represented by their two's complement. The four basic arithmetic operations are performed on command, with subtraction being accomplished by adding the two's complement of the subtrahend to the minuend.

The output of adder bit  $S_j$  may be entered into the accumulator at  $A_j$ ,  $A_{j+1}$ , or  $A_{j-1}$ , to allow shifting to be accomplished simultaneously with addition or subtraction during multiplication or division instructions. The accumulator data is shifted through this mechanism for shift instruction. The quotient register is operated as a normal bidirection shift register when shifting is required.

The cycle counter is used to control the number of iterations during multiplication or division and the number of places data is to be shifted a maximum of 32 places.

The index register is a three-bit register that may be loaded from the data bus and used to modify the three least significant bits of the address register during the data acquisition portion of an instruction. This address modification is accomplished by forming the logic sum (LUI) of L and I. The index register may also be used to control the number of times a subroutine is to be executed.

The data bus is an 18-bit parallel transfer system that may be used to transfer data from any place in the machine to another. These transfers are under the control of the timing and control section and are fixed for all instructions.

#### 2.1.2.3 Input/Output Logic

The I/O logic section of the AEA consists of the following major sections:

1. I/O control
2. Primary Guidance Navigation and Control System (PGNCS) input registers
3. Abort Sensor Assembly (ASA) input registers
4. Input telemetry register
5. Output telemetry register
6. Input discretes
7. Output discretes
8. Altitude/altitude rate register
9. Data Entry and Display Assembly (DEDA) I/O register
10. Input logic buffers.

The I/O control section selects the addressed I/O register and generates the appropriate read/load and reset strobes.

The PGNCS input registers are pulse-integrating registers whose contents are the difference between the total number of positive and negative count pulses that have been supplied to the register since the register was last commanded to clear. This is accomplished by using a shift register and a serial adder/subtractor.

The ASA input registers are 11-bit ripple counters that are advanced one count for each pulse received from the corresponding ASA channel. These

registers are read and cleared at precise 20-millisecond intervals.

The input telemetry register is an 18-bit shift register that accepts the first 18 bits of a 24-bit data word. The PGNCS downlink stop discrete indicates to the computer when the telemetry register is loaded.

The output telemetry register is a 24-bit shift register that is loaded from the accumulator with two output addresses. The AGS telemetry stop discrete is set by the LM telemetry system to signal the computer that the telemetry register has been unloaded.

The input discretes are divided into two words. Word 1 contains all the discretes associated with the LM vehicle and word 2 contains the GSE and DEDA discretes. These discretes are of two types: (1) switch closures and (2) pulse discretes that are sampled and held. The pulse discretes are cleared when the discrete word containing them is sampled.

The output discretes are transistor switches that are fed from a high-impedance power source. When the discretes are set, the voltage drop across the switch is 2 volts or less. When the discrete is not set, the voltage drop across the switch is 14 volts. These discretes are transformer coupled into the computer to maintain the required isolation. This is accomplished by feeding the primary of the transformer with a 512-Hz square wave when the discrete is set. This square wave is rectified on the secondary of the transformer and used to bias the transistor switch on.

The altitude/altitude rate outputs are generated by one common register. Before the information is loaded into the register, the program sets a discrete to identify the type of data the next word will be. When the register is loaded, the data is shifted out automatically.

The DEDA I/O register is a four-shift register that accepts from or outputs to the DEDA. Two related dis-

cretes, shift four bits in or shift four bits out, inform the DEDA of the appropriate action to be taken.

The input logic buffers accept all the pulse inputs and synchronize them with the internal computer clock prior to forwarding these inputs to the appropriate input register. The input logic buffers also provide temporary storage for pulses entering the computer while registers for which they are intended are being sampled.

All signals into and out of the AEA are ac coupled, with the exception of certain discretes and one dc D/A converter. These circuits are isolated from the LM vehicle ground on the receiving end, thus preserving the single-point ground system.

### 2.1.3 Functional Description of the Data Entry and Display Assembly (DEDA)

#### 2.1.3.1 General Description

The DEDA is a general-purpose, manually-operated, input-output device for use with the AEA. Its major external features are a keyboard and electroluminescent data display devices. Figure 2-3 shows the DEDA front panel. The DEDA keyboard consists of ten decimal digit pushbuttons, two sign pushbuttons, and four control pushbuttons. The display registers provide for a three-octal-digit address, a sign plus a five-octal-digit or a five-decimal-digit word, and an operator error indication. The display devices are activated (1) by use of the appropriate pushbuttons, (2) by extraction of data from the AEA, or (3) in the case of the operator error indicator, by certain improper procedures in the use of the keyboard.

Each of the four pushbuttons, CLR, READOUT, ENTR, and HOLD, when pressed, causes corresponding DEDA control discretes to be set in the discrete word 2 registers of the AEA. The DEDA control discretes are buffered switch closures to ground that remain set only as long as the corresponding DEDA control pushbutton remains pressed.

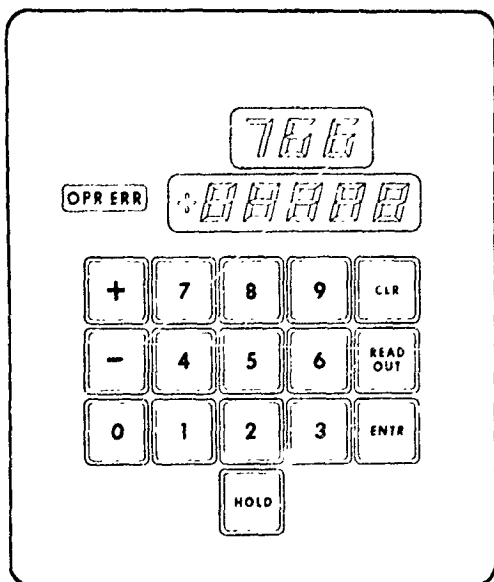


Figure 2-3. DEDA Front Panel

The DEDA is used for manual insertion of data into the AEA and manual readout of data from the AEA. In addition, selection of certain of the operating modes of the flight program and AGS generally is made by appropriate inputs via DEDA.

#### 2.1.3.2 Displays

In addition to the pushbuttons, the front panel contains an electroluminescent panel for numeric display and an incandescent status indicator that lights whenever an operator error condition exists. The status indicator remains lighted until the CLR control pushbutton is pressed. The electroluminescent display three address digits, a sign, and five data digits. Each digit consists of seven line segments.

#### 2.1.3.3 Operation

The DEDA operations is initiated by pressing the CLR control pushbutton. This action enables entry from the digit pushbuttons. As each digit pushbutton is pressed, its code is placed in the register for display in the order that it is pressed (most significant digit first). When the appropriate digits have been entered, the ENTR or READOUT pushbutton can be pressed. To enter information, nine digit pushbuttons must be pressed prior to pressing the ENTR

control pushbutton. To request a readout, three pushbuttons must be pressed prior to pressing the READ OUT pushbutton.

The DEDA register, a four-bit input/output shift register in the AEA, provides temporary storage for data that is being transferred between the AEA and DEDA under the control of the DEDA processing routine in the flight program. The DEDA processing routine initiates or terminates the data transfer in response to the recognition of the setting of the various DEDA control discretes.

A minimum time interval of 80 microseconds is allowed between subsequent settings of either the DEDA shift-in discrete or DEDA shift-out discrete to allow sufficient time for the data transfer.

A maximum of 512 memory locations is accessible in the AEA for data input and output via the DEDA. All of these memory locations are in a fixed designated section of the softwired memory.

The AEA computer recognizes the enter or readout signal and sends the DEDA a shift-in discrete. The DEDA then provides a serial sequence of a data pulse and a shift pulse that is repeated four times and results in the transfer of a digit code to the AEA computer. The computer issues further shift-in disretes and the process is repeated until all digits have been transferred. If the READOUT pushbutton has been pressed, following the entering process, the DEDA will receive a shift-out discrete from the computer. The DEDA will then provide a sequence of four shift pulses and receive four bits of data from the computer in return. The computer issues further shift-out disretes and the process is repeated until the entire word is received. The information is displayed until the AEA computer updates the word or the CLR pushbutton is pressed, the AEA computer will stop sending shift-out disretes after the next complete word has been received. Pressing of the READOUT pushbutton in this mode will cause the AEA computer to resume updating the displayed data.

#### 2.1.4 DEDA Design Characteristics

##### 2.1.4.1 Shift Register

The DEDA shift register accumulates and holds all information loaded from the pushbuttons or transferred from the AEA computer for display. The shift register contains thirty-six bits comprising nine digits. Codes presented from the pushbuttons are loaded directly into the four least significant bits of the register and positioned for display. Address and data bits transferred from the AEA computer are loaded into the least significant bit position of the register. Address and data bits to be transferred to the AEA computer are taken from the most significant bit position of the register. The digit positions of information in the shift register are as follows:

---

MSB			SHIFT REGISTER				LSB		
1	2	3	4	5	6	7	8	9	
Address Digits			Sign Digit	Data Digits					

---

##### 2.1.4.2 Bit Counter

The DEDA bit counter is a six-bit ripple counter that accumulates the number of clock pulses gated to the shift register. This counter is used in conjunction with the digit counter to control positioning of digit codes in the shift register as they are loaded from the pushbuttons. The DEDA bit counter also is used to control the transfer sequence as information is transferred either to or from the AEA computer.

##### 2.1.4.3 Digit Counter

The digit counter is a five-bit shift register counter that is incremented on the final count of the bit counter. The digit counter is used to control positioning of digit codes in the shift register as they are loaded from the pushbuttons. In addition, the digit counter is utilized to detect operator error conditions.

##### 2.1.4.4 Operator Error Indication

An operator error condition arises when pushbuttons are pressed out of sequence during loading of the shift register. A flip-flop is set and the OPR ERR status indicator lights.

##### 2.1.4.5 Data Transfer Sequencer

The data transfer sequencer consists of a two-step counter and miscellaneous flip-flops that buffer control and data pulses transferred from the AEA computer. The sequencer controls the timing of shift pulses information bits transferred to or from the computer and provides control for shifting the contents of the shift register during the transfer. The sequencer is inhibited during loading of the shift register from the pushbuttons.

##### 2.1.4.6 Display Decoding

The display segments for each digit are activated via drivers by outputs from the decoding logic associated with the respective four-bit digit positions of the shift register. As shown below, the three most significant digit positions (1, 2, and 3) of the shift register are decoded to form the address display; the next position (4) is decoded to form the sign display; and the remainder of the digit positions (5, 6, 7, 8, and 9) are decoded to form the data display.

The digit decode for each numeric display provides an output for each segment of the display. The segments are activated in such a manner as to form the decimal numbers. Two outputs are provided by the fourth digit decode to form the sign. The all ONE's code in any digit position of the shift register deactivates the decode outputs, blanking the digit display.

##### 2.1.4.7 Digit Display Decoder

The display decoder provides seven outputs for each four-bit numeric digit position of the shift register. Two outputs are provided for the sign digit. Each output activates an electroluminescent segment of the associated digit display (via a segment driver) when it is logically true.

#### 2.1.4.8 Clock Regenerator

The DEDA logic operates at a clock rate of 128 KHz. The master clock, supplied by the AEA, enters the DEDA via a transformer-coupled circuit and is fed to the clock regenerator. Two clocks of different pulse widths are supplied by the clock regenerator. The clock regenerator consists of two one-shots triggering consecutively. The first clock has a pulse width of 2 microseconds and is used in gating signals from the DEDA to the AEA. The second clock has a pulse width of 400 nanoseconds and is used for internal DEDA logic clocking.

#### 2.1.4.9 Electroluminescent Driver

The electroluminescent driver supplies approximately 19.625 milliwatts for each electroluminescent segment. With 10 vdc impressed across a segment, the brightness of a segment when viewed in a totally dark environment is approximately 0 foot-lambert. The circuit provides protection against electroluminescent segment shorts, thus safeguarding the 115-volt transformer driver from overload.

#### 2.1.5 Environmental Conditions

The AEA and DEDA have been designed to meet the environmental conditions of the LM vehicle and have successfully completed the qualification testing required to establish conformity with these requirements. A summary of these conditions follows.

##### 2.1.5.1 Vibration and Temperature

The following vibration tests were performed on the AEA and DEDA at temperatures of 30°F and 160°F:

##### 1. Non-Operating (30°F)

Sinusoidal 3 octaves per minute each axis

5 to 18.5 Hz at  
0.154-in. double  
amplitude

18.5 to 100 Hz at  
2.7 g

##### 2.1.5.2 Acceleration

Acceleration inputs of +4.7 g and -2.6 g were applied to the AEA along the X-axis in a non-operating condition.

Random 5 minutes per axis,  
15 minutes total

10 to 23 Hz, 12  
db/octave rise to

23 to 80 Hz,  
0.015 g<sup>2</sup>/Hz

80 to 110 Hz,  
12 db/octave rise  
to

110 to 950 Hz,  
0.044 g<sup>2</sup>/Hz

950 to 1200 Hz,  
12 db/octave roll-  
off to

1200 to 2000 Hz,  
0.015 g<sup>2</sup>/Hz

##### 2. Operating (160°F)

Sinusoidal 1/2 octave per  
minute each axis

5 to 30 Hz at  
0.023-in. double  
amplitude

30 to 100 Hz at  
1.1 g

Random 21 minutes per  
axis, 63 minutes  
total

10 to 20 Hz, 12  
db/octave rise to

20 to 100 Hz,  
0.0059 g<sup>2</sup>/Hz

100 to 120 Hz,  
12 db/octave roll-  
off to

120 to 2000 Hz,  
0.003 g<sup>2</sup>/Hz

#### 2.1.5.3 Thermal - Vacuum

Four thermal-vacuum tests were performed on the AEA with the chamber pressure at  $1 \times 10^{-5}$  mm Hg. Test conditions are tabulated below.

#### 2.1.5.4 Shock

A shock test was performed on the AEA in accordance with MIL-STD-810, Method 516, Procedure 1. Test conditions were as follows:

1. Modified shock pulse to saw-tooth, 15 g peak
2. Rise time,  $11 \pm 1$  milliseconds
3. Three pulses per axis, 18 pulses total.

### 3. AGS SOFTWARE

Software is defined as the total computer (AEA) program contained in the hardwired and softwired portions of the memory. The equations programmed into the hardwired portion of the memory are identical in all flight computers (except for a few early prototype computers used for test purposes). The equations programmed into the softwired portion of the memory are subject to change from mission to mission.

In general, the AGS software development has been a highly successful effort with only minor problems encountered. Major changes were necessary to accommodate changing mission requirements. These changes were made without undue difficulty in a timely fashion, although some minor compromises were effected because of AEA memory limitations. This notable success is attributed to the software development and test techniques developed at TRW over a number of years and applied to this program.

#### 3.1 AGS SOFTWARE REQUIREMENTS

##### 3.1.1 Mission Requirements

The AGS must have the capability to successfully guide the LM vehicle to rendezvous with the CSM in the event of

failure of the primary guidance system at any time during LM lunar operations. Abort capability is required from any point in the powered descent (LM landing phase) and powered ascent (lift-off from the lunar surface) trajectories.

The flight profile (Figure 3-1) used to rendezvous the LM vehicle with the CSM is described by the following sequence of events: AGS active guidance begins with abort in powered descent, on the lunar surface, or in powered ascent. The LM ideally undergoes powered ascent to a prescribed altitude above the surface of the moon where it is injected into an orbit that is nearly coplanar with the orbit of the CSM and has a specified perigee and apogee. A fixed amount of time is allowed for coasting, then a horizontal burn maneuver is initiated (thrust parallel to orbit plane of target vehicle and along horizontal of chase vehicle). Given a perfect horizontal burn and a burn into an orbit co-elliptic with that of the CSM at the predicted time of apogee (or perigee) passage, a fixed LM CSM line-of-sight should be acquired at a prescribed time. The orbit of the LM is made concentric with the orbit of the CSM in the process of performing the co-elliptic burn (with the lines of apsides aligned). Then the LM coasts

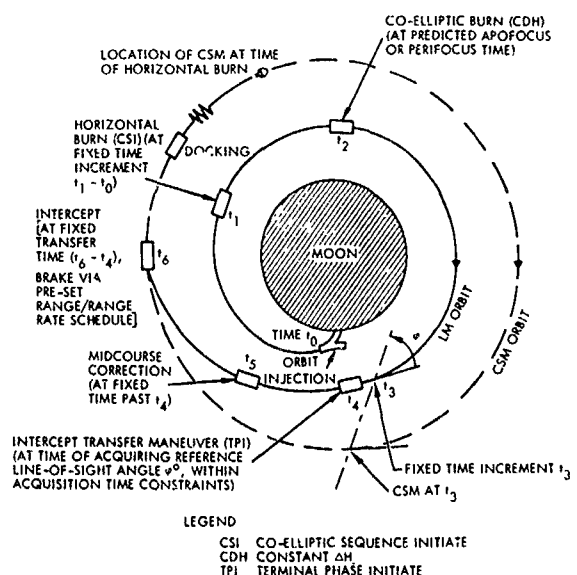


Figure 3-1. Co-Elliptic Rendezvous Flight Profile

in parking orbit. A navigation update can be telemetered to revise the guidance estimates of the vehicle ephemerides. Such a navigational update may also be required, for instance, before the horizontal burn. When the desired line-of-sight between chase and target vehicles is acquired (within certain time constraints), the maneuver to effect rendezvous with the CSM after a fixed transfer time is initiated. This time corresponds nominally to travel through 130 degrees central angle. There exist mechanization errors associated with the execution of the intercept transfer maneuver. The AEA digital radar filter processes information from onboard radar range and range rate observations of the CSM to furnish a relative navigational estimate for the LM vehicle. Midcourse corrections are applied at fixed times past the direct transfer maneuver. The braking maneuvers are executed according to a prescribed range/range rate schedule of events.

### 3.1.2 Basic Computer Program Requirements

The requirements of the program are that it provide the capabilities of:

1. Aligning the AGS to a selected inertial coordinate system
2. Maintaining vehicle attitude information with respect to inertial space
3. Calibrating and compensating the gyro and accelerometers
4. Initializing the LM and CSM state vectors
5. Navigating LM and CSM vehicles
6. Providing monitoring data to displays and ground channels
7. Solving the abort guidance equations according to the co-elliptic flight plan
8. Providing an inflight check of the system logic and memory.

### 3.1.3 Performance Requirements

Three basic accuracy requirements apply.

1. Navigation computation: The maximum error incurred through the powered descent to the lunar surface (about 600 seconds), through 120 seconds of hover, and through powered ascent to orbit insertion (about 420 seconds) shall be less than 2500 feet in each position coordinate and 4 ft/sec in each velocity coordinate.
2. Orbit insertion shall be achieved with pericynthian altitude greater than 5 nautical miles.
3. Abort to rendezvous shall be achieved within a specified sensed  $\Delta V$  expenditure.

## 3.2 AEA SOFTWARE FUNCTIONS

To satisfy the previously mentioned AGS flight program requirements, the following capabilities are provided.

### 3.2.1 Attitude Reference Equations

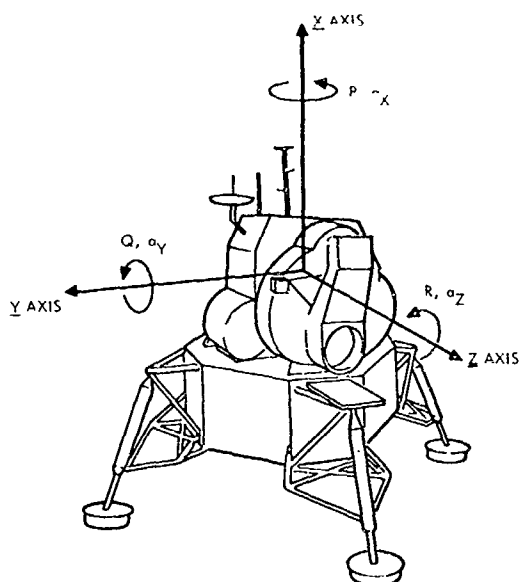
The attitude reference equations maintain an inertial attitude reference in the form of a transformation matrix that relates the vehicle coordinate axes to corresponding inertial coordinates. The equations update the transformation matrix by using angular increments about the vehicle axes received from vehicle strapped-down gyros. The equations provide for alignment of the transformation matrix to reference attitude information.

The attitude reference equations compute and output attitude errors for attitude control. The equations also compute the output attitude in the form of Eulerian angles for attitude display. The inertial attitude reference is maintained in a 3 x 3 orthonormal direction cosine matrix [A] that relates vehicle coordinates X, Y, and Z to the inertial coordinates x, y, and z as follows:

$$\begin{bmatrix} X \\ Y \\ Z \end{bmatrix} = [A] \begin{bmatrix} x \\ y \\ z \end{bmatrix}$$

body                      inertial

The vehicle coordinates are depicted in Figure 3-2 and the inertial coordinates are specified in Subsection 3.2.3.



THE DIRECTIONS OF THE ARROWS ABOUT THE VEHICLE BODY AXES UNIT VECTORS INDICATE POSITIVE ANGULAR RATES (P, Q, R) AND DISPLACEMENT ( $a_x$ ,  $a_y$ ,  $a_z$ ). THE DIRECTIONS OF THE ARROWS ALONG THE AXES INDICATE THE DIRECTION OF POSITIVE TRANSLATIONAL ACCELERATION AND VELOCITY ( $v_x$ ,  $v_y$ ,  $v_z$ ).

Figure 3-2. Vehicle Reference Axes

The equations use compensated gyro inputs to update the transformation matrix whenever vehicle rotational motion has occurred. The equations compensate the gyro inputs for fixed gyro drift and gyro scale factor errors as well as gyro mass unbalance terms along the main (X) thrust axis.

The ASA provides the equations with incremental angular information about the vehicle X, Y, and Z axes and incremental velocity changes along the vehicle X, Y, and Z axes (see Figure 3-3).

### 3.2.2 Navigation

#### 3.2.2.1 LM Navigation

The LM navigation function consists of the computation of the current value of LM position and velocity in the AGS inertial frame. This coordinate frame is nominally aligned as defined in paragraph 3.2.3.1 with the origin at the center of the attracting body.

The navigation equations accept the velocity increment inputs from the ASA accelerometers and transform them from body coordinates to inertial coordinates using the attitude transformation matrix. These inputs are employed to sense LM velocity changes caused by (1) thrust from ascent or descent engine operation, (2) reaction control operation, or (3) external forces. These inputs are accepted by the navigation computations when the acceleration caused by thrust or external forces is greater than a prescribed threshold. The equations compute the velocity changes caused by gravity by assuming a spherical gravity model for the attracting body.

LEGEND:  
i Input Axis  
o Output Axis  
s Spin Axis  
p Pendulous Axis

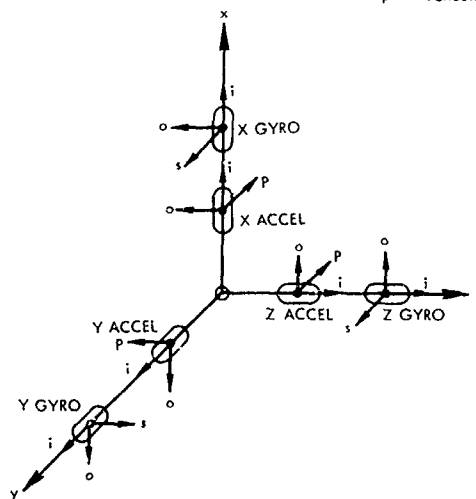


Figure 3-3. ASA Sensor Tread Configuration



The inertial navigation of the LM, when located on the lunar surface, assumes that the velocity remains constant at the initialized value. This navigation is valid within  $\pm 30$  minutes of nominal liftoff time.

### 3.2.2.2 LM Navigation Initialization

If the PGNCS is operating, LM navigation initialization consists of accepting the PGNCS downlink data. If the PGNCS is not operating, LM navigation initialization consists of accepting data inserted in the DEDA accessible memory.

When the initialization is performed in flight, the epoch of the input data is no more than one orbital period earlier than current time, but subsequent to the last time of LM powered flight. When the initialization is performed on the lunar surface, the epoch of the input data should be within 10 minutes of the nominal liftoff time.

### 3.2.2.3 CSM Navigation Initialization

If the PGNCS is operating, CSM navigation initialization consists of accepting the PGNCS downlink data. If the PGNCS is not operating, CSM navigation initialization consists of accepting data inserted in the DEDA accessible memory. The epoch of the input data is no more than one orbital period earlier than current time, but subsequent to the last time of CSM powered flight.

### 3.2.2.4 Time Initialization

The absolute time initialization consists of synchronizing the AGS clock with an external reference time provided via the DEDA.

Absolute time is initialized through the DEDA each time the AGS is placed in operate mode, and will be the difference in current mission time and a known time bias constant. Current mission time is the difference in current Greenwich Mean Time (GMT) and the GMT of liftoff from the earth. The absolute time entered via DEDA is an exact multiple of 0.1 minute.

## 3.2.3 Alignment and Calibration

### 3.2.3.1 Alignment

Alignment consists of initializing the elements of the transformation matrix to obtain attitude reference to a desired inertial reference frame. Given an alignment submodule instruction, the inertial reference frame is aligned to one of the three reference frames described below.

3.2.3.1.1 Inertial Measurement Unit Align (Align to Primary Guidance System). The transformation matrix is initialized to align the computational inertial reference frame to the coordinate system defined by the PGNCS Inertial Measurement Unit (IMU).

For lunar missions, prior to landing, this coordinate system is selenocentric with the X-axis passing through the nominal landing site at the nominal landing time, positive outward from the lunar center. The vector product of the CSM angular momentum vector and the X-axis defines the positive direction of the Z-axis. The Y-axis completes the right-handed orthogonal triad. After landing, the coordinate system is similarly defined except that the X-axis is defined to pass through the launch site at the nominal time of launch.

PGNCS Eulerian angles  $\theta$ ,  $\psi$ , and  $\phi$ , which are the IMU gimbal angles, are used by the equations for this alignment.

The PGNCS provides continuous attitude information to the AGS by means of direct connections between the AEA and the three Coupling Data Units (CDU) associated with the three gimbal angles of the IMU. The AEA contains three 15-bit integrator registers, each of which accumulates the pulses transmitted on a pair of lines from a corresponding CDU. Each pulse produces a one count increment or decrement in the register depending on whether the signal arrives on the plus or minus line.

The receipt of a single pulse represents an angular change of  $360/2^{15}$

degrees in the corresponding gimbal angle. Thus, the range of the data word in each register is 0 to 360 degrees.

**3.2.3.1.2 Lunar Align.** The transformation matrix is initialized so that the x, y, and z axes coincide with the axes of a selenocentric coordinate frame with the X-axis along the lunar local vertical positive outward from the lunar center, and the Z-axis direction obtained by forming the vector product of the unit angular momentum vector of the CSM orbit with a unit vector along the X-axis.

The compensated velocity increments from the ASA Y and Z accelerometers are used by the equations to determine local vertical with respect to the instantaneous vehicle coordinates.

The vehicle azimuth angle with respect to the CSM orbit plane at lunar touchdown is determined by storing, upon command via the DEDA, the AGS azimuth reference, as defined by appropriate elements of the direction cosine matrix.

An azimuth correction angle can be subtracted from the stored azimuth reference to compensate for the effects of lunar rotation during lunar stay time and for any CSM plane changes (computed by Mission Control). The azimuth correction angles,  $\Delta\delta$ , is inserted via the DEDA, in octal, prior to commanding lunar align. The angle is limited to  $\pm 5$  degrees. For azimuth correction angles greater than  $\pm 5$  degrees, alternate terms can be input via the DEDA, in octal, prior to commanding lunar align.

**3.2.3.1.3 Body Axis Align Submode.** The transformation matrix is set to a unit matrix. Thus, the inertial reference frame is aligned to the vehicle reference frame at the time of alignment completion.

### **3.2.3.2 Gyro Calibration**

**3.2.3.2.1 In-Flight Calibration.** The AGS program provides inflight calibration to automatically update gyro drift

compensation. This calibration takes place during free-fall periods. The time required is 5 minutes. The gyro drift calibration uses the PGNCS IMU Eulerian angles as the reference.

**3.2.3.2.2 Lunar Surface Calibration.** The AGS program provides gyro calibration to automatically update gyro fixed drift compensation while the LM is resting on the lunar surface. The calibration time is restricted to 5 minutes. An IMU align or lunar align must take place prior to lunar surface calibration. The program initially stores the existing direction cosine matrix to provide a reference attitude. The input angular increment is corrected for the lunar rotation rate. As for inflight calibration, angular errors of the AGS indicated attitude (as defined by the direction cosine matrix) with respect to the reference attitude are computed and used to maintain the AGS attitude aligned with the stored reference attitude and also to correct the gyro drift compensation.

### **3.2.3.3 Accelerometer Calibration**

The AGS program provides inflight calibration to automatically update accelerometer static bias compensation. This calibration will take place during free-fall periods. This calibration can take place concurrently with the inflight gyro calibration or upon separate command. The calibration requires 30 seconds. The accelerometer bias calibration is based upon the accelerometer outputs during free fall.

### **3.2.4 Radar Data Processing**

Radar updating consists of accepting and processing rendezvous radar data input via the DEDA and updating LM navigation. The radar data consist of:

- Radar range
- Radar range rate
- An instruction entered into the AEA via DEDA at the instant when the radar pointing error, with respect to the Z-body axis, is nulled. The instruction causes the Z-axis direction

cosines to be stored in the AEA. Radar range is entered into the AEA within 30 seconds of the instant when the pointing error is nulled.

The equations accept the input data without any data editing or ambiguity checks. This data is processed in a manner to reduce velocity error of the LM with respect to the CSM. The radar data is combined with the inertial data to estimate relative position and velocity of the LM. Radar misalignments, systematic errors, drifts, and biases are not determined in the estimation process.

### 3.2.5 Guidance Routines

The AGS program contains the following guidance routines:

- Orbit insertion routine
- Co-elliptic sequence initiate (CSI) routine
- Constant delta h (CDH) routine
- Terminal phase initiate (TPI) routine
- External  $\Delta V$  routine

These routines are available for selection via the DEDA.

The orbit insertion routine provides attitude commands and engine off commands to obtain predetermined cutoff conditions.

The co-elliptic rendezvous maneuver is initiated by the co-elliptic sequence initiate (CSI) burn followed by the constant delta h (CDH) burn. The co-elliptic sequence initiate routine computes the magnitude of the horizontal velocity increment (parallel to the CSM orbit plane) required to satisfy the targeting conditions, input via the DEDA.

The magnitude of the CSI burn is computed such that, after the CSI and CDH maneuvers, the LM arrives at the desired TPI time with the desired LOS angle to the CSM.

The constant delta h (CDH) routine computes the attitude commands and velocity increment required to make the the LM and CSM orbits co-elliptical. The computation is based on the predicted positions and velocities of the LM and CSM at the time of the CDH burn. This predicted time of the CDH burn need not be updated following the CSI maneuver. The CDH routine provides commanded attitude such that the horizontal component of the vehicle X-axis thrusting is parallel to the CSM orbit plane.

The terminal phase initiate (TPI) routine calculates the necessary LM velocity increments to place the LM on a direct intercept transfer trajectory with the CSM. A DEDA input of the desired LM transfer time is required.

The external delta V routine accepts the components of a  $\Delta V$  vector input via the DEDA. A commanded attitude is generated to maintain the X-axis toward the vector resultant of these components in real time, independent of the required burn time.

### 3.2.6 Attitude and Engine Control

The attitude errors are defined as angular errors of rotation about the three vehicle axes X, Y, and Z. The corresponding attitude error signals are designated  $E_x$ ,  $E_y$ , and  $E_z$ , and are functions of the particular system operating mode.

1. In the alignment mode, the attitude error signals are set to zero.
2. In the attitude hold mode, the attitude errors cause the LM to maintain the same inertial attitude existing at entry into the submode.
3. In the guidance mode, the attitude error signals produce that vehicle attitude and thrust direction required to satisfy the guidance logic.
4. In the acquisition mode, the attitude error signals cause the +Z-body axis to be pointed

in the estimated direction of the CSM. This facilitates radar lock-on.

When in active control, the AGS issues an engine on command only if the flight crew provides manual ullage with the reaction control system jets. The AGS must sense a low acceleration for approximately six seconds before an engine on command is issued. The engine off command is generated automatically when the velocity-to-be-gained decreases to a prescribed value.

### 3.2.7 Displays

#### 3.2.7.1 Total Attitude Display.

The sines and cosines of the flight direction attitude indicator Eulerian angles,  $\alpha$ ,  $\beta$ , and  $\gamma$  are computed from the transformation matrix to provide outputs for total attitude display. This total attitude information is computed every 40 milliseconds for all vehicle attitudes.

#### 3.2.7.2 Attitude Error Display

The attitude errors are output for displays at all times. Actual utilization of these errors depends upon several switch settings in the LM cockpit.

#### 3.2.7.3 Navigation Display

The following quantities are computed from the navigation computations to provide outputs for navigation displays:

1. Altitude — The difference between the magnitude of the position vector of the LM vehicle in the AGS attracting body centered coordinate system and the value of the LM launch site radius is computed and output at a rate of five times per second.
2. Altitude Rate — The altitude rate of the LM vehicle is computed and output at a rate of five times per second.

3. Lateral Velocity — The Y-body axis component of the LM vehicle total inertial velocity in the AGS attracting body centered coordinate system is computed and output at a rate of five times per second.

Special computations for DEDA display are as follows:

1. Velocity — The magnitude of the LM vehicle inertial velocity is computed and made available for output via the DEDA.
2. Range to CSM — The magnitude of the relative position vector of the CSM with respect to the LM is computed and made available for output via the DEDA.
3. Range Rate — The range rate along the LM line of sight to the CSM is computed and made available for display via the DEDA. Range rate is positive for opening range.

### 3.2.8 AGS Downlink

The AGS supplies one digital output telemetry word every 20 milliseconds. Each output word contains 24 bits, the most significant 6 bits being an identification (ID) code and the least significant 18 bits comprising one AGS computer word.

The output data is comprised of a 50-word block of computer memory, the output of which is repeated every second. At the end of each second, the program is initialized such that the next word output will be the first word of the block. At the same time, six current direction cosines are stored in the block for later output.

### 3.2.9 PGNCS Downlink Telemetry

Data is transmitted serially over the PGNCS downlink telemetry line to the AGS at a rate of fifty 40-bit words per second. The downlink telemetry

register in the AEA, an 18-bit shift register, provides a means for accepting the PGNCS downlink data under appropriate conditions.

The data is loaded into the downlink telemetry register under the control of clock pulses supplied by the instrumentation subsystem at a rate of 51,200 pps.

### 3.2.10 GSE Service Routine

The hardwired portion of the AEA flight program contains a GSE service routine to provide the capability for loading the softwired (erasable) portion of the AEA memory with data supplied from ground support equipment, either BTME or ACE to the downlink telemetry register. Initiation of data transfer is controlled by the ground support equipment.

For loading the softwired portion of the flight program via ACE, where verification of the accuracy of data transfer is required, the flight program load and verify routine is used. In this event, the flight program load and verify routine is loaded into the AEA in advance of the flight program by means of the GSE service routine.

### 3.2.11 Inflight Self Test

The inflight self-test checks on a continuous basis that the computer's logic and memory are functioning properly. A DEDA selection is used in conjunction with the test to indicate test results and to allow resetting of error indications.

The logic test checks the operation of all computer instructions except those associated with input/output operations. The memory test performs a checksum of all hardwired memory plus a portion of the softwired memory that contains fixed data.

### 3.2.12 DEDA Processing

The DEDA processing routine provides for read-in, decoding and storage of instructions and data, and processing and readout of stored flags and data

through the DEDA. All transfer of information is initiated under control of the DEDA discretes.

Data is processed in two forms, octal or decimal. Octal words consist of a sign and five octal characters. Decimal data consist of a sign and five characters. Decimal parameters have an associated scale factor stored in the computer's memory.

All data transfer is initiated by the clear discrete. Upon sensing the clear, the routine sets up the clear mode, during which it awaits either an enter or a readout discrete.

Upon sensing an enter discrete, the routine inputs and processes the data contained in the DEDA shift register.

Upon sensing a readout discrete, the routine reads in the address of the requested data from the DEDA shift register. Thereafter, the requested data is output twice per second until either a hold or a clear discrete is sensed. A hold discrete will cause the last output data to be held until the readout discrete is again sensed. This will reinitiate output twice per second.

The program accepts data without any reasonableness checks except that the program checks input data for the presence of the DEDA error code, indicating operator procedural errors.

### 3.2.13 AEA Program Coding Organization

The AEA program is distributed time-wise between 20-millisecond, 40-millisecond, and 2-second routines. The ASA input data is processed every 20 milliseconds. The attitude error signals (steering commands) and engine signals are generated every 40 milliseconds. The guidance routine computations are repeated every 2 seconds.

The coding is divided equally between permanent (hard) and temporary memory.

The hard memory contains:

- ASA data processing

- Attitude reference
- Navigation (about one-half of the navigation equations)
- Self-Test
- Certain guidance subroutines
- Auxiliary routines (sines, cosines, etc.)
- DEDA Processing (about half of this logic)
- Alignment
- Tape load

The soft memory contains:

- All program constants and instrument compensation
- Guidance routines
- Calibration routines
- Executive logic (for the most part)
- Radar filter
- DEDA processing
- Navigation
- Scratch pad

### 3.3 SOFTWARE DEVELOPMENT AND TESTING

#### 3.3.1 Software Development Concept

The software development concept implemented by TRW for the AGS software is based on a set of formal procedures and documentation developed on other programs beginning with the Ranger program (launch) vehicle guidance) in 1963. The objectives of these procedures are to ensure software:

- Technical adequacy
- Accuracy
- Compatibility with program objectives

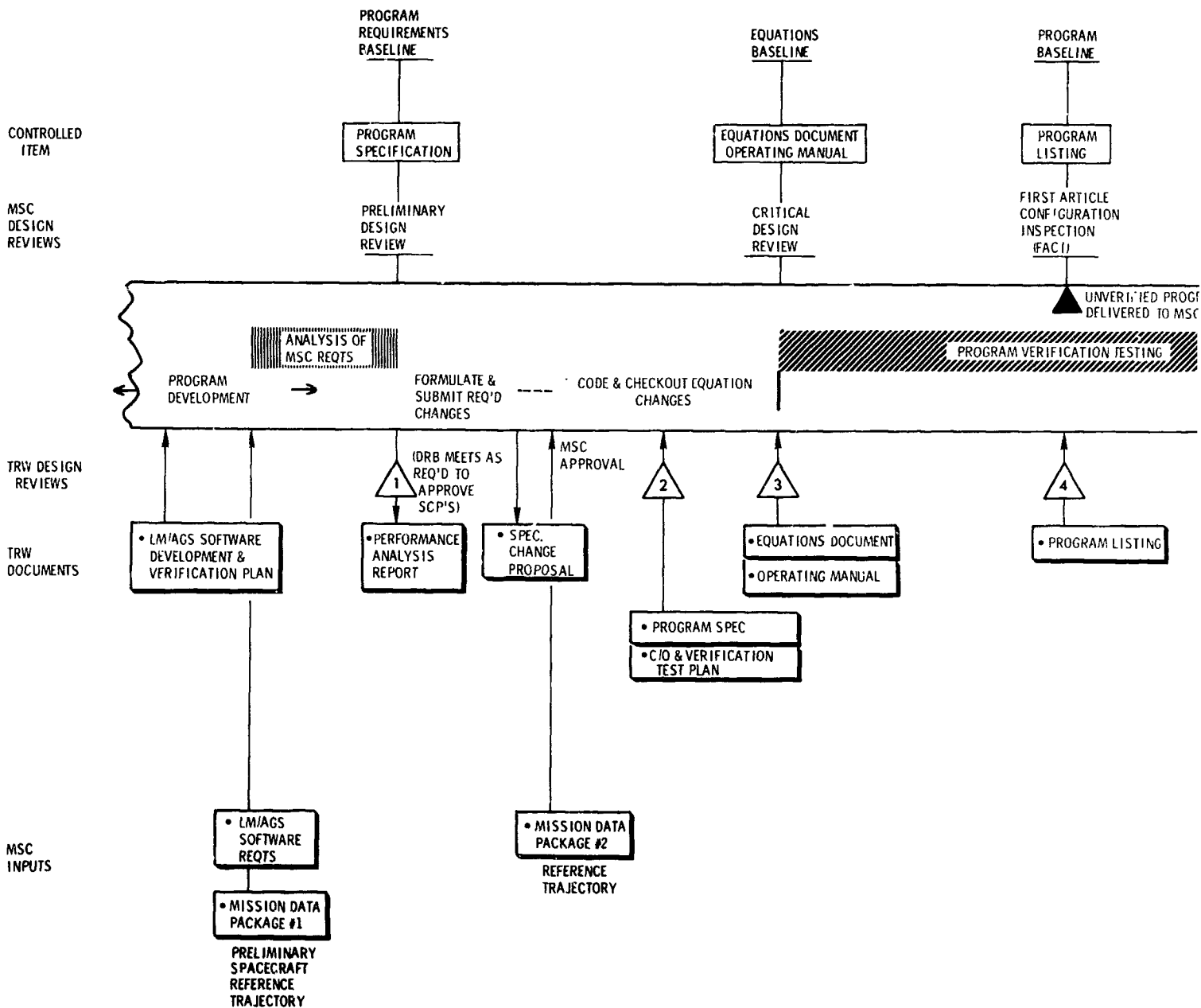
This is achieved by:

- Systematic documentation
- Software configuration control
- Comprehensive design reviews
- Simulation
  - Scientific flight simulation (FS)
  - Performance analysis
  - Interpretive computer simulation (ICS)
  - Hybrid (analog/digital)
  - Combined ICS/FS
- Hardware/software compatibility testing

Figure 3-4 shows the development flow for the AGS software, and also indicates the major design reviews conducted during the development process. Also shown are the baseline documents used for software configuration control and their relationship to the development flow.

#### 3.3.2 Software Verification Testing

The importance of thorough verification of a flight guidance program is obvious because even a single mistake may result in serious consequence. The AGS verification is conducted in accordance with test plans for the ICS/FS tests (interpretive simulation) reviewed by senior engineers. The results of the test are carefully examined and compared with results of similar tests conducted on other simulations (e.g., the scientific simulation). The test results are also compared with specification values. The program specification, a TRW document, is generated early in the program development cycle to provide a record of TRW's interpretation of the general mission and functional requirements for the AGS. This specification is consistent with the Grumman performance of interface specification on the AGS, which details vehicle and other data applicable to the software.



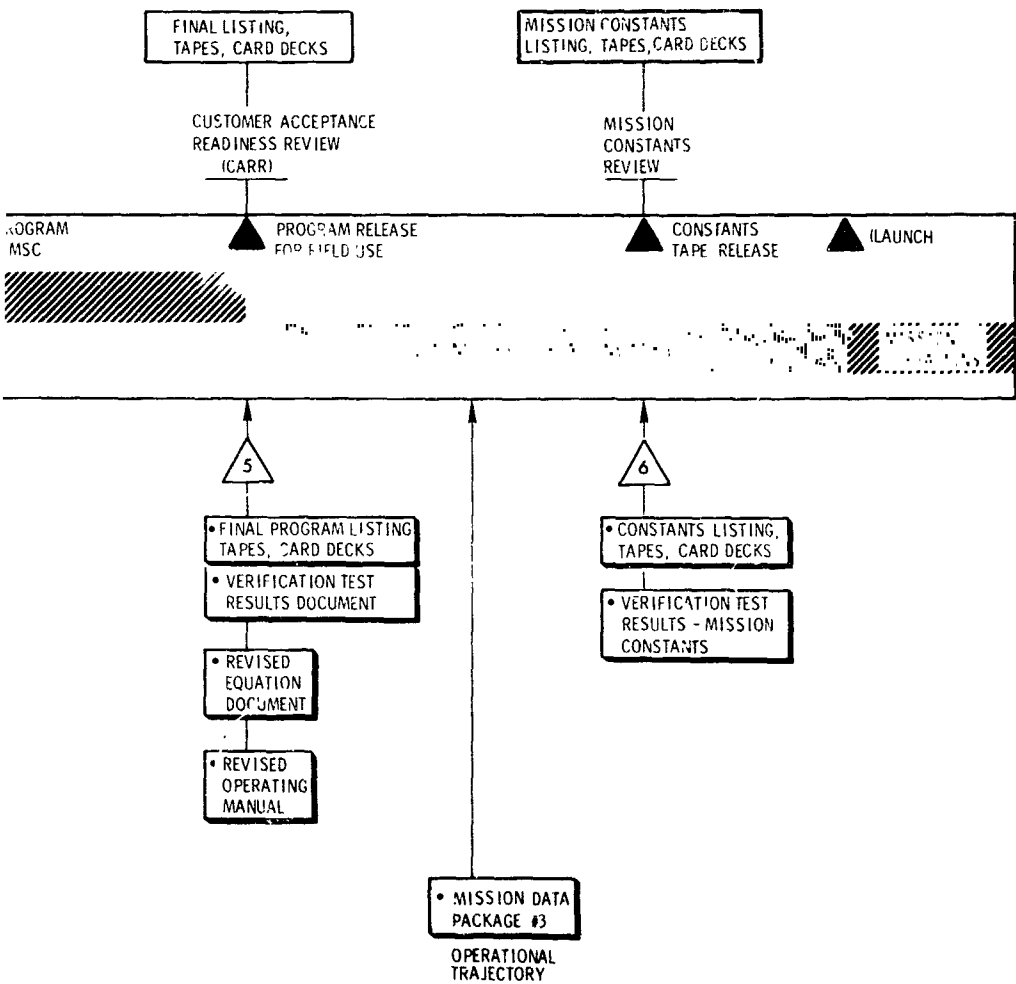


Figure 3-4. Configuration Control and Documentation for LM/AGS Software



Additional control over the program verification is exercised by the generation of documents that explain in detail the purpose, the nature, the theory, and the coding of the flight program.

All program development and verification are reviewed by a Design Review Board (DRB). This board examines requirements, concepts, test plans, analysis results, equation formulation simulation results, and equation and program documentation.

#### 4. SYSTEM LEVEL TESTING

##### 4.1 OVERALL TEST PROGRAM DESCRIPTION

AGS system level testing performed at TRW included three types of tests:

1. Design proof (engineering) tests
2. Qualification tests
3. Acceptance (compatibility) tests

Design proof tests provided data for an engineering evaluation of AGS performance by verifying design principles, proving modifications, and exploring unexplained phenomena. Extensive qualification tests proved the system could perform according to the specification in the environments of the Apollo Mission. Acceptance (compatibility) tests verified workmanship and compliance with the approved design of each production system. All of the above tests can be considered system performance verification tests.

This test program included measurement of system performance during linear vibration, angular vibration, EMI, thermal vacuum, sway and coning environments, exercising system functions of attitude reference, navigation, and self calibration. It is believed that, during these environments, testing of system performance (accuracy) as opposed to survivability testing, was more extensive than previously accomplished on an inertial guidance system.

Another aspect of the TRW test program not in common use elsewhere is the performance of mission analyses for the acceptance test of each production AGS.

Due to the complex and critical nature of the mission, the conventional acceptance test practice of bounding all of the individual terms in the AGS error model is not an efficient way of controlling or estimating the mission performance.

As an integral part of each AGS acceptance test, a detailed error model is prepared, using actual test data where available on an individual system. Other errors are modelled statistically from the ensemble data for all AGS's tested, and from qualification and proof test results.

Using this statistical error model, a Monte Carlo type mission simulation is flown, and the critical parameters (total fuel required and pericynthian altitude) are evaluated against specified limits.

Conventional limits are also applied to each measured parameter as reliability indicators. Each AGS is therefore accepted on the basis of individual mission performance as well as on conformance to reliability criteria.

##### 4.2 AGS INTEGRATION

###### 4.2.1 Initial Integration Testing

The first phase of design proof testing successfully demonstrated that the three major assemblies of the AGS would function properly as a system. The demonstration included use of the bench test and maintenance equipment and some of the flight software programs. The test was designed to verify that each assembly operated as part of the AGS and that interfaces between assemblies and between each assembly and the test equipment were satisfactory. With some logic changes to the test equipment and evolution development of test software, the system compatibility was satisfactorily demonstrated.

The power supply voltages to the assemblies were checked and satisfactory operation of the assemblies was verified. The AEA was exhaustively tested with several softwired memory programs, which were loaded via the test set and performed to verify computer memory and input/output functions.

The critical AEA/ASA interface was checked out during the performance of the input/output test. The portion of this test that verified the AEA/ASA interface was called the ASA input counters test. It compared the AEA pulse counts and the test set pulse counts, made simultaneously from the ASA under various operating conditions. additional verification of this interface was accomplished as part of the subsequent testing.

The next test of the series checked the DEDA functions and the DEDA/AEA interface. The required DEDA functional routine was loaded into the AEA and all DEDA logic and pushbuttons were exercised. This operation included reading data into and out of the AEA, performing improper commands to verify the error logic, etc.

The performance of the ASA was verified by a series of sensor calibrations. A special program was loaded into the AEA to accumulate pulses from the ASA in the six calibration positions and to compute the calibration coefficients. In this test the AEA served as a data collector and processor. Compensations were computed by the same calibration program for use in the flight program to correct for the deviations of the inertial sensors from nominal.

As an additional system test, the portion of the flight program that computes the direction cosines of the attitude reference was inserted into the program and checked. The compensations from the automatic calibration were inserted via the DEDA, and the ASA attitude was varied. The ASA inputs were processed internally to the AEA to give the direction cosines, which were compared with the expected values.

An integral part of the aforementioned tests was testing the AGS software. The routines for memory access were checked out in loading a program and in making normal and special readouts from the memory. When a problem arose in testing, it was sometimes necessary to perform a memory dump to obtain data to isolate the problem.

Another phase of the integration test was the waveform test, which consisted of measuring the characteristics of every signal between AGS assemblies and of every AGS signal output. Characteristics measured and then compared with design control and interface specifications included: period, amplitude, rise time, fall time, pulse-width, noise levels, etc. for pulse signals; period, amplitude, and noise levels for ac signals; and amplitude and noise levels for dc signals. The criterion for issuance of each discrete signal was verified along with the response to each discrete input signal. These tests produced excellent results, giving a general confirmation of the AGS hardware and hardware/software interfaces.

#### 4.2.2 Test Set

The AGS test set, with analog test capability and limited counting and logic capability, was designed and built to test the AGS or any of its assemblies. This special purpose test set was selected over a general purpose computer originally because of the limited digital capability of the AGS. Subsequent program redirection greatly expanded the digital requirements. Ultimately, the capability for digital processing, storage, special programs, high-speed recording, etc. was developed external to the test set. Had it been known what final form the AGS would take, the best approach would have been to design the test set around a high-speed data recording and general purpose computer test facility at the onset.

#### 4.3 SYSTEM PERFORMANCE TESTING

The following performance tests were planned to evaluate the performance of the AGS as part of the design

proof test, qualification test, or acceptance test:

- Linear vibration
- Angular vibration
- Thermal/vacuum
- Earth prelaunch gyro calibration (sway)
- Navigation
- Coning
- Calibrations
- Electromagnetic interference.

The AGS test program attempted actual measurement of total performance errors, and isolation of all important dynamic error terms (e.g., anisoelastic, spin input rectification coning, scale factor asymmetry rectification, vibropendulous rectification, etc.) under mission level sinusoidal and random vibration, both linear and angular. During the test program planning and execution, considerable attention was given to the reduction of spurious motion, cross vibration, coning, etc. Vibratory test facilities and techniques were selected and modified to assure inertial stabilities and position repeatabilities of arc seconds, and sophisticated data recording and analyses techniques had to be employed to separate the residual equipment errors. For example, determination of unwanted coning in random vibratory motion was achieved by means of cross-spectral density analyses of recorded gyro data.

In every dynamic test environment attempted (random vibration, sinusoidal vibration sway) resolution of performance measurements to the desired level (approximately 0.1 or 0.2 degree per hour) was accomplished with some difficulty.

#### 4.3.1 Linear Vibration

The ASA was subjected to various linear vibration environments (both cardinal and skewed) while the AEA accumulated pulses and computed

velocity and position. These parameters were initialized to zero at the beginning of each test run, so that the values at the end of a given time were easily compared to the expected values from prior computations. The ASA vibration was initiated immediately after the beginning of the data collection interval and was terminated before the end of the interval.

Errors in velocity caused by vibration were also determined from the differences in the results of the dynamic run and a preceding static run of the same duration. As an intermediate step in the evaluation, the pulse counts accumulated by the AEA were also evaluated. Differences in performance could be traced to the assembly generating the differences.

The equipment used for the test was a simple shaker actuating a plate restrained to linear motion by special V-grooved and T-shaped bearings. Inputs were random between 10 and 2000 Hz with amplitudes and profiles dependent upon the test purpose. Sinusoidal sweeps were also employed. All test levels were based upon the design specifications.

The problems of (1) determining the attitude of the ASA and (2) utilizing the then current sensor biases and scale factors to compute expected values from the vibration runs were bypassed by the differencing method. Performance during each vibration run was determined by differencing the results of the dynamic run and a preceding static run of the same duration. This differencing technique removed all sensor errors except short-term sensor instability. Subsequently, the method was altered to help reduce the short-term instability error by replacing the static run with the average of two stat. runs, one made before and one after the dynamic run.

#### 4.3.2 Angular Vibration

The angular vibration test was conducted similar to the linear vibration test. The ASA was vibrated about the cardinal axes and the 45-degree skewed axes. Performance during each vibra-

tion run was determined by the difference between the attitude rates for the dynamic run and the average of two adjacent static runs. The orientation at the beginning and end of the test was maintained within arc seconds to minimize test errors.

A large flat plate riding on an oil-film-coated granite block was used for the test. The plate was pivoted in the center and was oscillated about the pivot by two linear shakers (one on each side) connected to perform push-pull motions.

The ASA was attached to the flat plate and various fixtures were used to obtain the desired orientations. The resulting test motions were relatively free of extraneous inputs such as coning and linear vibration. Closed-loop control of the vibration amplitude and frequency was maintained by use of a feedback signal from a linear accelerometer located 30 inches from the center of the rotation.

Specially shaped profiles of random vibration from 10 to 100 Hz were normally used. Some testing was also conducted with sinusoidal inputs to study the effects of the gyro scale factor asymmetry problem on the system outputs. Performance evaluation during angular vibration test was accomplished by using the same differencing technique employed for the linear vibration test.

#### 4.3.3 Thermal/Vacuum

The thermal conditions of space flight were simulated with each assembly in a vacuum. The temperature profile was varied during the 14-day period of the test to simulate the expected flight conditions. A series of drift tests was made with the AGS computing attitude and velocity. The results obtained were compared with the results of tests conducted in room environment with the ASA in the same position. The DEDA was operated to demonstrate the functions and logic under the thermal vacuum conditions.

The AEA self-test programs were also performed. These tests indicated generally satisfactory AGS performance. However, it should be pointed out that extensive performance testing was not warranted because of the instability of the ASA in the chamber that is subject to industrial noise (motion).

#### 4.3.4 Earth Prelaunch Gyro Calibration Program Test Under Sway Environment

Because of the long time interval between laboratory calibration and actual vehicle flight, the gyro bias changes, thereby invalidating the compensations in the flight program. Therefore, the gyro biases will be re-determined shortly before launch (with the ASA in the vehicle) and the compensations updated. The calibration technique is complicated by the fact that the vehicle sways in the wind and hence is not a stable platform.

Calibration of the gyro biases will be accomplished with the AGS in the vehicle, using a special computer program. The program establishes an inertial reference, using averages of the accelerometer outputs to obtain the ASA leveling data. The azimuth information is supplied from an external source. The gyro biases are then computed and filtered to smooth out the effects of vehicle motion. At the end of the 20-minute program, the gyro bias data are printed out. The flight program must be reloaded and the compensation (including the new gyro biases) must be reinserted. A series of tests was performed in the laboratory to prove the acceptability of this scheme. The ASA was subjected to the simulated sway motion while the program computed the gyro biases. The resulting values were compared to the best estimate of bias determined from other testing. The swaying motions of a fueled vehicle and of an empty vehicle were simulated for winds from different directions. The sway motion was simulated by a specially developed machine that causes the ASA to move in an elliptical path over a very small segment of the surface of a very large sphere.

#### 4.3.5 Navigation

Portions of the AGS flight program were read into the AEA to allow navigation. The program was altered only by the addition of the data readout logic. The AGS was operated in the same manner as for flight while it accumulated the position and velocity data, issued steering commands, and issued discretes. These outputs were compared with the expected values.

#### 4.3.6 Coning

The ASA will be subjected to the coning motions while the AEA utilizes the outputs to compute the direction cosines of the attitude and the velocity. For low frequency coning, the system attitude reference and velocity computations are not expected to be affected (assuming the inputs do not saturate the gyros). As coning frequency increases, however, the sampling error increases to 100 percent at 25 Hz for the particular sampling rate (50 Hz) employed by the AGS. Also, gyro phase shift or pseudo coning errors will occur. The test was designed to verify the above errors. The AGS outputs will be compared with the expected values.

A special test design was required to separate the coning errors from the rectification of vibration inputs by the gyro asymmetry. The basic coning motion induces error with the same sign as the input motion. The asymmetry-rectified vibration error is independent of the direction of coning input; however, the coning error will be separated from the asymmetry error by coning in both clockwise and counter-clockwise directions. The coning angles were chosen to give an input of 80 percent of the gyro loop saturation level at each of the input frequencies.

#### 4.3.7 Calibrations

The values of all ASA sensor parameters must be determined from test data to ascertain the condition of the

ASA and to obtain data for use in compensating for sensor off-nominal conditions.

Routine calibrations of the ASA were generally performed using the AEA as a computer. The time logged therefrom and experience gained thereby added considerably to the reliability and confidence in the AGS.

The method chosen for calibration of gyro fixed drifts and imbalances and accelerometer biases, scale factors, and misalignments was a six-position rate test. Sensor input axes were located along north and east lines and the local vertical for several minutes (precisely measured), then inverted for the same time period. Pulse accumulations were recorded from each position.

The gyro scale factor and misalignments were determined by rotating the ASA through a precisely known angle (720 degrees) clockwise and counter-clockwise to cancel the effects of fixed drifts and earth rate. Rotational rates were not critical. Error analyses and subsequent test repeatability and correlations have shown these schemes to be sound and adequate.

#### 4.3.8 Electromagnetic Interference

When the electromagnetic emittance of the AGS and the susceptibility of the AGS to external radiation were investigated, the only problem encountered was the degree of nonrepeatability resulting from the lack of a stable pier.

Subsequent testing has revealed a clock jitter problem associated with EMI. The test set clock jitter was particularly attributable to EMI within or between countdown chains, and was more severe on the trailing edges of the clock pulses. The problem was not evident until an ASA circuit modification shifted the trigger point from the leading to the trailing edges of the clock pulses.